Innovative tools for vascular disease

Dissertation discussed in partial fulfillment of

the requirements for the Degree of

DOCTOR OF PHILOSOPHY

Department of Sperimental Medicine (DIMES)
Translational biotechnology
Curriculum translational surgery
XXXIII cycle

PhD advisor:
Professor Domenico Palombo

Candidate:
Giulia De Negri Atanasio

Index

Abstract

In the Western World, pathologies related to cardiovascular apparatus as coronary and peripheral arterial represent one of the prevalent causes of mortality. Atherosclerosis is an inflammatory and progressive disease characterized by the presence of an accumulation of low-density lipoprotein. The accumulation is commonly called plaque and it can occlude the blood flow in the arteries. The evolution of the plaque can represent a target in all stages of its progression. In the early-stage of atherosclerotic plaque, nanocarriers can be used as a system for targeted drug deliver, and during its progression it could be necessary to replace the vessel by using innovative engineered biodegradable vascular grafts. Nanoparticles can inhibit the progression of the plaque when correctly functionalized on the surface to target the atheromatous site. The first part of this Ph.D. thesis is focused on the production of nanoparticles with a comparative study between liposomes produced trough the thin layer hydration technique and polylactic co glycolic acid (PLGA)-based nanoparticles produced using the double emulsion technique. In this preliminary work, both carriers were loaded with different concentrations of albumin as model protein. A study of morphology, dimension, size, entrapment efficiency, cytocompatibility, and hemocompatibility was performed. Both particles analyzed present positive points however, the studied polymeric nanocarriers can be considered as a good model to be engineered with antibodies on their surface in order to be employed in the vascular field as a nanosystem for protein drug delivery.

A second work on PLGA nanoparticles was performed at the Instituto de Investigação e Inovação em Saúde da Universidade do Porto (i3S) at the University of Porto, under the supervision of Professor Bruno Sarmento. Here, it was optimized the encapsulation of bevacizumab, a commercial antibody, Avastin®, active against the vascular endothelial growth factor (VEGF) receptor commonly expressed at the atheromatic site. The functionalization process with immunouteroglobin-1 (IUG1) a human recombinant antibody (scFv) specific for extra-domain B (EDB) of fibronectin, a well-known

marker of angiogenesis was considered and tested. These polymeric and functionalized nanoparticles were analyzed in terms of morphology, size, ζ-potential, entrapment efficiency, conjugation efficiency, release studies at 37° C, FTIR, CD, biocompatibility with endothelial cells (EA.hy926), macrophage (RAW 246.7), and hemocompatibility.

This part of the work involves an innovative therapeutic approach for the treatment of the early-stage of atherosclerosis, the most common disease in cardiovascular field.

The second part of this Ph.D. thesis is focused on the development of synthetic grafts for vessels with a diameter smaller than 6 mm. In the clinical practice, when the vessel is obstructed by the atheromatous plaque is essential to reconstruct the blood flow, maintaining all the functions of the downstream tissue, is necessary to introduce a bypass. It is preferable to use autologous veins but, if not available, the use of synthetic grafts is required. Non-biodegradable vascular prostheses such as poly (ethylene terephthalate fibers and expanded poly (tetrafluoroethylene), commercially known as Dacron® and Gore-Tex®, respectively) have been successfully used as vascular grafts for aortic and iliac replacement. These materials are not used to substitute small caliber vessels (inner diameter < 6 mm) because the longer contact of the blood with the wall of the vessels due to the lower pressure can induce thrombogenic event, there is the absence of endothelialization after the implantation, it can occur infection of the synthetic grafts and related inflammatory response to the foreign materials.

Nowadays, it looks essential to fabricate vessel grafts to replace these small vessels, and several approaches have been used to fabricate small-caliber blood vessel grafts as 3D printing, film casting, electrospinning, decellularization matrices from animals, and cell-seeding. An ideal vascular graft should be biodegradable acting as a scaffold to help the regeneration of a native vessel. The mechanical properties result to be essential to mimic the native arteries, being resistant to thrombosis, dilatation, good flexibility, and no kinking, showing good suture retention,

hemocompatibility and have an appropriate degradation kinetic. Given these problems in the clinical procedure, small caliber vascular prostheses made of biodegradable and bioabsorbable polymers through electrospinning have been developed through electrospinning and then functionalize with bioactive compounds.

The electrospinning technique is considered one of the most promising methods in the tissue engineering area, in particular for the development of synthetic vascular tissue producing structures similar to the extracellular matrix. In this process, the solvent evaporates immediately, and the applied electrical fields induces the deposition of the polymeric solution on a tubular collector. The prostheses thus produced, are composed of a blend of two different polymers: poly (ε-caprolactone) (PCL) and poly (glycerol sebacate) (PGS) in a ratio 1:1 both 20 % m/v. These constructs, due to the high permeability, need a coating with gelatin which significantly reduces the water permeability.

One of the aims of this project is to produce grafts that can influence the cells inducing the regeneration process. Furthermore, the post-surgical inflammation is able to negatively affect the cellular attachment and can induce several damages to the structure of the biomaterials compromising it's the characteristics. In order to modulate the inflammation, scaffolds were functionalized with antioxidants. Quercetin (3, 3', 4', 5, 7-pentahydroxyflavone) is an antioxidant popular in different kinds of fruit and vegetables.

The addition of quercetin to the studied polymeric vascular grafts did not change both their morphology and their overall performances. Also, the presence of quercetin counteracted the activity of TNF-α inducing a decrease in MMP-9 expression level, showing the capability to modulate the inflammatory process.

To develop a suitable construct is important to study its behavior in different conditions; for this reason, a study in static-conditions, dynamic-conditions and a study in bioreactor have been

performed. The latter was fundamental to understand the behavior under different pression regimes mimicking the peripherical district.

During or at the end of the experimentations vascular grafts were always by characterize at different point of view: morphological (SEM, fiber distribution and dimensions), chemical physical (release of bioactive compounds, degradation , fluid uptake and degradation at different pH), mechanical (tensile strength, young modulus and elongation percentage).

The novelty of this second part is the fabrication of small-diameter biodegradable and bioabsorbable vascular graft and its characterization in several conditions (Static, dynaminc and bioreactor) showing promising results.

Introduction

Cardiovascular diseases (CVDs) represent one of the major causes of death in the Western world[1]. In 2016, ischaemic heart disease and stroke were the most common cause of death globally, representing a 27 % of the total deaths. These diseases have been the main causes of death worldwide in the last 15 years. In 2017, there were 108.7 million people living with CVDs in the 54 European Society of Cardiology (ESC) member countries[2], 92.1 million people[3] in the United States of America and more than 200.1 million people globally. According to the World Health Organization (WHO), more than 23.6 million of death will be reached by 2030[4].

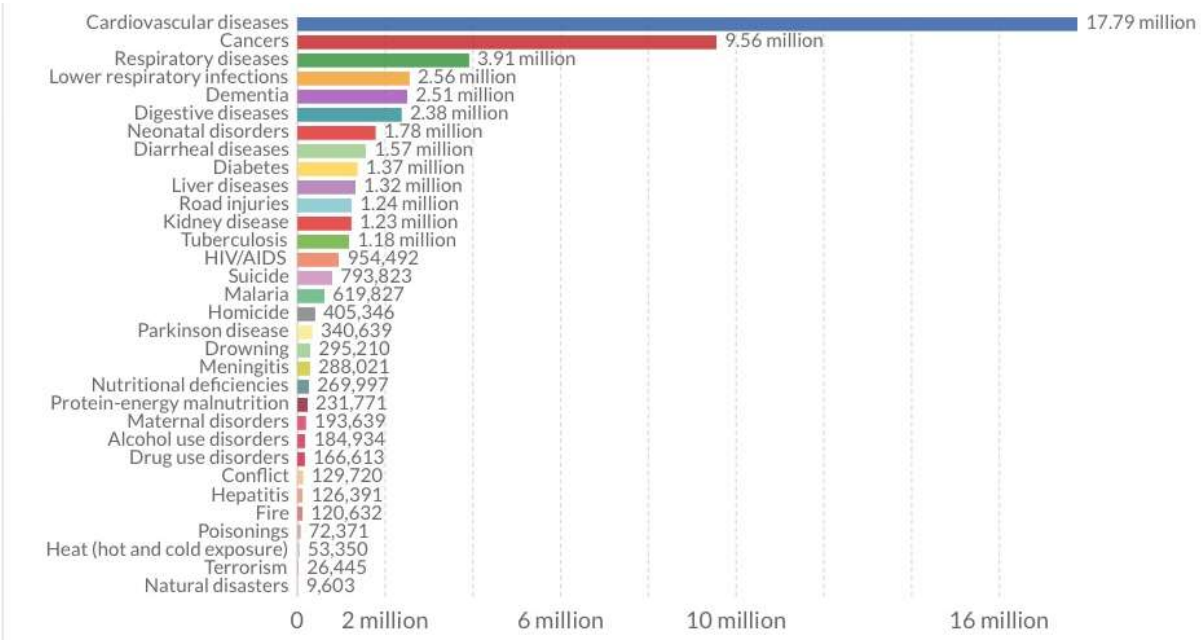

Figure 1. Number of deaths in the western world. Source: IHME.

CVDs include mainly peripheral arterial diseases, cardiomyopathy, rheumatic heart disease, endocarditis, hypertensive heart disease, atrial fibrillation, ischemic heart disease, stroke, and aortic aneurysm [5]. 24 % of people with CVDs were living with peripheral vascular diseases in 2017 in the 54 ESC member countries with a heavy impact on each singular National Health System. Peripheral arterial disease (PAD) is referred to all the anomalies that have as a final result the obstruction of

arteries serving the legs, stomach, arms, and head [6]. PAD can be manifested as atherosclerosis (ATH) of the abdominal aorta, iliac, and lower extremity arteries[7].

ATH can be called the new plaque of the modern world due to the new lifestyle, as the sedentary life, unbalanced diet, smoke, and chronic disease as diabetes[8]. Is a silent disease which increase and get worst during the hear if is not treat using common drug as statin, the elective drug.

It is described as a disease characterized by the presence of inflammation where lipid-rich plaques are present in large or medium size vessels due to the accumulation of low-density lipoproteins (LDLs). The deposition of LDLs close to the endothelial layer represents the basis of their oxidation, becoming oxidized LDL (oxLDL), and stimulate phagocytosis by macrophages. After phagocytosis of oxLDL, macrophages are engulfed, and they modify their appearance as foam cells. This event represents the basis of the trigger of an inflammatory environment due to the secretion of pro-inflammatory cytokines (e.g. tumor necrosis factor-α, (TNF-α) and interleukin 1 (IL-1)). These two molecules are responsible for the expression of adhesion molecules that play a pivotal role in the leukocyte's recruitment. Furthermore, they are able to induce the production of platelet-derived growth factor (PDGF) and fibroblast growth factor (FGF) which are responsible of the migration of smooth muscular cells (SMC) from the tunica media to the intima[9]. This pathologic scenario is mainly due to lifestyle factors (i.e. sedentary lifestyle, obesity, tobacco consumption, consume of food rich in salt, sugar, and saturated fats, hypertension, diabetes, and dyslipidaemia) that are, in some cases coupled with genetic contributions[10][11] [8]. The most frequent clinical evidence of ATH comprise myocardial infarction, angina pectoris, intermittent claudication, ischemic stroke, and ischemic attack [12].

Structures of arteries and atherosclerosis description

The mammals' arteries are organized in three different layers. The inner layer is called intima which is in contact with the blood and it is formed by a monolayer of endothelial cells with an elongated shape toward the blood flow. These cells have connected each other by tight junctions and are anchored to a connective tissue that is fundamental for nutrient and growth factor diffusion.

The tunica media is the thicker layer. It consists of layers of elastin, collagen, and smooth muscle cells (SMC). In small-medium size arteries, the muscular portion is more developed while in the bigger ones prevails the composition of elastin.

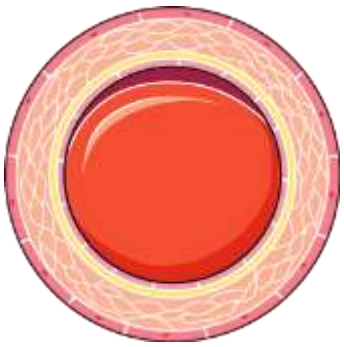

Figure 2. Schematic representation of vascular vessel. Source from: smart Servier medical art.

The external layer is the tunica adventitia whereby fibroblasts secrete the collagen. This represents the limit of expansion of the vessels, moreover, has a close interaction with the vasa vasorum which provide addition of oxygen and nutrients to this layer[13].

Blood vessels have the primary role of distributing the nutrients and of removing wastes from all the body. It occurs that, due to different kinds of pathologies, such as atherosclerosis, the blood flow is compromised with the possibility to have severe damages to the vascularised organs. Atherosclerosis (ATH) is a disease that represents the first cause of death in industrialized countries and the next years, it will represent an epidemic pathology. ATH is a slow and progressive morbidity characterized by the presence of plaques due to the accumulation of fatty molecules. This process happens mainly in large and medium size arteries, and, for the earlier stages is asymptomatic being symptomatic only in the case of thrombosis or other complications. The main risk factors are smoking, hypertension, dyslipidaemia, diabetes, a sedentary lifestyle, and obesity. For many years, it was believed that the ATH was a passive accumulation of cholesterol in the arteries wall. Today,

it is described as a multiple aetiology-based disease in which an inflammatory process involving the activation of the endothelial cells in the intima is present. Felix Marchand was the first scientist who coined the term 'atherosclerosis' in 1903, which derives from the Greek noun "athere" meaning "gruel" and "scleros" meaning "hard".

Usually, the first damage can occur near the arterial bifurcation. This behaviour suggests a correlation between a hydrodynamic stress and the development of the plaque[14]. The first modification of endothelium, which precedes the development of the atherosclerotic plaque, is represented by an increase of the endothelial permeability to lipoproteins[15]. The LDLs undergo oxidative changes becoming oxLDLs which promote the establishment of a pro-inflammatory environment [15]. The oxLDLs, accumulating in the intima, stimulate the endothelial cells to express cellular adhesion molecules (CAMs) like VCAM-1 (Vascular Cell Adhesion Molecule-1), ICAM-1 (Intercellular Adhesion Molecule-1), ICAM-2, PE-CAM (platelet endothelial CAM) and selectin P and E[16][17]. This activation promotes the recruitment of lymphocytes T and monocytes. The latter, once penetrated in the intima, differentiate in macrophages. The macrophages expose on their surface a scavenger protein which is responsible of the removal of the oxLDL. These oxidized forms of LDL is responsible in the turning of the macrophages in foam cells [18]. This first lesion is called fatty-streak and is composed prevalently by foam-cells and is potentially reversable with the application of a diet which reduces the lipoproteins in the blood[14]. The lymphocytes T and macrophages promote the release of chemokines like IL-1 and TNF-α which trigger the inflammatory process and stimulate the SMC migration from the tunica media to the tunica intima [19]. The SMC build a fibrous cap known as atheroma which surrounds the lipidic core [13]. These cells produce the collagen and elastin as a response to the PDGF released from the foam cells forming the extra-cellular matrix (ECM) which promotes the wall arteries thickening. The production of ECM is offset by the matrix metalloproteinases (MMPs) which catalyse its remodelling. This degradation

facilitates the SMC migration from the media to the intima and it could weaken the fibrous cap potentially provoking its rupture[18]. When the fibrous cap breaks, procoagulant factors are released from macrophages and SMC. This pro-inflammatory cascade leads to the activation of thromboxane A2 which is responsible of vasoconstriction and promotes platelet aggregation and the possible formation of thrombotic events [18].

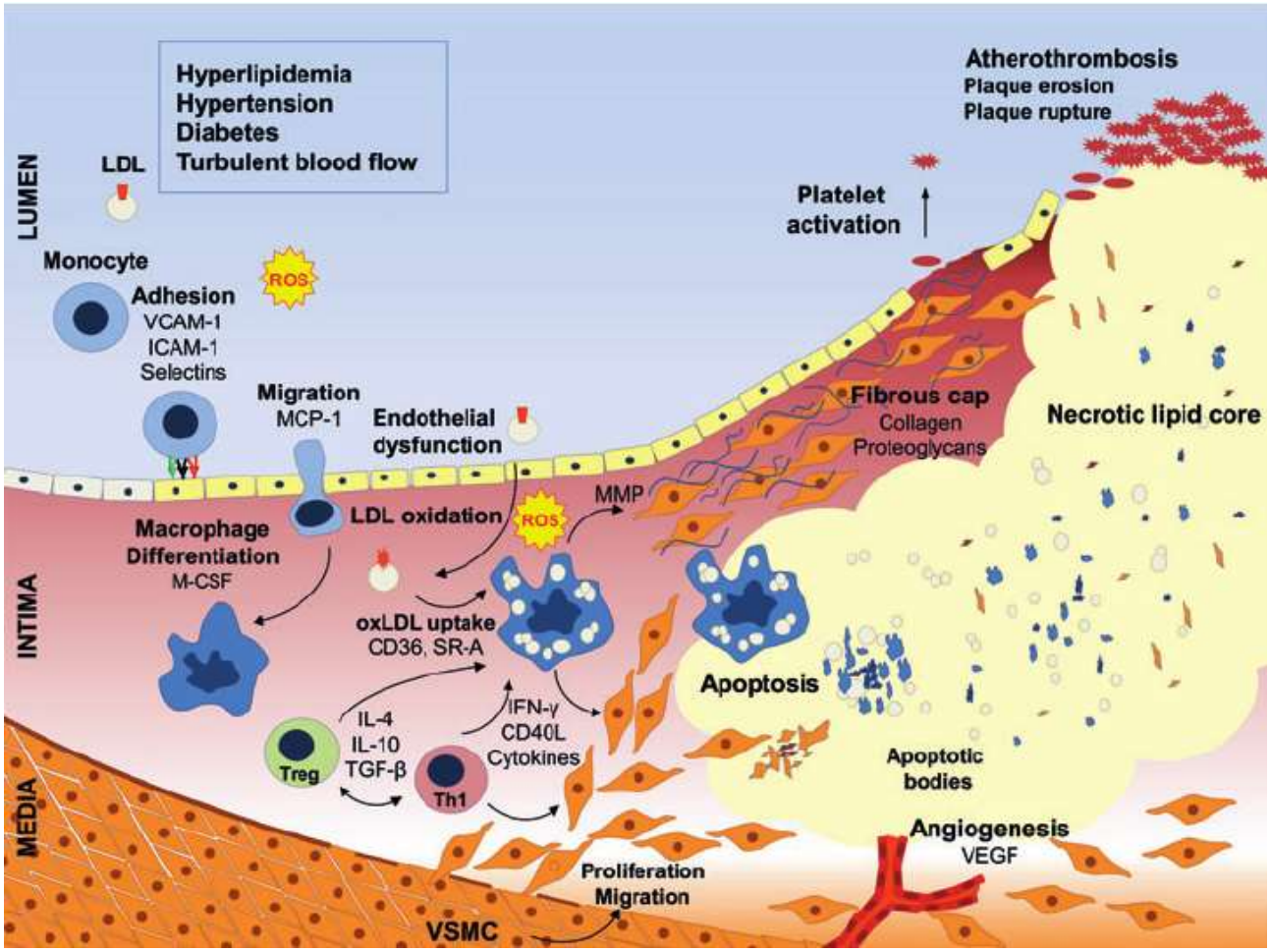

Figure 3. Schematic representation of inflammation process in atherosclerosis. Adapted from Wilck et al.[20]

Classification of atherosclerosis plaque

The American Heart Association classified the atherosclerotic plaques in six different types based on a histological description[21] [22].

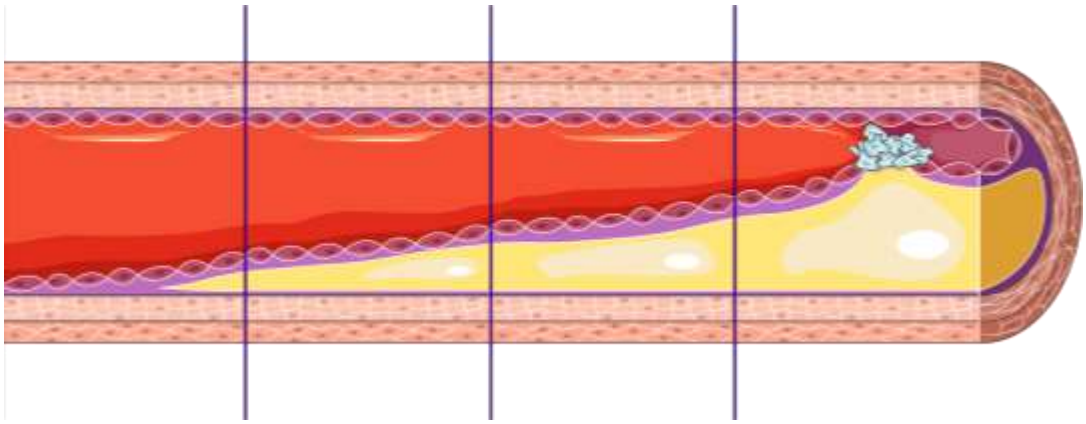

Figure 4. Schematic representation of atherosclerosis plaque progression. Source from: smart Servier medical art.

LESION TYPE I: it derives from the first small accumulation of foam cells in the intima. This type of lesions is the most recurring in children and these phenomena are interpreted as an intima thickening adapting to the mechanical shear stress forces induced by the blood on the arteries. Typically, they do not decrease the vessel lumen.

LESION TYPE II: this type of lesion consists of layers of foam cells and SMC. Generally, this step is known as fatty streak and it could be reversible if a decrease concentration of cholesterol in the blood with a proper diet or a specific therapy occurs.

LESION TYPE III: these lesions are a bridge between the lesions type II and the atheroma (type IV) and they are called pre-atheroma. It is characteristic to find foam cells and extracellular drops between the SMC which increase the thickness of the intima. At this stage, the lipid core (a massive accumulation of extracellular lipids) is not developed yet.

LESION TYPE IV: it is called atheroma. In the lesions of type IV, there is the development of a lipid core in the intima. It is the first critical stage because of the presence of an endothelial disorganization caused by the lipid core. This core evolves from extracellular lipid drops characteristic of the pre-atheroma.

LESION TYPE V: this lesion is characterized by the presence of fibrous connective tissue. When this new tissue belongs to a lesion with a lipidic core, it is called fibroatheroma or lesion type Va. The lesion type Vb is represented by a lipidic core or other part presenting calcification. If the lipidic core is absent and the intima is replaced by a fibrous tissue, it is called lesion type Vc.

LESION TYPE VI: these lesions are complicated lesions. They are usually divided in several sub-types: lesion type VIa, characterized by ulcerations of the endothelial cells and type VIb, characterized by hematoma of the lesion. If there is thrombosis, it is classified as a type VIc lesion, while the type VIabc presents all the characteristics reported above.

Looking this classification several strategies can be follow according to the type of lesion found in the patient.

When lesions are type III or type IV it is possible to use a pharmacological strategy, if the plaque is type V or type VI is necessary a surgical procedure. In the following chapter these two types of strategies will be discussed in depth.

Pharmacological approach

The pharmacological approach for the treatment of atherosclerosis are used to stabilize the lesions there are clinical evidences studies for statins, anti-platelets agents, β-blockers, and renin-angiotensin-aldosterone system inhibitors[23] . The most common pharmacological treatments for ATH are here reported:

STATINS

Statins were isolated for the first time from the fungus *Penicillium citrinium* [24]. The first statin approved for humans was lovastatin of natural origin. Nowadays, the statins present in the market

are synthetic, i.e. fluvastatin, atorvastatin, rosuvastatin and pitavastatin. The common structural element between the natural and the synthetic statins is the presence of 3,5 - dihydroxypentanoic acid 3,5 - dihydroxy 2- pentanoic, depending on the presence of a double bond in position 2. This chain could be in a cyclic lattonic shape where the carbossilic and hydrossilic groups are condensed or not. The statins (e.g. lovastatin and simvastatin) which present the lactonic group are pro-drugs, which means the hydrolyzation and the open of the ring occur in the intestinal tract, forming the molecule with the inhibitory activity. The administration of a statin in the form of lactone or acid changes the solubility and the pharmacokinetics of the drug itself. The mechanism of the statins is related to a decrease in the synthesis of cholesterol in the liver and to a decrease level of cholesterol in the hepatocytes, with a consequent reduction of the degradation of the receptor of low density lipoprotein (LDL) and an increase of the expression for the gene for the LDL receptor through the activation of the transcription factor SREBP (sterol regulatory element-binding protein). This event involves the increase of the number of LDL receptor and consequently an increased removal of LDL from the blood [25]. The use of statins for the primary and secondary prevention requires a long-term therapy. For this reason, it is important to consider the tolerance and safety of these drugs: usually statins in monotherapy present a good tolerability and a low percentage of side effects. The interaction between the statins and other drugs, like anticoagulant (e.g. warfarin), macrolides, digossin, calcium antagonists, and antifungal, can give myopathy which can aggravate in rhabdomyolysis, a particular pathological condition which affects the muscles and take them to deterioration. The interactions are especially due to the inhibition in induction of the isoenzyme members of the cytochromes P450 family, in particular to the inhibition of cytochromes 3A4. The co-administration of statins and bile acid sequestrants causes a decreasing bioavailability of statins themselves[26]. The introduction of this class of drugs has proved the correlation between the

hypercholesterolemia and ATH. The benefits obtained by the treatment with statins could be a combination of LDL reduction and inflammatory inhibition[27].

BILE ACID SEQUESTRANTS

This class of drug was used before the launch of the statins. These molecules represent probably the safest ones in the treatment of atherosclerosis because they are not absorbed from the intestine. Cholestyramine and colestipol are the two-bile acid sequestrants found in commerce. Cholestyramine is a quaternary amine while colestipol is a mixture of ternary and quaternary diamines. These molecules are positively charged and bind themselves to the bile acids which are negatively charged before being eliminated with the stools. Because of this decrease of bile acids, the hepatic cells increase the conversion from the cholesterol, involving an increasing of the synthesis of LDL receptor[28][29]. Despite their high tolerability, this class of drug can interact with the absorbance of vitamins which are soluble in fat like vitamin A, D and K, giving also some abdominal pains and constipation.

Lipid lowering agents

The cholesterol assumed with the diet is normally absorbed by the enterocytes with a proper carrier in the intestine. Ezetimibe was the first lipid-lowering agent to have been used starting from the first years of this century. It is able to inhibit the intestinal protein Niemann-Pick C1-Like 1 (NPC1L1) that is responsible of cholesterol transport in the intestinal lumen[30] . This inhibition reduces the amount of cholesterol in the liver without affecting the absorption of vitamins, triglycerides, and bile acids. How this drug can decrease the entrance of cholesterol in the cells is not completely clear but some studies assume a change of shape of the NPC1L1 preventing the binding with sterols[31]. Usually, these drugs are administered with the statins as adjuvants[32].

Drugs controlling the inflammation process

Another strategy in the treatment of atherosclerosis could be the control of the related inflammation. The most well-known class of these therapeutics is represented by the salicylate like acetyl salicylic acid (aspirin) which belong to the non-steroidal anti-inflammatory drugs[33]. Low-dose of aspirin reduces vascular inflammation and the levels of proinflammatory cytokines in the plasma [34] . The anti-inflammatory properties result from a high-dose treatment inducing an inhibition activity of NF-kB which has an important activity during the generation of the atherosclerotic plaque [35][36]. Another molecule that could be pharmacologically controlled is IL-1. In CANTOS trial a monoclonal antibody, Canakinumab, was studied [37]. In the atherosclerosis, the IL-1 has a pivotal role for the plaque development[38]. It promotes the adhesion of monocytes and lymphocytes T to the endothelial cells and stimulates the growth of the SMC which build the fibrous cap surrounding the atheroma. Canakinumab binds to IL-1 receptor, excluding this molecule to recognize it activating all the biochemical pathway that give rise to a pro-inflammatory environment.

B-blockers

These drugs reduce heart rate and blood velocity inducing a lower turbulence and lower wall stress. The pooled analysis of four IVUS trials has demonstrated that β-blockers reduce the rate of ATH progression[39]. The inflammation process associated with ATH could be modulated even by administering molecules that block angiotensin II. Clinical trials, e.g. HOPE and ONTARGET, have reported a stabilization of the plaques by the pharmacological reduction in blood pressure[2].

Anti-cancer agents

In the recent years, some researchers have made an interesting parallelism between cancer and atherosclerosis. Cancer represents the second leading cause of mortality in industrialized countries,

after CVDs. This pathology is characterized by an unregulated excessive cellular proliferation together with the loss of cellular differentiation and enhanced invasiveness. For many decades, ATH and cancer were considered unrelated pathologies to be treated by different therapeutic approaches. Despite this classical concept, modern medicine uses to place side by side these two pathologies. Emerging therapeutic strategies present similar targets as the reduction of oxidative stress, the use of anti- agents, like methotrexate (MTX), have been used for the treatment of the atherosclerosis and it was demonstrated that in animal models it has an inhibitory activity around 50% on the macrophage's migration, in the early- stage, when the monocytes differentiate in macrophages/foam cells [40].

Actual nanoparticles strategies for atherosclerosis

In the last years, the development of drug delivery systems for the pharmaceutical industry has represented an important tool to broaden the drug market[41]. This innovative technology can enhance the release of non-hydrophilic molecules or the instable ones in biological fluids. It could manage also the co-release of two or more drugs in the combined therapy[42]. Moreover, due to the small size (200 nm), nanocarriers, can pass through small capillaries and can be internalized by the target cells. The nature of the shell of the nanocarriers usually is chosen to be a biodegradable material increasing the biodistribution and the shelf-life of the loaded drug and decreasing its toxicity. The target drug delivery can be achieved using the active or passive targeting. The active one is represented by the binding between nanocarrier and specific ligand for the target site. The passive targeting is reach with a nanocarrier's preferential accumulation in the lesion; this phenomenon is known as EPR (enhanced permeability and retention) [43]. On the other side, nanocarriers, beyond the advantages described above, possess some drawbacks like the rapid uptake from the RES (reticule endothelial system) with a consequent hepatic or splenic elimination.

To overcome this problem, it is become a common use the addition of PEG (poly ethylen glycol) on the nanocarriers' surface (stealth nanocarriers) which decreases the rapid elimination and increases the payload release time. In literature, it has been reported that the half number of stealth nanoparticles accumulate in the liver in comparison with the non-stealth ones. PEG is an adaptable polymer, cheap and approved by Food and Drug Administration[44]. In the last decades, many attempts have been proposed in this field and different carrier have been studied for various applications, i.e. liposomes, micelles, polymeric nanoparticles, dendrimers, and phytosomes.

In the case of ATH, it has been proposed the approach of decorating the particles' surface with specific ligands to adhesion molecules, i.e. VCAM-1, integrins and selectins. These molecules are massively expressed by the activated endothelium during the inflammatory process. Once the recognition between receptor-ligand occurred, the nanoparticles could link to the endothelial cells or become internalized according to the carriers' properties[45].

These technologies are widely used even in the diagnostic field. The recent developments in this topic offer the possibility to reach biological processes at molecular level. However, many of these engineered devices are now been considered in other medicine fields such as CVDs and ATH. In this part of the thesis, the two major carriers can be applied towards CVDs and ATH diagnosis and treatment will be discussed.

Liposomes

Liposomes are carriers made of phospholipids which give rise naturally to particles with the interaction of water[46]. These vesicles were produced for the first time by Bangham in England in 1961. They represent an efficient drug carrier which can preserve the activity and increase the payload shelf-life. The diameters of the liposomes range between 20 nm to

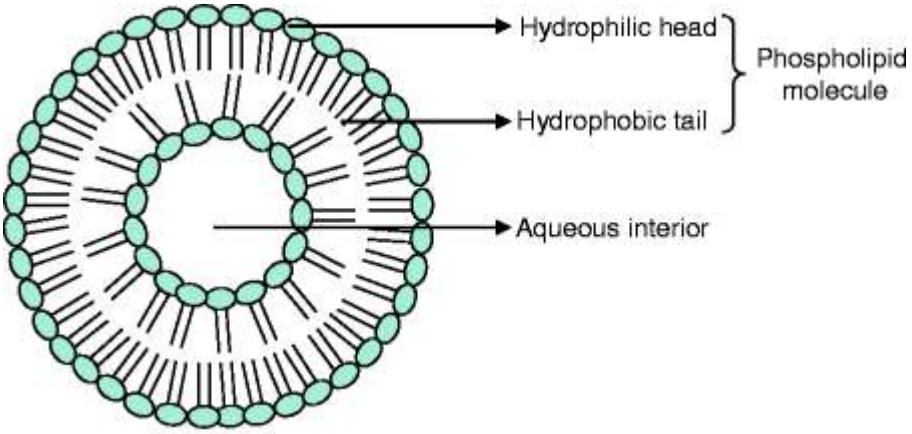

Figure 5. Schematic representation of liposome. Adapted from Swaminathan et [47]

several micrometres. Usually, they are classified on the number of lamella, indeed when liposomes present a single bilayer are called unilamellar vesicles (ULV) which could be divided in small unilamellar vesicles when the diameter is less than 100 nm and large unilamellar vesicles (LUV) if the diameter is larger than 100 nm. The multilamellar vesicles (MLV) are liposomes exhibiting a concentric number of lipidic bilayers[48]. Liposomes could be chemically modified on their surface producing good carriers for the targeting therapy.

For the atherosclerosis therapy, different studies based on liposomes have been reported [49]. Saito et al. [50] demonstrated that liposomes loaded by fasudil, a rho-kinase inhibitor, and decorated on the surface to bind the LOX-1 antigen expressed on the plaque, reduce the thickness of the atherosclerotic lesion. This treatment reduces the MMP-9 expression and the SMC migration. Another approach described by Cho et al. consisted of the production of liposomes loaded by PC phosphatidylcholine that can increase the HDL levels. In this way, the balance between HDL and LDL

was modified and there was a reduction of the lipidic fraction in the plaque thereby inhibition of oxidation of LDL with a limited inflammatory process. This study reported a significant decrease plaque thickness after just 5 weeks of treatment[51].

Polymeric nanoparticles

Polymers have become an important material class in the biomedical field. Polymers can be used for clinical applications like the production of vascular grafts, ocular implants, orthopaedic prostheses etc. [52]. In the context of nanotechnology, polymers can be used to product carriers which can be loaded with therapeutic agents to increase their therapeutic properties[24] . In literature, several polymers,

Figure 6. Schematic representation of polymeric nanoparticle. Created with Bioreder.com

of synthetic or natural origin, are used to product carriers for the atherosclerosis treatment. Giannouli et al. [53] produced nanoparticles of poly (lactic-co-glycolic acid) (PLGA) loaded with quercetin which presented a strong antioxidant activity and an inhibitory role against the matrix metalloproteases (MMPs). They demonstrated that quercetin-release consisted of two steps, an early phase during the first hours of release and a second one with a slow and sustained release of quercetin which was prolonged for 59 days. The results obtained highlighted how it is possible to product a drug delivery system loaded with a flavonoid with a long drug release making it a potential construct for atherosclerosis treatment. The aim of the paper by Hirpara et al. [54] was to investigate chitosan PEGylated nanoparticles loaded with rosuvastatin. This drug is an anti-hyperlipidaemic largely used for the atherosclerosis therapy and is an inhibitor of the enzyme HMG CoA reductase. In order to increase its bioavailability, the drug was encapsulated in chitosan PEGylated nanoparticles and it

has been demonstrated its sustained release in vitro. The in vivo studies reported a higher half-life accompanied by a reduction in the concentration of cholesterol and triglycerides in the serum in comparison to the free rosuvastatin. Sanchez et al.[55] produced nanoparticles with a PLGA core and presenting a HDL-like coating. These nanoparticles were produced by microfluidic technology. The results have shown that carriers were recognised preferentially by the macrophages and monocytes in the plaque. Yang et al. [56] produced PLGA particles loaded with heparin and demonstrated a decrease of the growth of the SMC induced by the PDGF. This encapsulation technique improved heparin half-life. In the last years, cyclodextrins (CD) have been of interest for atherosclerosis treatment for their ability to bind to hydrophobic molecules, like cholesterol, but they present a poor pharmacokinetic. To increase it, they were conjugated with polymers (CD-polymer) presenting consequently a higher half-life and a better therapeutic effect both in vitro and in vivo[57] .

As described above, macrophages play a pivotal role in the atherosclerotic plaque development. They express the glycoprotein CD36 which is involved in the endocytosis of the ox-LDL. PEGylated liposomes produced by Yu M, et al. [58] were functionalized with the extra-domain B of fibronectin specific aptide (APTFN-EDB). This aptide was immobilized on the liposomes surface loaded with cyanine as a small model drug to study the biodistribution and the pharmacokinetic. The results obtained reported a prolonged blood circulation and an increased accumulation in the plaques compared to the free drug[58] . Li et al. [59] have produced liposomes loaded with atorvastatin and curcumin and have decorated them with a peptide specific for the E-selectin. It has been reported that the liposome vesicles had a high uptake rate through endocytosis and it has been reported that both in vitro and in vivo treatment with liposomes had a higher anti-atherosclerosis effects related to the single drug treatment (i.e. with atorvastatin and curcumin alone).

Is a common strategy to improve the half time of the nanocarrier in the organism to use the polyethylene glycol (PEG) which can control the opsonization, improve the stabilization and reduce the toxicity increasing the biocompatibility profile [60]. This technique has been introduced in the 1970s and it has been demonstrated have activity in terms of circulation time in all the nanocarriers for polymeric nanoparticles and liposomes.

When the lesion reach V or VI level is necessary to proceed surgically, several different strategies can be applied.

Small blood vessel cardiovascular pathology treatment

Atherectomy

A possible procedure to remove the plaque from the vessels is the atherectomy. Usually this procedure is applied to make the lumen artery wider in order to facilitate the blood flow to reach the heart muscles. In an atherectomy, the plaque is shaved or vaporized away with tiny rotating blades or a laser on the end of a catheter.

This procedure is usually performed in peripheral vessels disease and coronary artery disease. Sometimes is used for severe plaque or in patients who present in their medical history have already had angioplasty and stents, but who still have plaque blocking the flow of blood.

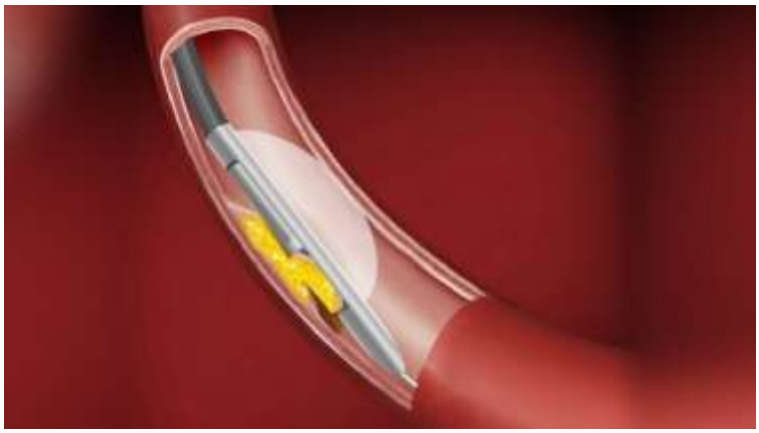

Figure 7. Schematic representation of atherectomy. Adapted from Willis-Knighton Cardiology site.

Angioplasty

Angioplasty is a procedure which re-establish the blood flow to the heart muscle without open-heart surgery usually used to open blocked small vessels.

In this procedure a catheter is used, placed in the vessel and directed to the blocked coronary artery. The catheter presents a balloon at its tip and, reached the interested place, the balloon is inflated at the restricted area of the heart artery. The plaque or the blood clot are pressed the wall of the artery, making space for blood flow. This strategy is usually used when the inner lumen is less than 70%.

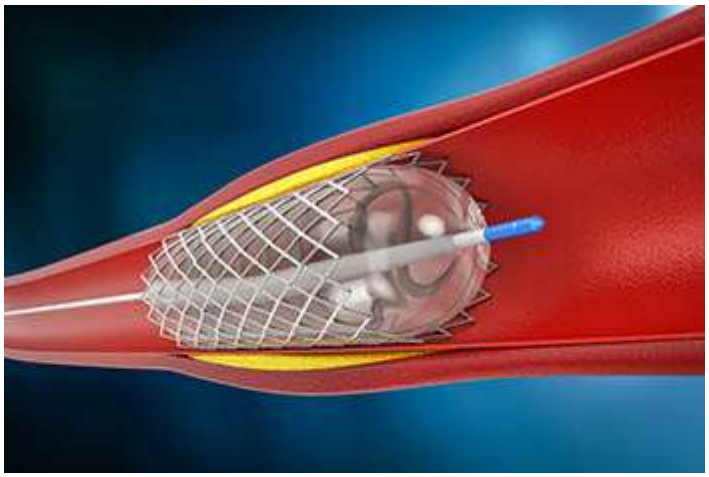

Figure 8. Schematic representation of angioplasty. Adapted from Trinity Health Mid Atlantic

BYPASS

A strategy to avoid the blocked of vessels is the use of piece of a healthy blood vessel from elsewhere in own patients' body bypassing the portion of the vessels blocked. Not always is possible to perform an autologous transplant so is necessary to use synthetic graft. The actual alternatives largely used for vessels with diameter higher than 6 mm are synthetic graft in Dacron or ePTFE. Conversely, for small diameter vessels this commercial grafts can be used because thrombogenic events may occur considering the higher contact of the blood with the wall of the vessels due to the lower pressure.

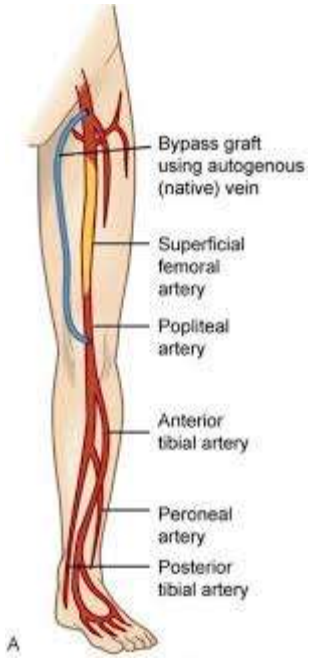

Figure 9. Schematic representation of bypass. Adapted from society of vascular surgery

Considered these problems is necessary to fabricate grafts for the replacement of small diameter vessels, a goal of my Ph. D. theses is the fabrication of synthetic scaffold realized with biodegradable polymer using the electrospinning.

Chapter 1

Introduction

In this chapter it will be describe the nanoparticles section of my Ph.D. work. These nanotools can be used for the treatment of ATH when the disease and the lesions are in an early stage. In literature nanoparticles are largely used for the treatment of cancer, but currently the idea of small targeted tools for specific site has been extended to other pathologies. Nowadays the most common particles in commerce are the liposomes and the polymeric nanoparticles the PLGA can be considered the Holy Grail among the synthetic polymer[61].

Liposomes are self-organizing colloidal particles made of bilayer membranes able to entrap molecules in a confined core. The presence of amphiphilic membranes makes it possible to encapsulate both hydrophilic and hydrophobic compounds inside liposomes.

PLGA is a copolymer of lactic and glycolic acid and the degradation occurs by hydrolysis of its ester. Lactate and glycolate, derived from LA and GA, respectively, are considered the products of PLGA biodegradation and, from a biochemical point of view, the Krebs cycle is the mechanism responsible for their elimination inside the human body.

To study deeply these two types of carrier an *in vitro* comparative investigation was performed using albumin (BSA) as protein control for the low cost and the easy detection.

Materials and Methods

Polymeric nanoparticles (PNPs) were produced using poly (d,l-lactide-co-glycolide) (PLGA) 50:50 (Mw = 54,000–69,000 g/mol) (RESOMER® RG 505, Evonik Industries, Essen, Germany). Poly (vinyl alcohol) (PVA) (Mw = 31,000–50,000 g/mol), bovine serum albumin (BSA), and phosphatidylcholine (PC) from egg yolk to prepare nanoliposomes (NLPs) were supplied by Sigma-Aldrich (Saint Louis,

MO, USA). Ethyl acetate and chloroform used during the preparation and all the reagents for cell culture, as, Dulbecco's Modified Eagle's Medium (DMEM, high glucose w/l-glutamine w/sodium pyruvate), fetal bovine serum (FBS), trypsin, and Dulbecco's Phosphate Buffered Saline w/o calcium w/o magnesium (DPBS) were obtained from Carlo Erba (Milan, Italy). The bicinchoninic acid (BCA) protein assay kit (Euroclone, Pero, Italy) was used to quantify the proteins for calculating the encapsulation efficiency (EE) and for the in vitro release studies. CellTiter 96® AQueous One Solution Cell Proliferation Assay (MTS) for cell viability studies was bought from Promega (Madison, WI, USA).

Preparation of Polymeric Nanoparticles

PLGA based nanoparticles were obtained using an emulsion solvent evaporation method based on a water/oil/water (w/o/w) double emulsion technique. The water internal phase was prepared by dissolving BSA in Milli-Q water obtaining solutions at different concentrations (30, 35, and 40 mg/mL). Then, the oil phase was obtained by dissolving 100 mg of PLGA in 1.0 mL of ethyl acetate until complete dissolution. Adding an adequate volume of the water internal phase to the oil phase achieving a ratio between PLGA and BSA of 60% (w/w) the primary emulsion was obtained by ultrasonic process using a Vibra-Cell® ultrasonic liquid processor (Sonics & Materials, Inc., Newtown, CT, USA) with a 20 kHz ultrasonic generator probe at 70% amplitude in pulsed mode (30 s on and 30 s off) for 1 min, at room temperature (25 ± 2 °C). This value was selected on the basis of a previous optimization study aimed at entrapping BSA with high efficiency [62]. The water external phase was a PVA (2%, w/v) water solution. A fixed amount of water external phase of 4.0 mL was then added to the primary emulsion. The w/o/w emulsion was prepared by sonicating the obtained mixture at the same conditions mentioned above. At the end of the second sonication process, the w/o/w emulsion was diluted up to 7.5 mL with the same external phase solution of PVA as before mentioned. The obtained emulsion was left under magnetic stirring at ambient conditions to allow the complete evaporation of the organic solvent. The obtained nanoparticle solution was then

centrifuged three times at 12,984 x g for 30 min at 4 °C (centrifuge from Alliance Bio Expertise MF-20R, Guipry, France) and the pellet was redispersed with deionized water to remove the excess of free BSA. After preparation, polymeric nanoparticle suspensions were stored at 4 °C. Empty PNPs (PNP_E) were also produced following the same procedure described above and used as control during the entire experimentation.

Preparation of Nanoliposomes

Nanoliposomes were produced using the thin-film hydration method also known as Bhangam technique. Briefly, 500 mg of PC was dissolved in 100 mL of chloroform. Then, the organic solvent was removed and the lipidic layer hydrated with the aqueous internal phase. Previously, BSA was dissolved in Milli-Q water at three different concentrations (3.0, 4.0, and 6.0 mg/mL). The volume of water was always selected to maintain the ratio between PC and BSA equal to 60% (w/w) for comparison purposes with PNPs. The solution was left under magnetic stirring for 3 h at room temperature. Then, it was homogenized for 2 min using the same Vibra-Cell® ultrasonic liquid processor reported above at the same conditions. The obtained liposome solution was then centrifuged at 12,984x g for 30 min at 4 °C three times and the pellet were washed with deionized water to remove the non-entrapped BSA. Liposome suspensions were stored at 4 °C after preparation. Empty NLPs (NLP_E) were also produced following the same procedure and used as control during the entire experimentation.

Particles Size

Both PNPs and NLPs were characterized using Dynamic Light Scattering (DLS) with a Zetasizer Nano ZS (Malvern Instruments Ltd, Worcestershire, UK) to measure mean diameter (MD) and particle size distribution (PSD) of the obtained carriers. This instrument worked at 25 °C and was equipped with a 5.0 mW He-Ne laser operating at 633 nm with a scattering angle of 173°. For MD, at least three

measurements for each sample were performed reporting their mean value ± standard deviation (SD). In the case of PSD, it has been analysed after particle preparation for each batch.

Scanning Electron Microscopy

PNP and NLP morphology was studied by using a Phenom ProX desktop SEM (Phenom-World BV, Eindhoven, Netherlands). PNPE and NLPE were prepared as described above. Prior to being analysed, samples were filtered by using 0.22 µm pore size filters. After that, a drop of each preparation was poured over a glass slide and kept at room temperature until the complete evaporation of water.

Before scanning electron microscopy (SEM) analysis, samples were sputtered with gold in the presence of argon. At least three different images for each sample were acquired.

Entrapment Efficiency

The BSA entrapment efficiency (EE) was calculated by an indirect method. The amount of encapsulated BSA was calculated after collection of the supernatants. In detail, both PNPs and NLPs after their preparation were centrifuged at 12,984 x g for 30 min at 4 °C and the supernatants were collected and analysed in terms of protein content. EE was calculated according to equation (1):

$$EE(\%) = \frac{Amount\ of\ loaded\ BSA - amount\ of\ free\ BSA}{amount\ of\ loaded\ BSA} \times 100$$

Total amount of loaded BSA is referred to the BSA initially used during the preparation procedures while free BSA is the protein present in the supernatants after the centrifugation step; i.e., the non-entrapped. BSA was quantified by BCA assay following the manufacturer's instructions and the absorbance of the samples was read at 562 nm using a microplate reader (Tecan Spark® 20M, Tecan, Männedorf, Switzerland). This analysis was performed in triplicate

In Vitro Release Studies

The in vitro release studies were performed both with PNPs and NLPs. At first, nanocarriers were centrifuged at 12,984× g for 30 min at 4 °C with the same centrifuge reported above to remove free BSA. Then, PNPs and NLPs were resuspended in 10 mL of DPBS (pH = 7.4) and stored at 37 ± 2 °C (incubator VWR, Radnor, PA, USA) under constant stirring. For a period of 12 days at a fixed time, samples were centrifuged at 12,984 × g and an amount of supernatant corresponding to 3% of the total volume was collected and replaced with the same amount of fresh DPBS. In order to calculate the protein concentration, supernatants were analysed by using the BCA assay as mentioned before. The obtained values were expressed as percentage of released BSA over time and were determined by summing the released BSA mass at each time point. Release studies were performed in triplicate.

Hemolysis

The in vitro evaluation of the nanocarrier compatibility with the red blood cells (RBC) is an important preclinical test. Human blood was obtained by healthy volunteers the hemolysis experiments were performed following the Guidelines of the European Community Council in accordance with the Nuremberg Code (Directive 2004/23/EC). Blood was collected into ethylenediaminetetraacetic acid (EDTA) test tubes and centrifuged for 10 min at 867× g (centrifuge SL 8, Thermo Fisher Scientific, Osterode, Germany) in order to separate erythrocytes from plasma[63] . Then, the obtained pellets were washed three times with DPBS while supernatants were discarded. At the end of this procedure, erythrocytes were resuspended in DPBS. Different concentrations of nanocarriers were mixed with erythrocytes to have a solution with a final volume of 150 µL. The solutions were then incubated, under agitation at 25 °C (orbital shaker-incubator ES-20, Grant-bio, Grant Instruments Ltd, Shepreth, Cambridgeshire, England) for 2 h and then centrifuged for 5 min at 867 g (centrifuge Z 216 MK, HERMLE Labortechnik GmbH, Wehingen, Germany). The obtained supernatants were

spectrophotometrically analyzed at 540 nm using the plate reader reported before. The hemolysis percentage was calculated using equation (2):

$$Hemolysis(\%) = \frac{sample\ Abs - negative\ Abs}{positive\ Abs - negative\ Abs} \times 100$$

The negative and the positive controls were obtained treating erythrocytes with DPBS and deionized water, respectively [64]. For this test, the concentration of the particles to be used was calculated on the basis of the amount of entrapped BSA. Negative results were approximated to zero in the analysis and statistical studies were performed exclusively for samples showing a hemolysis percentage lower than 5.

Cell Viability

EA.hy926 human endothelial cells (ATCC® CRL-2922) were cultured in DMEM supplemented with 10% (v/v) of FBS and incubated at 37 °C and 5% CO2 until 70% confluency was reached. 4×10^3 cells were seeded in each well of a 96-well plate and incubated overnight before any treatments. Cells were treated with different concentrations (0.1, 1.0, 10, 100, 200, 300, and 500 µg BSA/mL) of both empty and loaded PNPs and NLPs. After 24, 48, and 72 h of incubation with PNPs and NLPs, cell viability was quantified by CellTiter 96® AQueous One Solution Cell Proliferation Assay (MTS). Daily, the medium of analyzing well was discarded, cells were washed with DPBS, and a mix of fresh medium (100 µL) and reagent (20 L) was added to each well and incubated for three hours. At the end of the incubation time, the absorbance of the samples was read at 490 nm by using the same plate reader indicated above.

For this test, the concentration of the particles to be used was calculated based on the amount of the entrapped BSA. For PNPE and NLPE, an equal amount of the BSA-loaded PNPs and NLPs, respectively, was used for each investigated concentration. Controls were represented by untreated

endothelial cells (without nanoparticles). All the experiments were performed in triplicate and results were expressed as a percentage with respect to the control (100%).

Statistical Analysis

All the experiments were done at least in triplicate and the results are expressed as mean values ± standard deviation. Statistical analysis was done by one-way analysis of variance (ANOVA), following Tukey's HSD post hoc multiple comparison test using Statistica v 8.0 software (StatSoft, Tulsa, OK, USA).

Results

Production and Characterization of BSA-Loaded Nanocarriers

Both PNPs and NLPs were successfully loaded with BSA with remarkable differences between them. To produce PNPs, a protocol based on w/o/w emulsion was adopted. The volume of the internal water phase, when this technique is applied, represents an important parameter which affects entrapment efficiency (EE). The required volume of the internal aqueous phase is mainly determined by the solubility of the compound that has to be encapsulated and it influences particle structure and therefore also the EE[65] . In this work, for the preparation of PNPs, the effect of the variation of the internal aqueous phase volume on mean diameter (MD), particle size distribution (PSD) and EE was studied, maintaining equal to 60% (w/w) the theoretical BSA loading with respect to PLGA or PC mass. Specifically, for PNPs it was used an internal volume of water equal to 2.00, 1.70, and 1.50 mL and the concentration of BSA solution was 30, 35, and 40 mg/mL, respectively.

Table1. BSA-loaded nanocarrier production conditions and results related to particle mean diameter and encapsulation efficiency.

	BSA concentration [mg/mL]	Total water volume [mL]	MD [nm]	EE [%]
PNPs	0	1.7	204 ± 20	-
	30	2.0	195 ± 11	97.15 ± 0.07[a]
	35	1.7	185 ± 10	97.82 ± 0.07[b]
	40	1.5	170 ± 12	98.01 ± 0.05[c]
NPLs	0	75	130 ± 51	-
	3	100	175 ±62	46.14 ± 14.17[a]
	4	75	152 ± 68	49.49 ± 2.18[a]
	6	50	144 ± 60	80.16 ± 7.46[b]

Particles prepared without BSA (PNP_E) were considered as control and taken into account for comparison purposes. Produced PNPs showed a MD between 170 ± 12 and 204 ± 20 nm. In Table 1 and in Figure 9A it has been reported that particle MD slightly increased at higher water internal phase volumes. Figure 9A highlights also a good control over PSD in all cases, particularly at the lowest water internal phase volume. In the case of PNPs, Table 1 shows a very high EE, up to 98.01 ± 0.05%. The EE slightly increased when the water internal phase volume was reduced. Probably, an increase in the water internal phase volume induces BSA losses towards the external water phase[66] . A higher volume of the internal aqueous phase can induce a decrease in the thickness of the particle polymeric layers allowing the migration of the water internal phase towards the water external phase[67]. The best condition for PNP production with good control of nanoparticle dimensions and high EE was at 1.5 mL of water volume with a BSA concentration of 40 mg/mL. NLPs were produced using the thin-film hydration method coupled with sonication. In this method, a lipidic layer is produced and then it is hydrated using a water solution containing the molecules of

interest, in this case BSA. Spontaneous formation of liposomes is obtained thanks to favourable interactions between water and phospholipids. When liposomes structure is formed, part of the water solution used for hydration is entrapped in the vesicles. The EE is markedly related to the amount of water that is effectively entrapped in the lipid bilayer, with respect to the total amount of solution used for hydration. Therefore, the amount of hydration water is a crucial parameter affecting EE. For this reason, for NLP production the effects of hydration water volume on liposome MD, PSD and EE were studied. Hydration volume was varied from 50 to 100 mL, changing the BSA concentration from 6.0 to 3.0 mg/mL and keeping constant at 60% (w/w) the BSA loading with respect to PC amount. Empty NLPs (NLPE), without BSA, were produced for comparison purposes. Operating process parameters and data referred to MD and EE of NLPs are reported in Table 1.

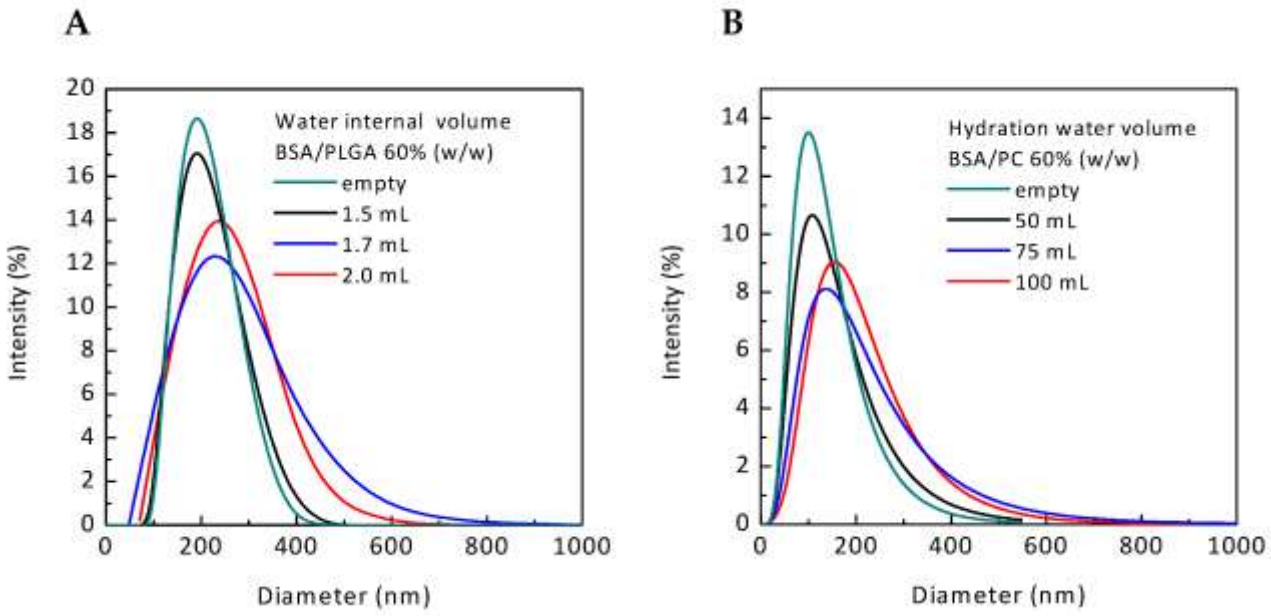

Figure 10. Representative particles size distribution of (A) PNPS and (B) NLPS.

It can be observed that NLPs were successfully produced with MD ranging from 130 ± 51 to 144 ± 60 nm by increasing the concentration of BSA in the stock solution used for their preparation. Figure 10B reports obtained PSD of liposomes produced with different water hydration volumes. From Table 1 and from Figure 10B, it can be noticed an increase of liposome MD when higher hydration

water volume was used. PSD data, showed in Figure 10B, showed also a good control of liposome dimensions in all the studied cases. Data reported in Table 1 showed remarkable differences in EE values between PNPs and NLPs. The samples produced with 100 and 75 mL of hydration water showed an EE of 46.14 ± 14.17 and 49.49 ± 2.18%, respectively. Conversely, by reducing the hydration volume at 50 mL and using a more BSA concentrated solution in order to have the 60% of theoretical loading, higher EE was obtained (80.16 ±7.46%). This result agrees with the related literature. By increasing the water hydration volume and fixing the PC content, less PC was available for unit of water, reducing the probability of entrapment of the water volume. The best condition for NLP production with good control over liposome dimensions and high EE was at 50 mL of water hydration volume with a BSA concentration of 6 mg/mL. Considering the two proposed nanosystems, EE was higher in the case of PNPs. The highest EE value (98.01 ±0.05%) was obtained working with 1.5 mL of water internal phase and a final BSA concentration in the water solution equal to 40 mg/mL. Figure 10 A, B report PSD of PNPs and NLPs, respectively. The loading of BSA did not interfere with PSD.

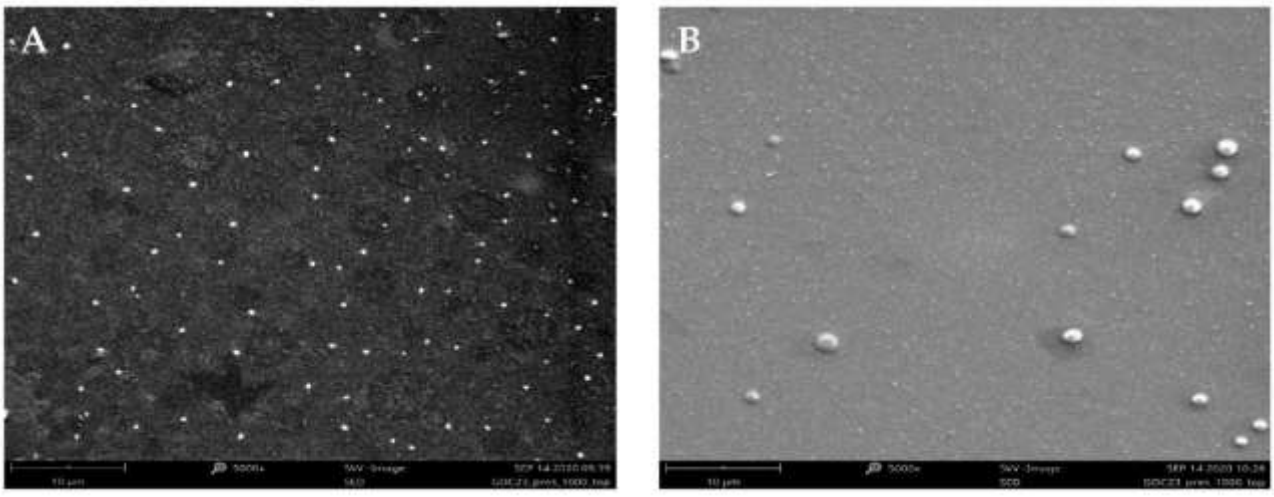

Figure 11. Representative SEM images (A) PNPE and (B) NLPE. SEM: scanning electron microscopy, PNPE: empty polymeric nanoparticles, NPLE: empty nanoliposomes.

As reported in Figure 11, the analyses of the morphological properties of empty PNPs and NLPs were performed using SEM. The studied nanocarriers appeared to show a spherical, well-defined morphology. *In vitro* release of BSA was studied at 37 °C over a period of 12 days. three different release curves obtained in the case of PNPs were compared with the three curves obtained working with NLPs.

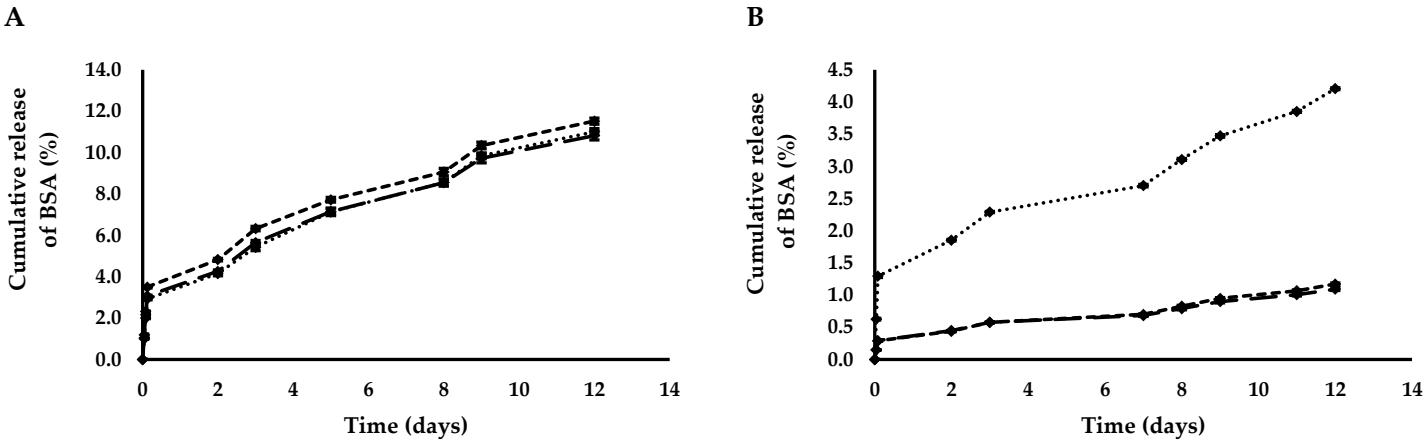

Figure 12. Release profile of BSA from (A) PNPs: ····· $PNP_{BSA\ (30\ mg/mL)}$, – – – – $PNP_{BSA\ (35\ mg/mL)}$, — — $PNP_{BSA\ (40\ mg/mL)}$ and from (B) NLPs: ····· $NLP_{BSA\ (3\ mg/mL)}$, – – – – $NLP_{BSA\ (4\ mg/mL)}$, — — $NLP_{BSA\ (6\ mg/mL)}$. BSA: bovine serum albumin, PNPs: polymeric nanoparticles, NLPs: nanoliposomes.

During this time, the maximum amount of BSA released from PNPs and NLPs was 11.01 ± 0.14% and 4.52 ± 0.01%, respectively (Figure 12A, B). This sustained release of the encapsulated bioactive compounds is desirable when they must reach a pathological site transported by nanocarriers. The delay that is evident in the release of the entrapped molecule is necessary for the nanoparticles to be internalized by the cells. In fact, once they are uptaken by cells, the carriers are able to release the encapsulated molecule that will start its therapeutic effects acting on specific cellular targets. A burst release is not desirable, as it would cause leakage before reaching the target of the pathological site. Working with both the nanoparticles, a burst released of BSA was avoided in all the cases, due to the physiochemical properties of the coating agent PLGA and PC.

Hemolysis Assay

Measuring hemolysis provides fast and valuable information of nanocarrier intravenous injections would have on red blood cell (RBC) membrane integrity. All the fabricated particles (PNPs and NLPs) were studied using fixed concentrations of 500, 300, 200, 100, 10, 1, and 0.1 µg BSA/mL. The concentration of nanoparticles was considered in terms of BSA content. All the produced samples reported in Table 1 were tested.

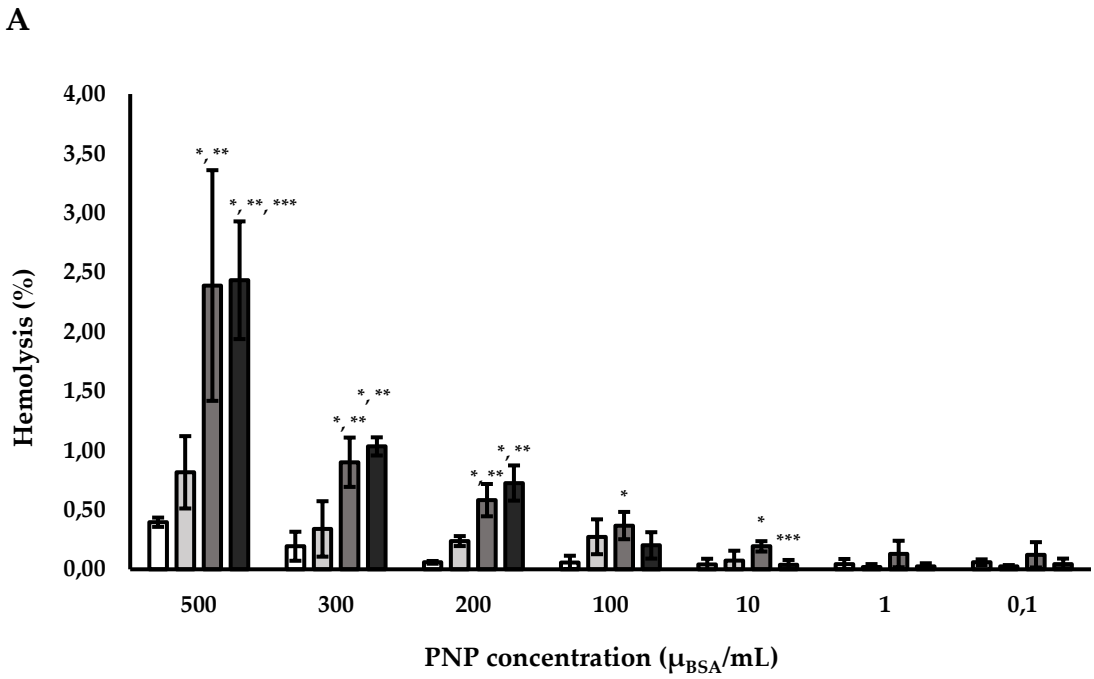

*Results are mean of three measurements ± standard deviation. Different symbols refer to statistically significant differences among results ($p < 0.05$, ANOVA with Tukey's HSD post-hoc multiple comparison test). *: statistically different to PNP_E, **: statistically different to $PNP_{BSA\ (30\ mg/mL)}$, ***: statistically different to $PNP_{BSA\ (35\ mg/mL)}$.*

B

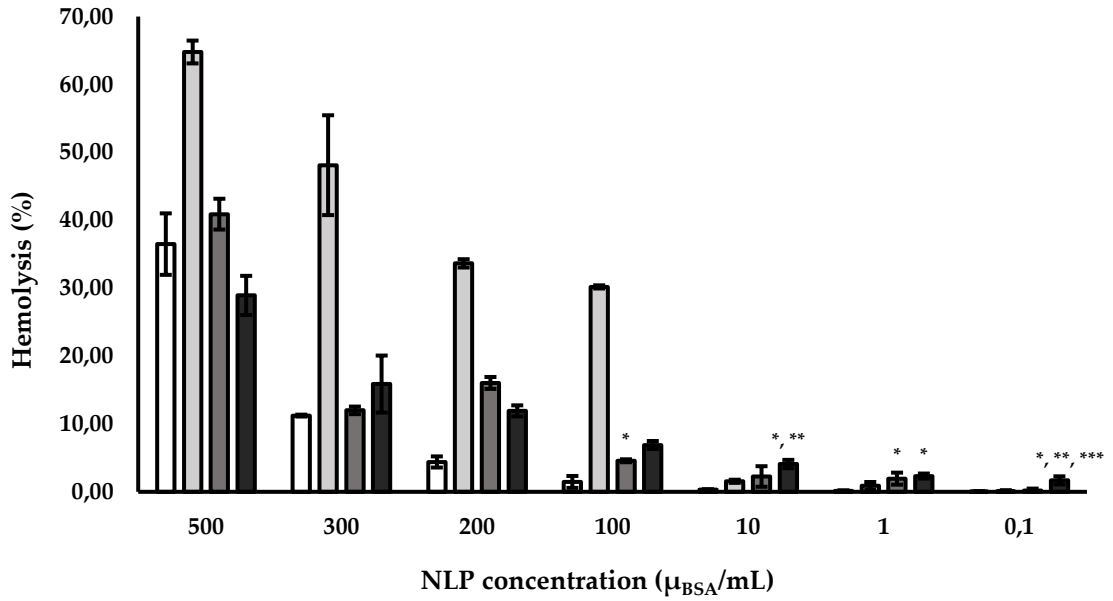

*Results are mean of three measurements ± standard deviation. Different symbols refer to statistically significant differences among results (p < 0.05, ANOVA with Tukey's HSD post-hoc multiple comparison test). *: statistically different to NLPE, **: statistically different to NLPBSA (3 mg/mL), ***: statistically different to NLPBSA (4 mg/mL).*

Figure 13. Hemolysis percentage of fresh blood after contact with different concentrations of (A) PNPs. □ PNP_E, ▒ $PNP_{BSA\ (30\ mg/mL)}$, ▒ $PNP_{BSA\ (35\ mg/mL)}$, ■ $PNP_{BSA\ (40\ mg/mL)}$ and of (B) NLPs □ NLP_E, ▒ $NLP_{BSA\ (3\ mg/mL)}$, ▒ $NLP_{BSA\ (4\ mg/mL)}$, ■ $NLP_{BSA\ (6\ mg/mL)}$.

The obtained results showed that the hemolysis was higher in the presence of NLPs in comparison to PNPs, testing the same concentration. Working with both the studied carriers, there was a direct correlation between the concentration of the payload and the toxicity on the erythrocytes. Figure 13A shows that in the case of PNP_E, there was a direct correlation between hemolysis percentage and PNP concentrations, especially for the concentration of 500, 300, and 200 μg_{BSA}/mL. Regarding the BSA-loaded PNPs, among all the different nanoparticle samples, 500 μg_{BSA}/mL resulted to have a higher hemolytic activity in comparison with the same concentration of the PNPE ($p < 0.05$). Furthermore, the hemolytic activity of PNP produced at BSA concentration in the water internal solution of 40 mg/mL (PNP_{BSA} (40 mg/mL)) was higher even at the concentrations of 300 and 200 μgBSA/mL. For all the tested samples, a hemolytic activity lower than 5% was reported and the formulated PNPs can be considered non-hemolytic at the tested concentrations[68].

Conversely, NLPs showed a hemolytic behavior, even for the empty sample at different concentrations. Concentrations of NLPs equal to 500, 300, and 200 g BSA/mL presented a hemolysis percentage over 5 (Figure 13B). This trend was reported even in the case of BSA-loaded NLPs, but in addition for the loaded liposomes also 100 µg BSA/mL concentration presented a hemolysis percentage over 5. The higher values of hemolysis reported for NLPs were probably caused by oxidation of their lipidic layer.

Cell Viability

Carriers can be considered as new therapeutic strategy only if they are biocompatible. Biocompatibility was studied in terms of cell viability. Once injected in the body, nanoparticles get immediately in contact with blood and endothelial cells. For this reason, the cell viability of the two studied nanocarriers was assessed on human endothelial cells EA.hy926 by using MTS assay (Figure 14). PNPs obtained with the lower water internal phase volume of 1.5mL and BSA concentration of 40mg/mL (PNP_{BSA} (40 mg/mL)) were assayed. In the case of NLPs, those obtained with 50 mL of hydration volume and 6 mg/mL of BSA concentration (NLP_{BSA} (6 mg/mL)) were chosen. These two samples were chosen since PNP_{BSA} (40 mg/mL) and NLP_{BSA} (6 mg/mL) represented the best compromise between the BSA release and the above-reported hemolytic properties among all the different prepared samples. They also represent the best condition for BSA EE and possess a good control over MD and PSD.

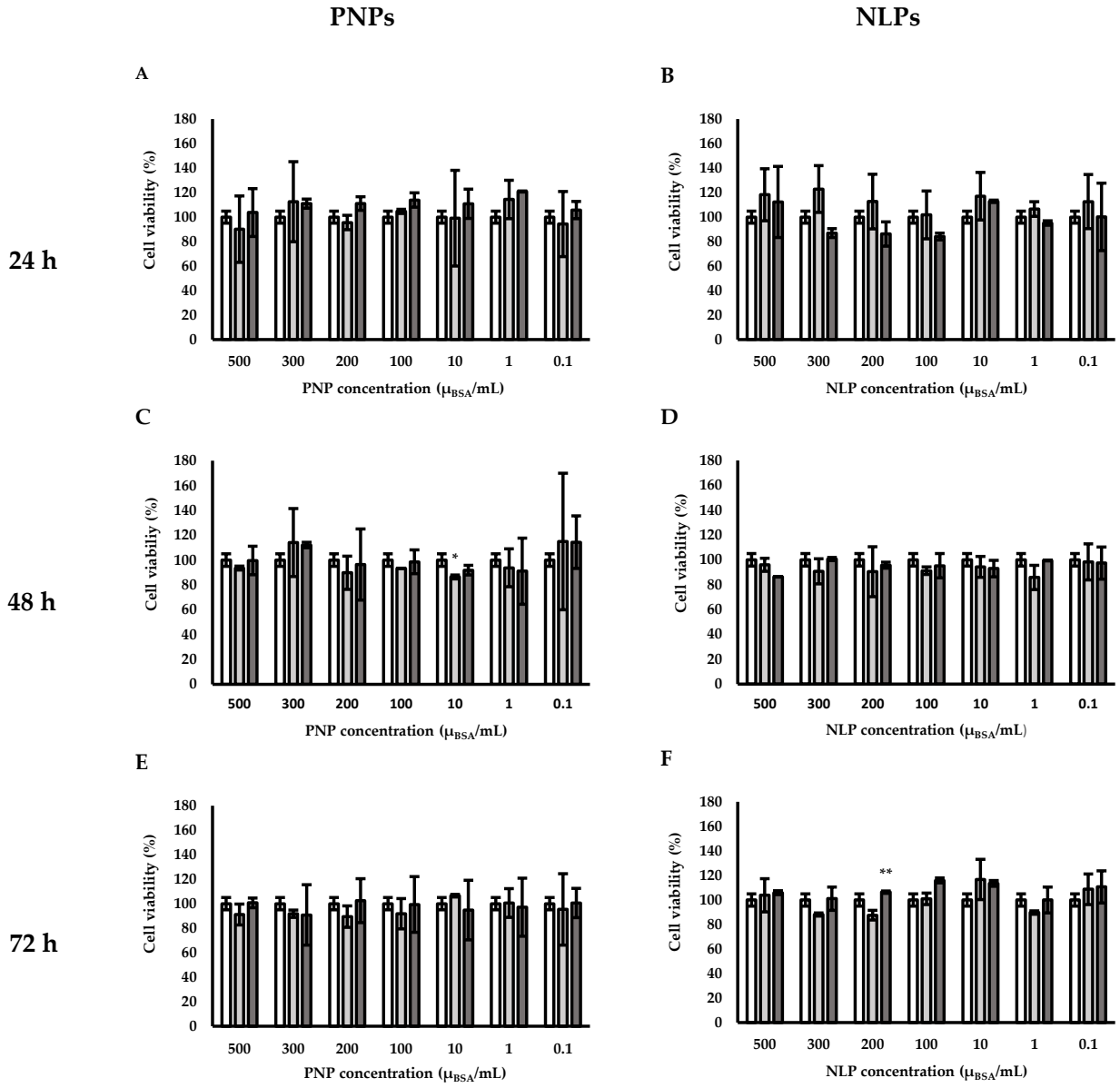

Figure 14: Cell viability of PNPs and NLPs by MTS assay after (A and B) 24, (C and D) 48 and (E and F) 72 hours. ☐ control, ▒ PNP_E (A, C, and E), ■ PNP_{BSA} (40mg/mL) (A, C, and E), ▒ NLP_E (B, D, and F), ■ NPL_{BSA} (3 mg/mL) (B, D, and F). PNPs: polymeric nanoparticles, PNP_E: empty polymeric nanoparticles, PNP_{BSA}: BSA-loaded polymeric nanoparticles, NLPs: nanoliposomes, NLP_E: empty nanoliposomes, NLP_{BSA}: BSA-loaded nanoliposomes.

PNPs present good biocompatibility for all the tested concentrations (0.1, 1.0, 10, 100, 200, 300, and 500 µg BSA/mL) and for all the duration of the experimentation (24, 48, and 72 h). No statistical differences were observed between the untreated (control) and the cells treated with PNPs for all the tested concentrations both for empty and for BSA-loaded nanocarriers. Similar results were obtained working with NLPs. No significant statistically differences were highlighted when

comparing cells treated with the same concentration of NLPs over time (24, 48, and 72 h). Furthermore, none of the tested NLP concentration caused any significant statistically decrease in cell viability at each time point. For both PNPs and NLPs, no statistically significant differences were noticed among different concentrations of the same nanocarriers at the same time point, at the same concentration, among different time point for both empty and loaded nanocarrier. One exception was the statistically differences between control and PNP_E at 10 µgBSA/mL after 48 h of treatment (Figure 14C) and between NLP_E and NLP_{BSA} (6 mg/mL) at 200 µgBSA/mL after 72 h of treatment (Figure 14F).

Conclusion

In this preliminary work, poly (lactic-co-glycolic acid)-based nanoparticles (PNPs) and phosphatidylcholine-based nanoliposomes (NLPs) were produced by a solvent emulsification evaporation method, based on a water/oil/water double emulsion technique, and a thin-film hydration method, respectively. Bovine serum albumin (BSA) was chosen as model protein to be easily replaced by specific therapeutic proteins useful for CVD treatment and was successfully encapsulated in both PNPs and NLPs, varying the volume of the internal aqueous phase. The two studied nanocarriers showed comparable mean size, particle size distribution, and morphological properties in terms of dimension and overall 3D structure. PNPs showed higher entrapment efficiencies presenting a maximum value of 98.01 ± 0.05%. Regarding BSA release, the two studied nanocarriers showed a different release profile: PNPs have released 11.53 ± 0.06% while NLPs have released 4.61 ± 0.02% of the encapsulated BSA after 12 days. In both the cases, considering the amount of released BSA, a burst release of the entrapped protein was avoided. The obtained results show that all the studied concentrations of PNPS have not induced erythrocyte membrane damages. Unlike PNPs, NLPs presented a hemolytic activity at all the concentrations higher than 10 µgBSA/mL. Both PNPs and NLPs showed a comparable biocompatibility with human endothelial cells. Based on

the obtained data, the choice of the better nanosystem strictly depends on the PNPs or NLPs final application. However, the studied nanocarriers can be considered as a good template to be engineered with antibodies on their surface to be employed in the vascular field as a nanosystem for protein drug delivery.

Future perspectives of this work will involve the engineering of the produced carriers by the decoration of the particle surfaces with specific antibodies to impart a peculiar targeting for atheromatous sites.

Chapter 2

Looking at that results obtained a deeply studied was performed on polymeric-based nanoparticles, this part of work was performed in collaboration with the Instituto de Investigação e Inovação em Saúde da Universidade do Porto in Porto, Portugal under Professor Bruno Sarmento's supervision.

Introduction

Bevacizumab (BEV) is a monoclonal antibody, usually used against several types of tumour like breast cancer or colorectal cancer, blocking the extracellular vascular endothelial growth factor (VEGF), specifically acting on the VEGF-A isoform[69]. This factor is extensively present in the carotid atherosclerotic plaques and its inhibition can be considered as a promising way to reduce the plaque neovascularization with a consequent decrease of the related risks[70].

In general, to improve the pharmacological properties of drugs, a possibility is their entrapment in nanoparticles (NPs). Indeed, these nanotools result useful for the delivery of therapeutic compounds bypassing their direct catabolism and maintaining unaltered their pharmacological activity thus making it possible to be active at the target site. A good candidate for nanoparticle production is represented by poly (lactic-co-glycolic acid) (PLGA) which is an Food and Drug Administration (FDA)-approved polymer largely used in nanomedicine[71]. Furthermore, the possibility to functionalize nanoparticle surface represents a hotspot of the actual nanomedicine. Coating agents include natural polymers, i.e. dextran, poly-L-arginine, and artificial polymers, i.e. poly-(diallyl dimethylammonium chloride) and poly-(allylamine hydrochloride). The coating exhibits different roles, such as being responsible of a sustained release over time [72], of a prolonged circulation eluding the reticuloendothelial system [73], impart a desirable surface charge, an improved stability and stimulate an enhanced cellular uptake[74]. Among the recently proposed

strategies to increase the nanoparticle shelf-life, one is the use of poly (ethylene glycol) (PEG) as coating agent which, in addition, can allow the functionalization of the coated surface with a resulted accuracy of drug release delivery in the active site [75].

The surface functionalization of nanoparticles consists of grafting of their surface with specific guide molecules, such as antibodies[76], ligands [77], and receptors[78].

Immunouteroglobin-1 (IUG1) is a human recombinant antibody (scFv) specific for extra-domain B (EDB) of fibronectin, a well-known marker of angiogenesis [79]. This protein is up-regulated in the extracellular matrix during tissue remodelling and it is over-expressed in atherosclerotic plaque as produced by activated macrophages [58] [80]. For these reasons, it can be considered as a good candidate to guide nanoparticles at the pathological site.

To the best of our knowledge, in this work it is proposed for the first time the encapsulation of BEV in PLGA-based nanoparticles functionalized using a PEG coating and a subsequent IUG1 grafting on the NPS surface as an innovative vascular drug delivery system. The aim of this study is, the production of PLGA-PEG nanoparticles loaded with BEV and functionalized with IUG1. the produced nanosystems are then characterized by morphological, chemico-physical characterization, and *in vitro* validation with EA. hy926 human endothelial cell line and human red blood cells.

Materials and methods

Chemicals

Poly (lactic-co-glycolic acid) (PLGA, 50:50, Mw 44.000) was offered by CorbionPurac Biomaterials (Amsterdam, Netherlands), poly (lactic-co-glycolic)-b-poly (ethylene glycol)-COOH (PLGA-PEG-COOH, Mw 5.000-40.000) was purchased from PolySciTech (Akina Division, Inc. West Lafayette, IN,

U.S.A.). The surfactant poly (vinyl alcohol) (PVA) (Mw 30.000-70.000), 1-ethyl-3-(3-dimethylaminopropyl) carbodiimide hydrochloride (EDC), N-hydroxysuccinimide (NHS), 2-(N-morpholino) ethanesulfonic acid (MES), Triton X-100, and penicillin/streptomycin for cell culture were acquired from Sigma-Aldrich (St. Louis, MO, U.S.A.). Bevacizumab (Avastin®) (BEV) was kindly given by the pharmacy of Centro Hospital do Porto, Portugal, while immunouteroglobin-1 (IUG1) was gently provided by Sirius-biotech S.r.l. (Genoa, Italy). Dichloromethane (DCM) from Fisher Scientific (Waltham, MA, U.S.A.) was used to dissolve PLGA and PLGA-PEG-COOH. The Amicon centrifuge filters (100 kDa MWCO) were acquired from Merck (Darmstad, Germany) and the micro bicinchoninic acid (BCA) protein assay kit (Thermo Fisher Scientific, Waltham, MA, U.S.A.) was used in order to quantify the proteins for calculating the encapsulation efficiency and for the in vitro release studies.

The human endothelial cell line EA.hy926 (ATCC® CRL-2922™), the 3-(4,5-dimethylthiazol-2-yl)-5-(3-carboxymethoxyphenyl)-2-(4-sulfophenyl)-2H-tetrazolium (MTS) (CellTiter 96® AQueous One Solution Cell Proliferation Assay, Promega, Madison, WI, USA), the cytotoxicity detection kit PLUS (LDH) (Roche Diagnostics, Florham Park, NJ, U.S.A.) and CyQUANT™ NF cell proliferation (Life Technologies, Carlsbad, CA, U.S.A.) were used to study cell viability.

All the reagents for cell culture, including fetal bovine serum (FBS), Dulbecco's Modified Eagle's Medium high glucose w/o L-glutamine w/o sodium pyruvate (DMEM), trypsin, and phosphate buffered saline (PBS) were purchased from Carlo Erba (Milan, Italy).

Preparation of PLGA nanoparticles

The technique used to prepare PLGA-PEG nanoparticles (NPs) was the water/oil/water double emulsion, with a ratio of 9:1 (w/w) of PLGA and PLGA-PEG-COOH. The total PLGA was dissolved in 1.0 mL of DCM for 20 minutes at room temperature (25 ± 2 °C)[81]. Then, 80 µL of the aqueous

inner phase, in which BEV was dissolved, was added and the obtained solution was homogenized for 30 seconds using a Vibra-Cell™ ultrasonic processor with 70% of amplitude. At the end of the first sonication the primary emulsion water/oil was obtained. After that, 4.0 mL of a PVA solution (2%, w/v), as surfactant, was added to the first homogenized solution primary emulsion and sonicated again under the same conditions reported above in order to have the second emulsion obtain the water/oil/water. Then, the produced emulsion was diluted using 7.5 mL of the same surfactant solution was added and left under magnetic stirring at 300 rpm in a fume hood for at least 3 hours to allow the organic solvent evaporation at room temperature. This final solution NPs suspension was washed with ultrapure water three times by centrifugation at 40.000 × g for 30 minutes at 4 °C, using a Beckman Avanti J26 XPI ultracentrifuge (Beckman Coulter, Brea, CA, U.S.A.). During After the third centrifugation, the formulation was dispersed in ultrapure water again at the desired concentrations. Both empty and BEV loaded NPs were produced. In the case of empty nanoparticles (NPE). Two types of NPs were obtained through this method: 80 µL of PBS were used as water internal phase; whereas, in the case of BEV loaded nanoparticles (NPBEV) or 80 µL of a BEV solution of at 25 mg/mL concentration were added to empty used as water internal phase. nanoparticles (NPE) or to loaded nanoparticles (NPBEV), respectively[82].

Functionalization of PLGA nanoparticles with immunouteroglobin-1

The conjugation of the NPs with immunouteroglobin-1 (IUG1) was obtained using the coupling reaction in the presence of EDC and NHS. First, NPs were washed three times with ultrapure water at 40.000 × g for 30 minutes at 4 °C, using the same centrifuge reported above, then the sample obtained from the last centrifuge was dispersed using a MES buffer with a pH= 5.0. EDC (0.1 M) and NHS (0.4 M) were added to this suspension with the aim of inducing the activation of the NPs and left for 1 hour at room temperature under mild agitation. Afterwards, the nanoparticles suspension was centrifuged to remove the reagents in excess, dispersed in PBS, and then 10 µL of IUG1 (2.0

mg/mL) was added to 1.0 mL of activated NPs, and left at 4 °C for 24 hours after homogenization. The functionalized NPs (IUG-1 NPs) were centrifuged using the same conditions above and the surnatant was collected for the ensuing analysis [83][84]. Performing this superficial modification, two types of nanoparticles were obtained: empty and BEV-loaded nanoparticles both functionalized with IUG1 (IUG1 NPE and IUG1 NPBEV, respectively).

Characterization of nanoparticles

Particle size and zeta potential

Once produced, all formulations were characterized in terms of average particle size, polydispersity index (PDI), and average ζ-potential by dynamic light scattering, using a Malvern Zetasizer Nano ZS instrument (Malvern Instruments Ltd, Welcheister, UK). For all the samples, three replicates were opportunely diluted in ultrapure water and before the analysis.

Bevacizumab association efficiency and IUG1 conjugation efficiency

The association efficiency (AE) was calculated using an indirect method. The amount of free BEV in the supernatant was obtained after centrifugation of the samples at the same conditions and with the same centrifuge reported above. The concentration of free BEV in the supernatant was detected by using the micro BCA protein assay, following this equation (3):

$$\mathrm{AE}\ (\%) = \frac{total\ amount\ of\ BEV - free\ BEV\ in\ supernatant}{total\ amount\ of\ BEV} \times 100$$

Similarly, conjugation efficiency (CE) was calculated using the micro BCA assay as follows, using the supernatant of functionalized nanoparticles, (equation 4)

$$\mathrm{CE}\ (\%) = \frac{total\ amount\ of\ IUG - free\ IUG\ in\ supernatant}{total\ amount\ of\ IUG} \times 100$$

Transmission electron microscopy

Transmission Electron Microscopy (TEM) analyses were performed to study the morphology of the NPs. The samples were washed with ultrapure water three times to eliminate the excess of surfactant at 40.000 × g for 30 minutes at 4 °C. One drop of the formulation to be analyzed was fixed in a grid and observed using a JEOL JEM-1400 TEM electron microscope (JEOL Ldt, Tokyo, Japan) after a treatment with uranyl acetate. All the obtained samples were studied using TEM.

In vitro bevacizumab release study

The NP_{BEV} loaded NPs suspensions were washed at the same conditions reported above to eliminate the non-encapsulated BEV still present in the supernatant. Then, NPsBEV were dispersed in 15 mL of PBS at pH= 7.4 and incubated at 37 °C under shaking condition (100 rpm). At determined time points (1, 2, 8, 24, 48, 72 and 168 hours), aliquots of 0.5 mL were taken and replaced with fresh PBS. The procedure was made in triplicate and the amount of released BEV was detected using the micro BCA protein assay.

ATR-FTIR analysis

After a freeze dryer cycle, the surface of all NPs was studied using Fourier Transform Infrared Spectroscopy (FTIR) equipped with a single reflection attenuated total reflectance (ATR) accessory. The IR spectra were acquired in the range of 4000-400 cm^{-1} and the accumulation of 32 scans with a resolution of 4 cm^{-1}. All the spectra areas were normalized for comparison purposes by using Origin 8 software (OriginLab Corporation, Northampton, MA, U.S.A.). All the samples were analysed in triplicate.

Circular Dichroism analysis

Circular Dichroism (CD) analysis was conducted to detect the secondary structure of the loaded drug. A Jasco J815 CD spectrophotometer (Jasco Incorporated, Easton, U.S.A.) was used to perform the analysis. The spectra were obtained working from 200 to 260 nm using a 0.1 cm cell, a bandwidth of 1 mm, a data pitch of 0.5 nm, a data integration time of 2 seconds, and a scanning speed of 50 nm/min. The CD spectrum of the buffer was subtracted to that of the sample and it was smoothed using 10 Savitzky-Golay points before conversion to absolute CD values. This analysis was performed by using native BEV, denatured BEV, and released BEV. The studied monoclonal antibody was thermally denatured following the protocol described by Sousa et al.[82] For native and denatured BEV, a solution of 0.150 mg/mL was used whereas denatured released BEV was obtained after 1 and 168 hours of IUG1 NPBEV incubation.

Cell viability

EA.hy926 human endothelial cells were cultured in DMEM supplemented with 10% (v/v) of FBS, 1% (v/v) of penicillin/streptomycin and grown at 37 °C and 5 % CO_2 until 70 % of confluency was reached. To investigate the cytocompatibility of the four different prepared nanoparticles, 4 x 10^3 cells were seeded in each well of a 96-well plate and incubated overnight before any treatments. Different concentrations (0.1, 1, 10, 100 µg/mL) of encapsulated BEV were tested. This analysis was performed by using NPE, NPBEV, IUG1 NPE, and IUG1 NPBEV after 24, 48, and 72 hours of cell incubation with the nanoparticles. For NPE and IUG1 NPE, cells were treated with an equal amount of NPBEV and IUG1 NPBEV, respectively, for each studied concentration. Control was represented by non-treated endothelial cells (without nanoparticles).

For the MTS assay, 20 µL of reagent was added to each well, incubated as mentioned above and after 3 hours, the absorbance of the samples was read at 490 nm using a multi-plate reader (Tecan

Spark® 20M, Tecan, Männedorf, Switzerland). Cell viability was calculated as percentage in respect with the control (100%).

For LDH assay, 100 µL of reagent was added to the supernatant of each well and incubated for 1 hour in dark condition. Then, the absorbance of the samples was read at 490 nm and 690 nm for background deduction. The positive control was represented by cells treated with Triton X-100 (1 %, v/v) whereas the untreated cells were the negative one.

Proliferation assay was performed following the manufacturer's instruction. Cell viability was calculated as percentage in respect with the control (100%).

Murine monocyte derived macrophage cell line RAW264.7 were cultured with RPMI-1640 medium supplementary with 10% (v/v) of FBS, 1% (v/v) of penicillin/streptomycin, 1% (v/v) of glutamine and grown at 37 °C and 5 % CO_2 until 70 % of confluency was reached. To analyse the cytocompatibility of the functionalized nanoparticles (IUG1 NPE, and IUG1 NPBEV) at the four concentration (0.1, 1, 10, 100 µg/mL of encapsulated BEV) 5 x 10^3 per well was seeded in a 96 well plate. The MTS assay was performed as describe above for the EA.hy926 human endothelial cells.

Confocal fluorescent microscopy imaging

Confocal imagines of RAW 267.4 were obtained using FV500 (Fluoview confocal Laser Scanning Microscope System, Olympus Europe GMBH, Hamburg, Germany) analyzed with FluoView 4.3b computer program (Olympus). Cells were seeded on a cover slip with IUG1 NP BEV in the 100 µg/mL (of encapsulated BEV) concentration. After 24 hours and 48 hours cells were washed with PBS, and fixed with paraphormaldehyde (PAF) at 2% for 5 min. Actin were stained with phalloidin (Thermo Fisher Scientific, USA) while nanoparticles were prepared using PLGA labelled with fluorescein (Sigma-Aldrich, USA)

Hemolysis

Blood obtained from healthy volunteers was collected in test tubes with ethylenediaminetetraacetic acid (EDTA) as anticoagulant agent following the Guidelines of the European Community Council in accordance with the Nuremberg Code (Directive 2004/23/EC). To separate the red blood cells (RBC) from the plasma, blood was centrifuged three times for 10 minutes at 870 × g (centrifuge SL 8, Thermo Fisher Scientific, Osterode, Germany). Pellet was washed with PBS three times. The samples were then added to the erythrocytes reaching a final volume of 150 µL for each concentration and left under agitation at 25°C for 2 hours (orbital shaker-incubator ES-20, Grant-bio, Grant Instrument Ltd., Shepret Cambridgeshire, Great Britain). After that, the samples were centrifuged for 5 minutes at 870 × g (centrifuge Z 216 MK, HERMLE Labortechnik GmbH, Wehingen, Germany). The supernatants were read at 540 nm by using the same plate reader mentioned before.

The hemolysis was calculated in percentage using the following equation (5):

$$\text{Hemolysis}(\%) = \frac{experimental\ value - negative\ control\ value}{pisitive\ control\ value - negative\ control\ value} \times 100$$

The negative control was represented by RBC treated with PBS while the positive one was treated with deionized water to induce RBC membrane breakage.

Statistical analysis

All the experiments were done at least in triplicate and the results are expressed as mean values + standard deviation. The statistically significant differences among results were put in evidence by the analysis of variance (ANOVA) with the Tukey's post-hoc test. Data were analysed by the Statistica v 8.0 software (StatSoft, Tulsa, OK, USA).

Results

Production of loaded and functionalized nanoparticles

Table 2: MD, PDI, ζ-potential, AE, and CE of NPE, NPBEV, IUG1 NPE, and IUG1 NPBEV. Results are expressed as mean ± standard deviation. Different letters (a and b) and (c and d) reported in the MD and in ζ- potential column, respectively, refer to statistically significant differences among the four different samples ($p < 0.05$) by ANOVA with Tukey's HSD post-hoc multiple comparison test. MD: mean diameter, PDI: polydispersity index, AE: association efficiency, CE: conjugation efficiency.

	MD (nm)	**PDI**	**ζ- potential (mV)**	**AE (%)**	**CE (%)**
NP_E	217.33 ± 1.25[a]	0.223 ± 0.020	-21.5 ± 0.252[c]	-	-
NP_{BEV}	225.60 ± 1.85[a]	0.221 ± 0.010	-20.7 9± 0.425[c]	77.12 ± 1.19	-
IUG1 NP_E	252.50 ± 2.90[b]	0.164 ± 0.031	-7.97 ± 0.448[d]	-	57.53 ± 0.008
IUG1 NP_{BEV}	265.47 ± 3.45[b]	0.247 ± 0.010	-8.11 ± 0.515[d]	74.35 ± 1.30	60.83 ± 0.048

The NP_E and NP_{BEV} were produced using emulsification-evaporation method based on the double emulsion technique. These NPs were functionalized by using IUG1, obtaining, respectively, IUG1 NPE and IUG1 NPBEV. All the formulations were characterized in terms of mean diameters, poly dispersity index (PDI), and ζ-potential (Table 2). Looking the mean diameter is possible to notice a non-statistical difference between the empty and the loaded NPs increased moreover a statistical difference is observable once immobilized the IUG1 probably due for the presence of the scFv both empty and loaded , PDI went was in the range between 0.164 and 0.247, and the ζ-potential decreased with the presence of the antibody, probably because of the less exposition of COOH groups exposed from the PEG involved in the link with IUG1, as reported in literature reinforcing the

hypothesis of occurrent functionalization[85]. The association efficacy (AE) of NPBEV and IUG1 NPBEV were 77.00 ± 1.19 % and 74.00 ± 1.30 %, respectively. As reported by several studies, the double emulsion technique represents a good option for the encapsulation of monoclonal antibodies. The percentage of conjugation efficiency (CE) was for the IUG1 NPE and IUG1 NPBEV 57.00 ± 0.008 % and 60.00 ± 0.048 %, respectively.

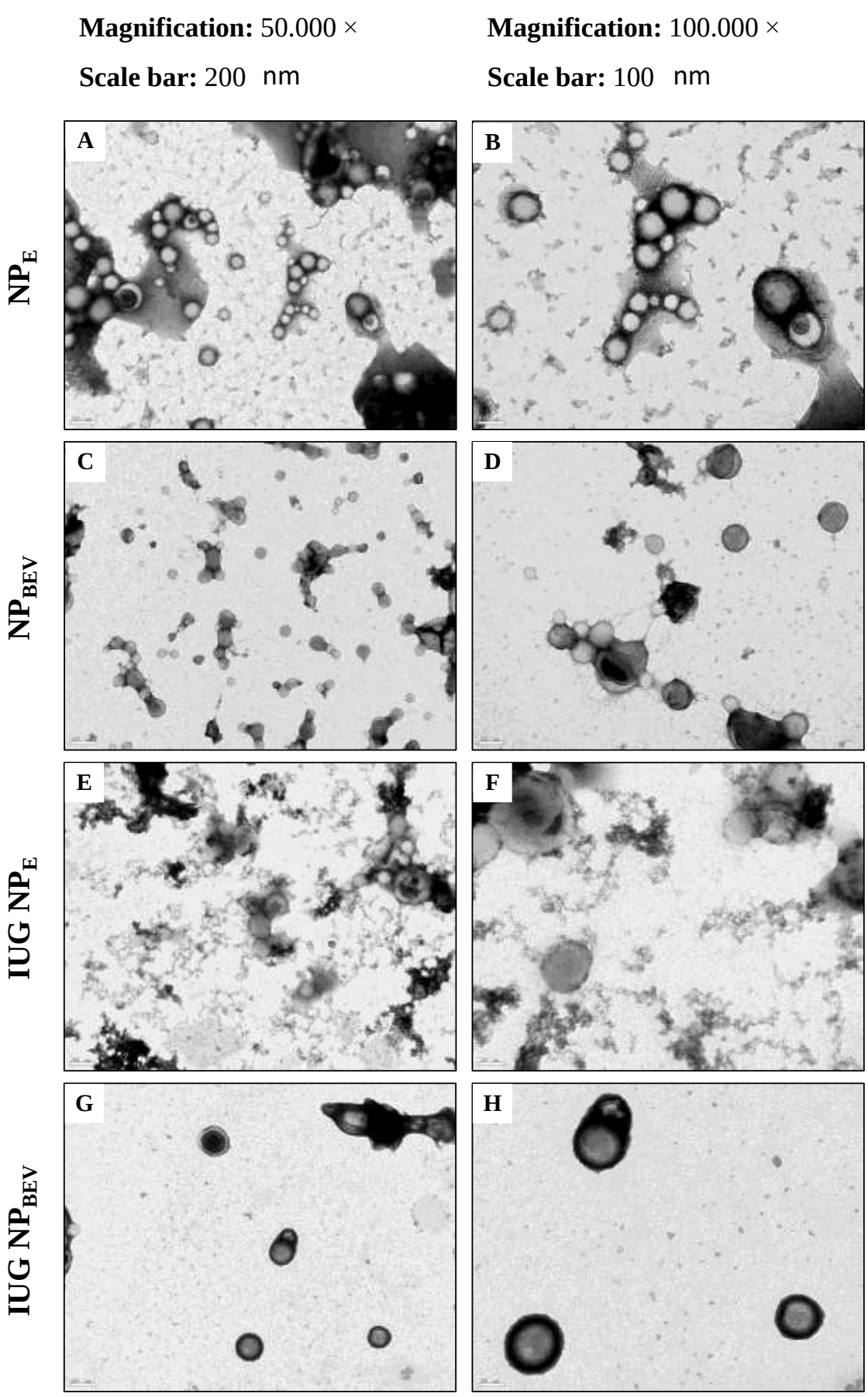

Figure 15. Representative TEM images of (A and B) NPE, (C and D) NPBEV, (E and F) IUG1 NPE, and (G and F) IUG1 NPBEV.

The shape of nanoparticles is an important characteristic to be investigated, as a spherical form is the easiest to be internalized by the target cells[86]. The images obtained using TEM confirmed the typical spherical shape of PLGA- based nanocarrier and the dimension of about 200 nm for all the studied samples. These data are in complete accordance with the results obtained with the DLS shown in Table 2. The BEV encapsulation as well as the immobilization of IUG1 did not interfere with the native shape of the PLGA NPs. Two different magnifications of the studied NPs are reported in Figure 15.

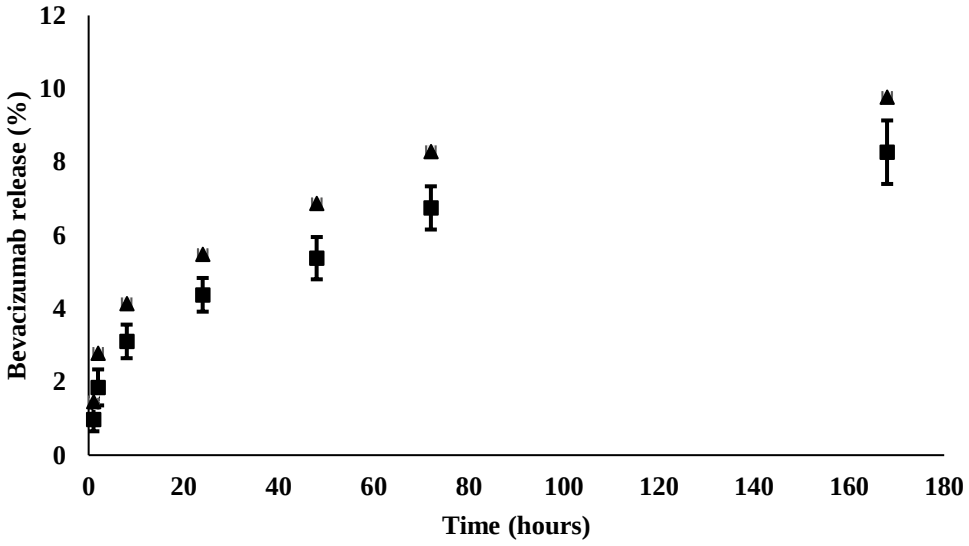

Figure 16. *In vitro* bevacizumab release profile from: (■) NP_{BEV} and (▲) IUG1 NP_{BEV}.

The use of PEG in the field of targeted drug delivery system is a popular strategy exhaustively described in the literature [60][87] since this concept has been introduced in 1970s [88]. PEG is a safe and FDA approved polymer: it is used to improve the circulation time of the nanoparticles in the blood streaming, in particular it has been demonstrating a reduced opsonization process with a consequent decrease number of required administration of the encapsulated drug [89]. The release of BEV was studied in vitro at 37° C for one week for both the produced samples of NPBEV and IUG1 NPBEV. The initial burst release was given by the presence of the residual drug absorbed on the nanoparticles surface. Looking at results reported in Figure 16, the release of BEV reached a

percentage of 8.260.50 ± 0.09 and 9.770.40 ± 0.04 after 168 hours in the case of NPBEV and IUG1 NPBEV, respectively (Figure 16). This low percentage of antibody release compared with the literature is probably due to the PEGylation of the studied carriers[90].

ATR-FTIR studies

To confirm the superficial immobilization of IUG1 on NPs, ATR-FTIR analysis was performed using native BEV, IUG1, and all NP formulations, results are shown in Figure 16. The peak at 1750 cm^{-1} is characteristic of PLGA and suggested the presence of a carbonyl group (C=O) [91]. The peak at 1660 cm-1[92] is characteristic of the chemical bond which identifies the amide bond C=N and that at 1380 cm -1 is characteristic of the aromatic amino group[93]. In the region from 1300 to 500 cm^{-1}, commonly known as "fingerprint", the profiles of the samples IUG1, IUG1 NPE, and IUG1 NPBEV are similar. These results proved the occurred functionalization of NP surface by IUG1.

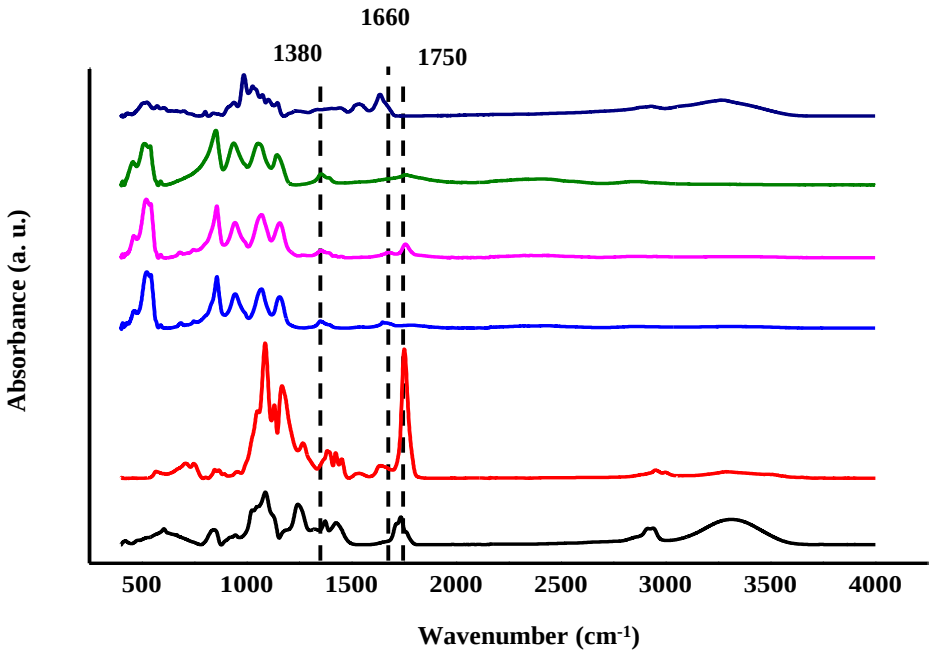

Figure 17. ATR-FTIR profiles of (▬) native bevacizumab, (▬) IUG1 NP_E, (▬) IUG1 NP_{BEV}, (▬) IUG1, (▬) NP_{BEV}, and (▬) NP_E.

Circular dichroism analysis

To study the stability of the secondary structure of BEV, CD analysis was performed. In Figure 18 the profiles of the native BEV, the thermally denatured form, the one BEV released after one hour and the 168 hours released BEV are reported. It is possible to notice that the released and the native form of BEV presented a comparable profile with a prevalence of β-sheet structure characterized by a maximum of the curve at 208 nm and a minimum of the curve at 215 nm in accordance with Varshochian et al.,[94] and Malakouti-Nejad et al., [95]. The thermally denatured BEV form presented a different CD profile. This result remarks the sustained release of the active form of BEV from NPs and demonstrated the potential of the formulation to protect this drug from the denaturation process.

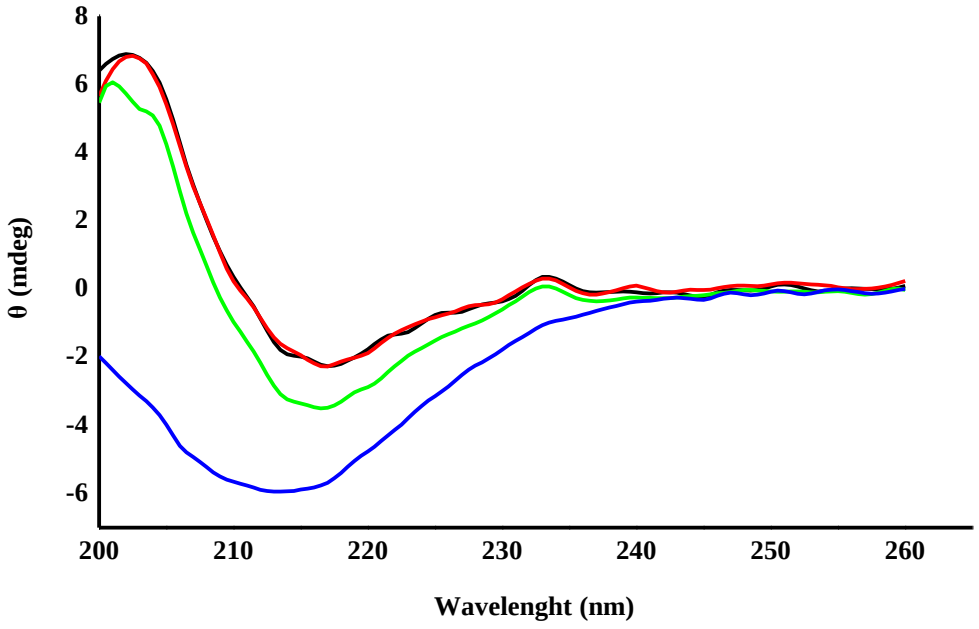

Figure 18. CD analysis of ( ) native BEV, ( ) denaturated BEV, ( ) BEV released after1 hour, and ( ) after 168 hours.

Cytotoxicity assay

A pivotal requirement of drug delivery systems is represented by their compatibility with living organisms. To validate them in a lab-scale in laboratory, different assays have been proposed over the last decade. In this work, in order to investigate the cytotoxicity of the studied nanoparticles with the EA.hy926 human endothelial cell line, three different assays have been performed: MTS, LDH, and DNA quantification. MTS assay provides information on the cellular mitochondrial activity[72].

The test was performed by using the four studied particles at the concentration of 0.1, 1, 10, and 100 µg/mL at fixed time (24, 48, and 72 hours). Considering results of Figure 19, it is possible to observe that for each day, no statistically differences were noticed considering the same concentration of each type of particle and the different concentration of each single type of particles in different days. In particular, in the case of IUG1 NPE a slight decrease of cell viability percentage was noticed only after 24 hours ($p < 0.05$), if compared with the other concentrations of the same sample. Furthermore, there were no differences between treated and non-treated cells, for each kind of sample, each concentration, and each time-point (Figure 19). Similar results were obtained by using LDH assay. In this case, it was measured the amount of LDH release from cells as indicator of cytotoxicity, results are reported in Figure 20. For all the tested concentrations and for all the time-points, considering each kind of particles, there were not statistically differences among the samples (Figure 20). Cell proliferation assay gives additional information regarding the biocompatibility of studied nanosystems. In accordance with MTS and LDH assay, even in this case no statistically significant difference among the four test samples, the four different concentrations and the three different time-points were noticed (Figure 21). Furthermore, a study of cytocompatibility on macrophage line RAW 247.6, was performed using the MTS assay. The analysis was conduct using the same nanoparticles concentration reported above for the same test on

endothelial cells, using the final functionalized PLGA-based nanosystem. Figure 22 shown the results obtained and no statistical difference were reported considering concentration of each type of particle and the different concentration of each single type of particles in different days. Moreover, there were no difference between the treated cells and no treated in all the time point, different concentration, and kind of sample.

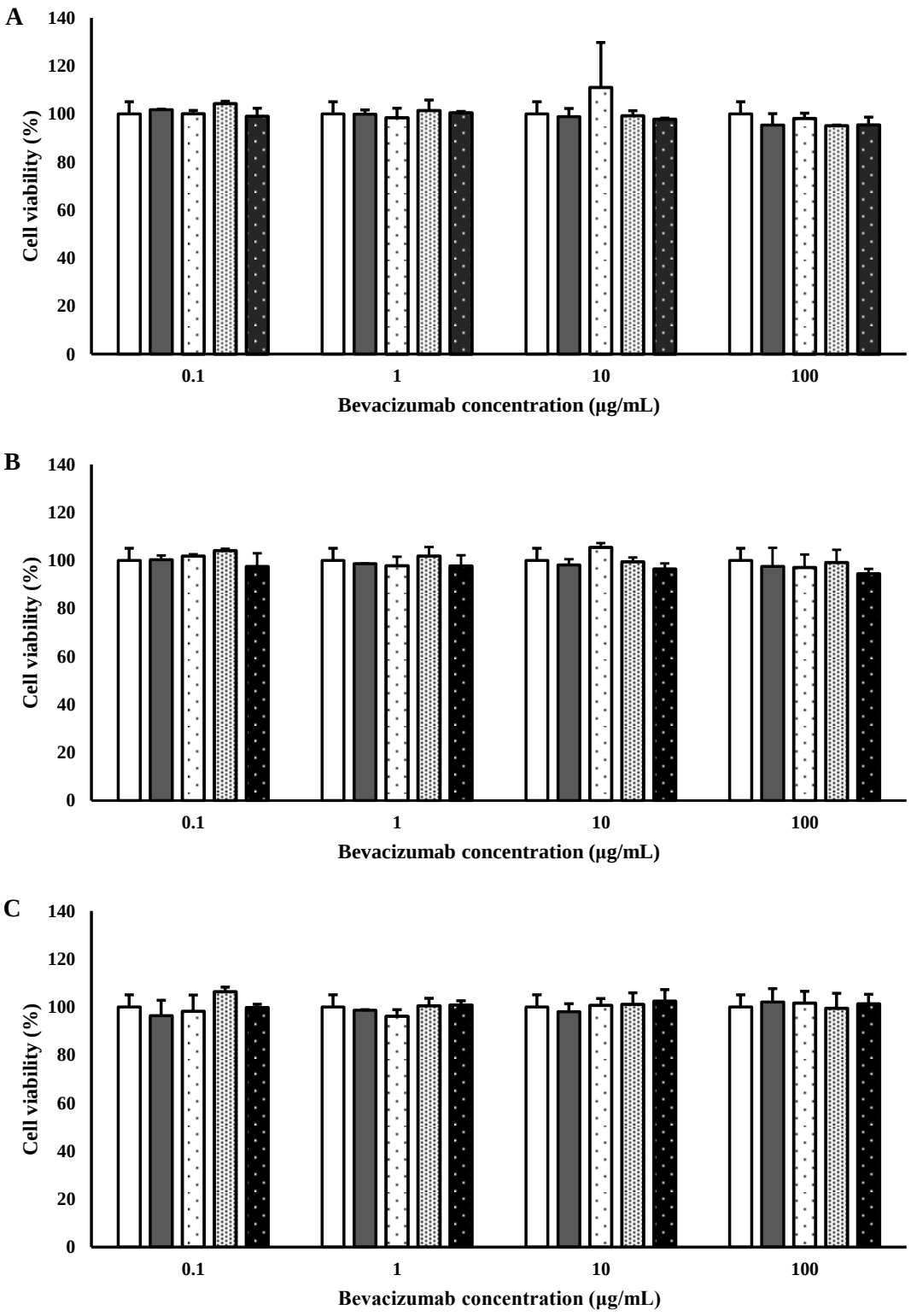

Figure 19. Cell viability on EAhy.926 of nanoparticles by MTS assay after (A) 24, (B) 48, and (C) 72 hours. Results are expressed as mean of three measurements + standard deviation. ☐ control, ■ NP_E, ⬚ NP_{BEV}, ▩ IUG-1 NP_E, ■ IUG-1 NP_{BEV}.

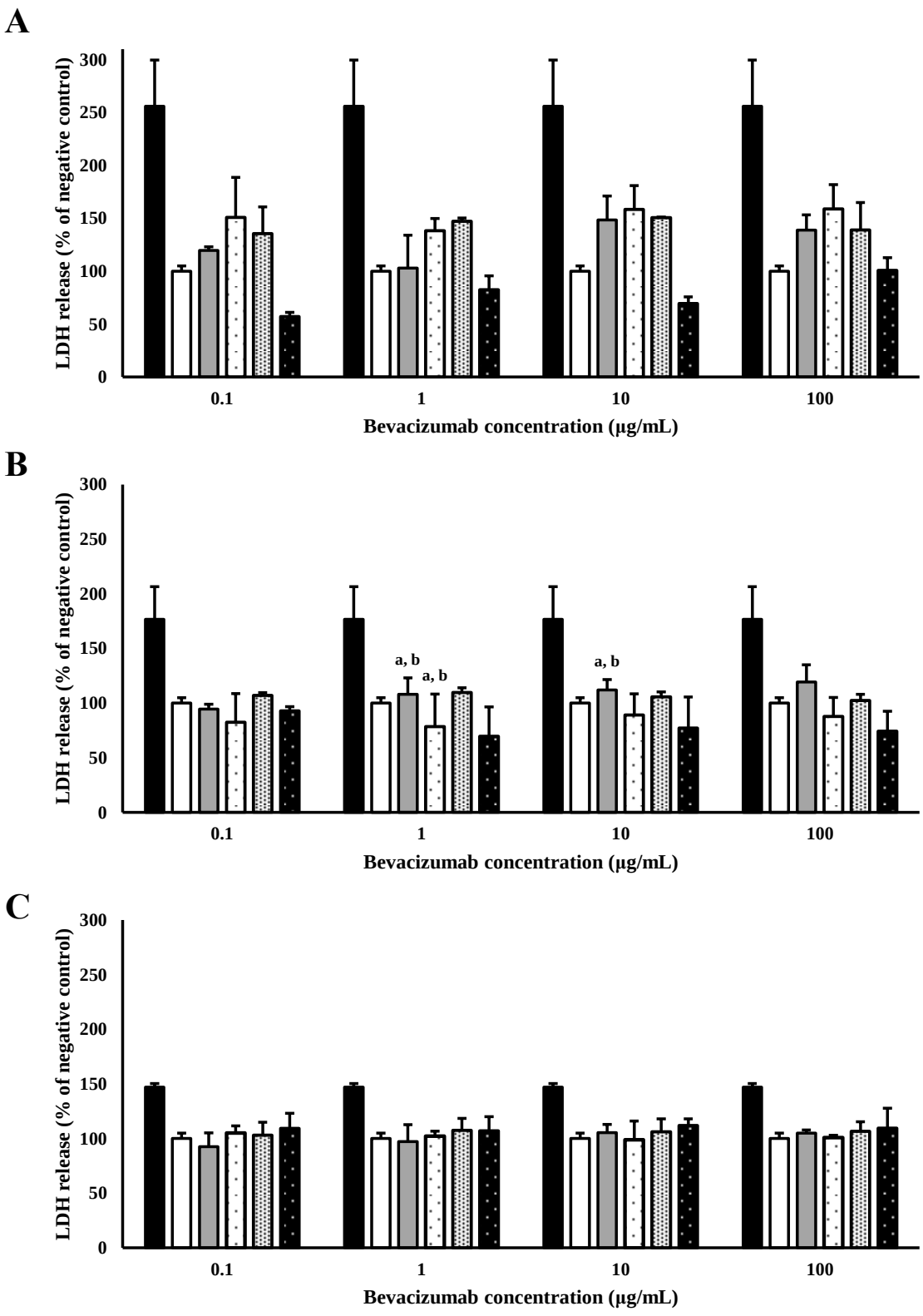

Figure 20. LDH release after (A) 24, (B) 48, and (C) 72 hours. Results are expressed as mean of three measurements + standard deviation. ■ positive control □ negative control, ■ NP_E, □ NP_{BEV}, ▩ IUG-1 NP_E, ■ IUG-1 NP_{BEV}. Different letters refer to statistically significant differences among results ($p < 0.05$, ANOVA with Tukey's HSD post-hoc multiple comparison test). $^{a, b}$: no statistically differences if compared with both positive and negative control.

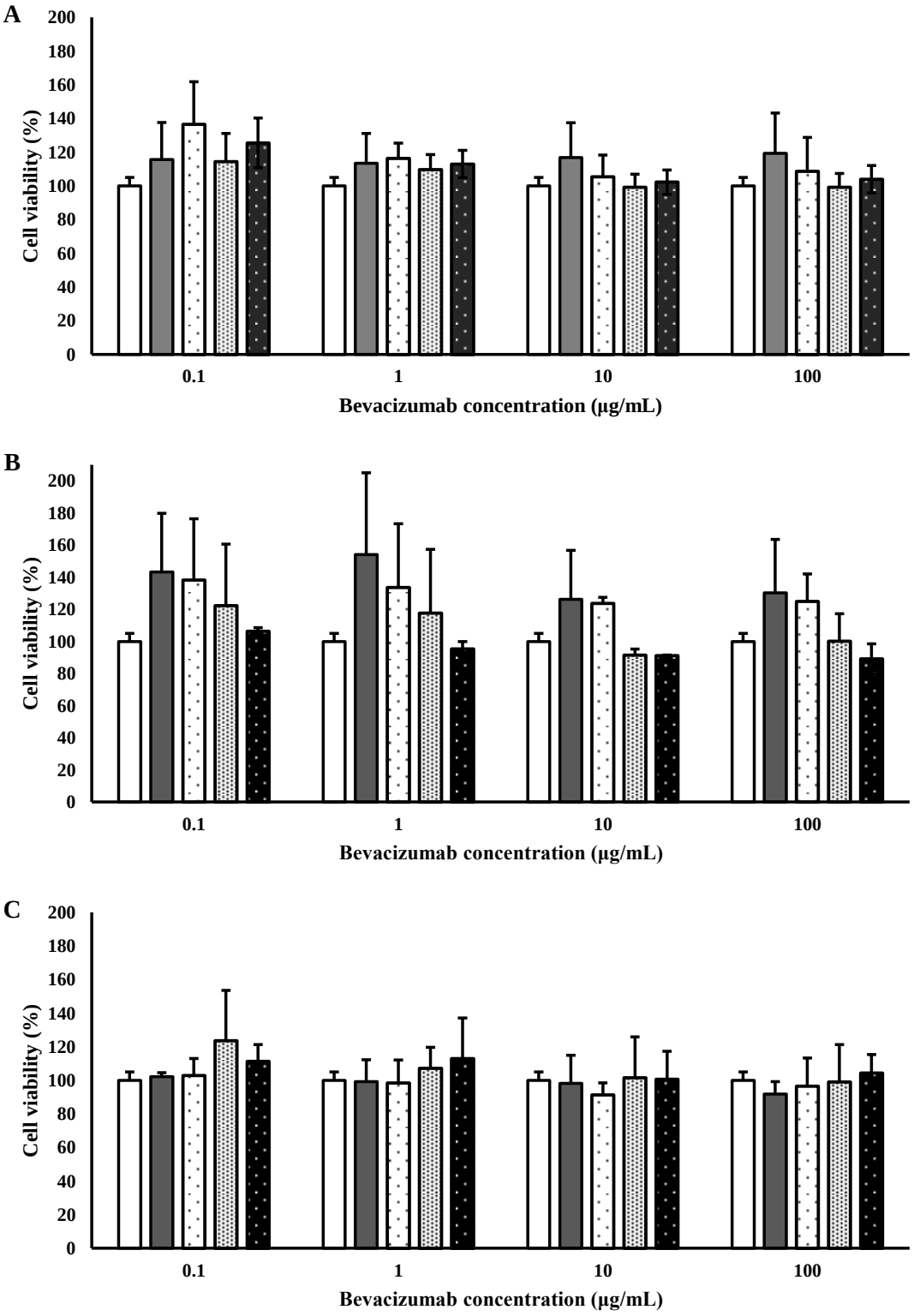

Figure 21: Cell viability on EAhy.926 of nanoparticles by DNA assay after (A) 24, (B) 48, and (C) 72 hours. Results are expressed as mean of three measurements + standard deviation. ☐ control, ■ NP_E, ⊡ NP_{BEV}, ▩ IUG-1 NP_E, ■ IUG-1 NP_{BEV}.

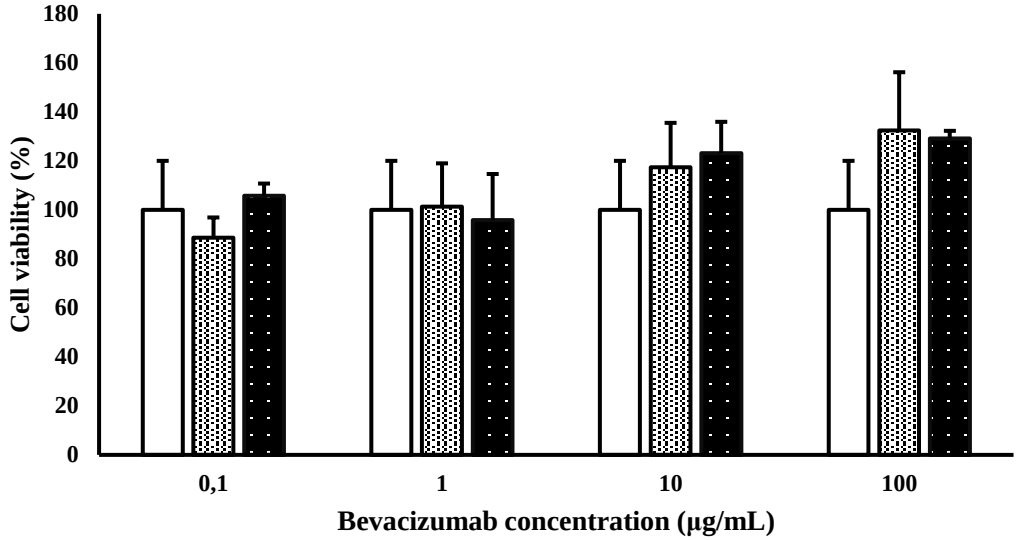

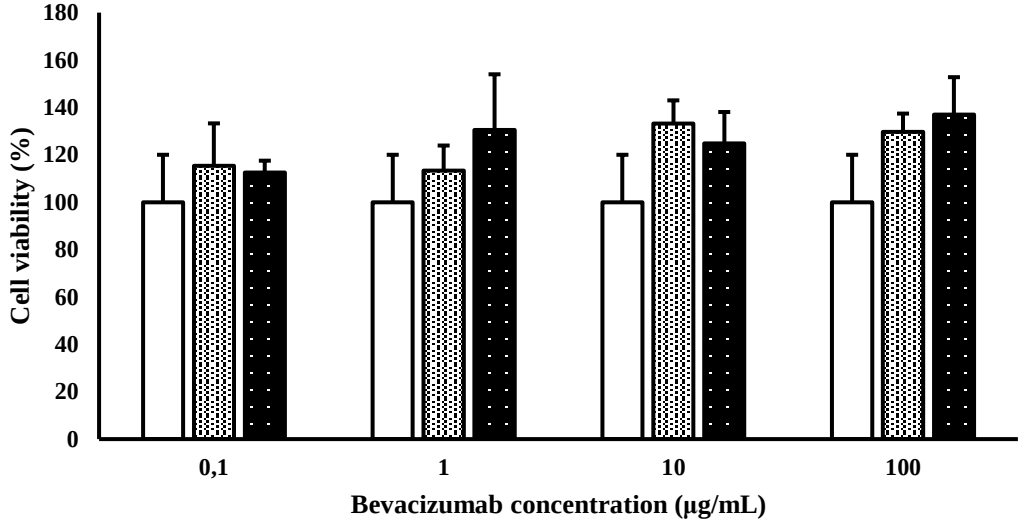

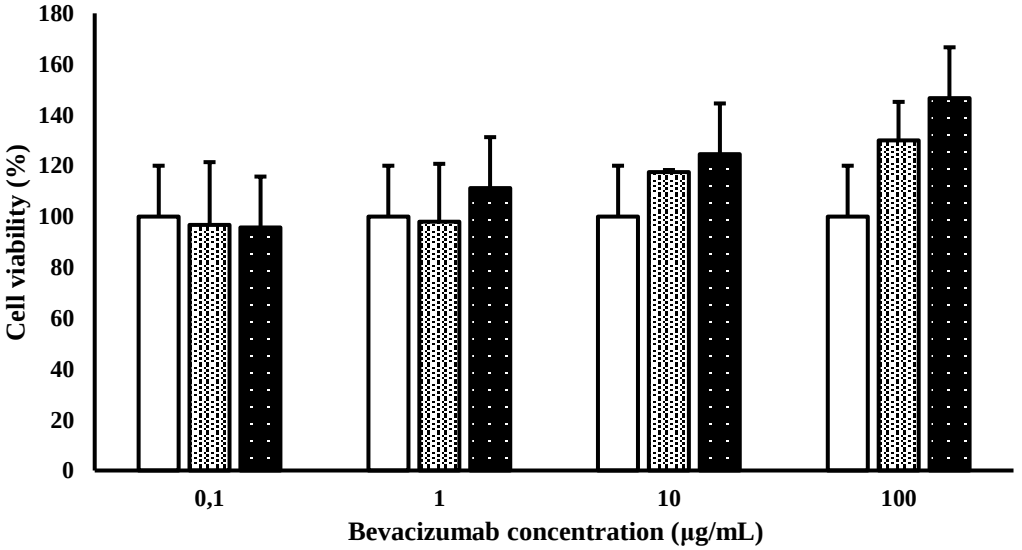

Figure 22: Cell viability on RAW 247.6 of nanoparticles by MTS assay after (A) 24, (B) 48, and (C) 72 hours. Results are expressed as mean of three measurements + standard deviation. ☐ control, ▩ IUG-1 NP_{BEV}, ■ IUG-1 NP_E.

Confocal fluorescent microscopy imaging

In order to deliver their therapeutic cargo, PLGA-based nanoparticles should cross the cells membrane and be uptake by macrophage. Therefore, the internalization of studied carriers was investigate assessed via confocal fluorescent microscopy. Figure 23 show representative confocal imagines of macrophage with two magnification, 20X and 40X, at two different time point, 24hours and 48 hours. It is notable that the nanoparticles after 24 hours are still in a peripherical cells area while after the 48 hours the nanoparticles are more internalized and located in an inner cell region.

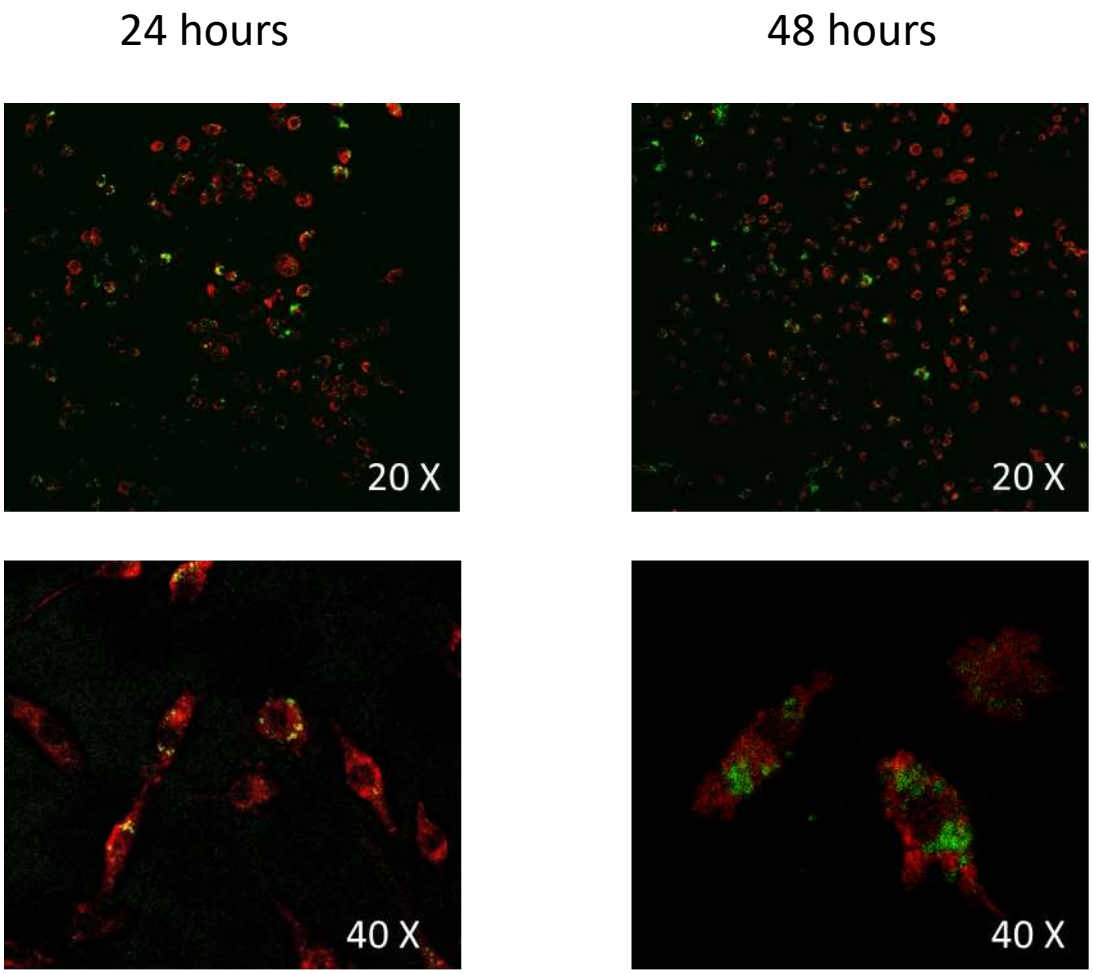

Figure 23. Representative confocal images of RAW 264.7 cellular line expose to IUG-1 NPBEV at different time points (24h and 48h).

Hemolysis assay

One key assay to consider a nanosystem as hemocompatible is represented by hemolysis assay in which haemoglobin released due to the breakage of red blood cell (RBC) membrane is measured [96]. The interaction of nanosystem with RBC depends on different characteristics of NP, i.e. surface charge, surface hydrophilicity, geometry, porosity, and surface engineering with specific molecules of chemical functional groups[97]. In the case of the breakage of red blood cells, haemoglobin is released. The quantification of this protein by using spectrophotometry is a valid method to study hemolysis percentage. For this assay, four concentrations of the different types of nanoparticles were studied. A condition to consider hemocompatible a material is a hemolysis percentage lower than 5 % and in this case it is considered non-hemolytic (American Society for Testing and Materials International) (ASTM, 2013). For all the tested concentrations and considering all the different studied samples, a hemolysis percentage lower than 5 % was found, as it is possible to see from (Figure 23). The presence of IUG1 on the nanoparticle surface did not induce a different hemolytic activity of NP for the tested concentrations of 0.1 and 1 µg/mL. In the case of 10, IUG-1 NPE showed a statistical significant higher hemolysis percentage, still lower than 5 %. For NPE and NPBEV, it can be noticed that the highest concentration tested (100 µg/mL) induced a higher hemolysis percentage ($p < 0.05$ and $p < 0.001$, respectively). In addition, the hemolysis percentage was higher ($p < 0.05$) in the presence of 10 and 100 µg/mL IUG-1 , both for NPE and NPBEV in comparison with the lowest studied concentrations (0.1 and 1 µg/mL). Expect these statistical differences, all the samples showed a hemolysis percentage lower than 5, guaranteeing the possibility to inject them in vivo without inducing lysis of erythrocytes.

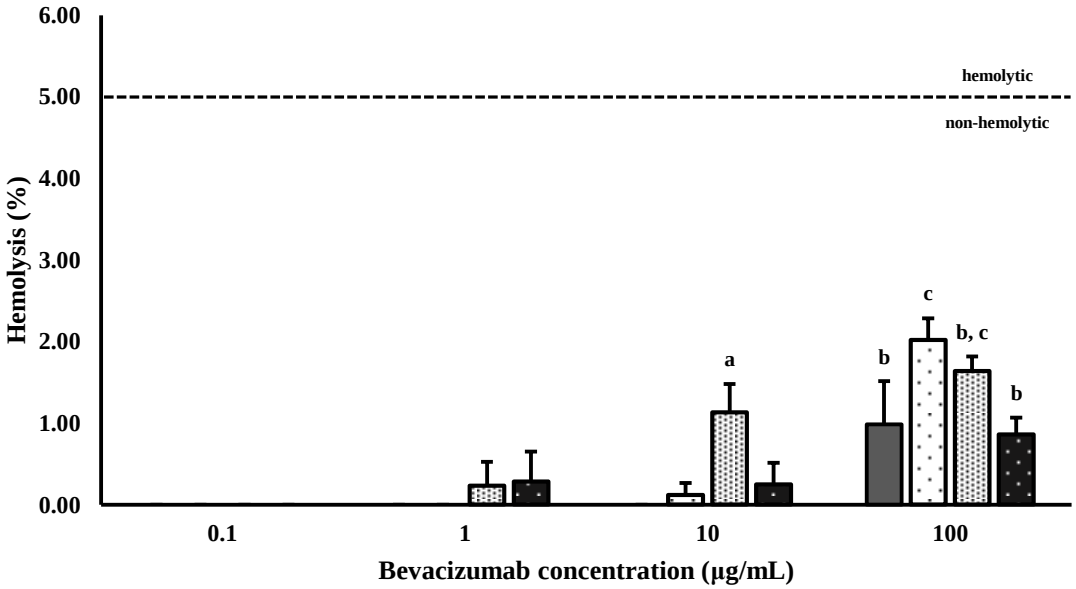

Figure 24. Hemolysis percentage of fresh blood after contact with different concentrations of nanoparticles. Results are expressed as mean of three measurements + standard deviation. Different letters refer to statistically significant differences among results ($p < 0.05$, ANOVA with Tukey's HSD post-hoc multiple comparison test). Different letters refer to statistically significant differences among results ($p < 0.05$, ANOVA with Tukey's HSD post-hoc multiple comparison test). The dotted line refers to 5% of hemolysis percentage. NP_E, NP_{BEV}, IUG-1 NP_E, IUG-1 NP_{BEV}

Conclusion

In this work, PLGA-PEG-based nanoparticles were successfully produced and functionalized on their surface with immunouteroglobin-1 (IUG1). Nanoparticles (NPs) were obtained through a method based on emulsification-evaporation technique. They were designed to entrap a monoclonal antibody, bevacizumab (BEV), commercially known as Avastin®. The potential of encapsulating bevacizumab paves open the way possibility to preserve its pharmacological properties, avoiding its early catabolism, and to enhance its biological activity, even at low concentration. The possibility to drive the encapsulated bevacizumab was achieved by immobilizing the IUG1 on the polymeric nanoparticles. This protein was chosen because its high affinity towards the fibronectin extradomain-B, a matrix protein largely expresses at the level of atherosclerotic plaque. Once fabricated, particles were morphologically characterized showing up a spherical geometry. The NP mean diameter was slightly influenced by the presence of IUG1 on particle surface as well as their

net charge. Probably, IUG1 was responsible of covering the COOH groups that give negative charge to the studied NPs. The immobilization of IUG on PLGA-PEG-derived NPs was demonstrated by FT-IR where characteristic peak of IUG1 remain in the spectra of bevacizumab loaded and IUG1-functionalized nanoparticles. The release profile of BEV was not negatively influenced by the functionalization of the NPs and circular dichroism analysis confirmed that, once encapsulated, BEV was structurally in its active form, thus maintaining its biological properties. Drug delivery system that are designed to be curative for atherosclerosis will enter directly in contact with blood and endothelial cells, once injected in the body. For this reason, cell viability and hemocompatibility with human endothelial cell and red blood cells, respectively were studied. Cell viability on endothelial cells was assessed by evaluating mitochondrial activity, lactate dehydrogenase secretion, and quantify the DNA. Moreover, on macrophage cells was evaluated the cell viability using the MTS assay. All the tests demonstrated the cytocompatibility of all the studied NPS up to 100 μg/mL of BEV over a period of three days on both cell lines. The percentage of red blood cells that undergone membrane breakage was for all the different type of NPs and for all the studied concentration always lower than 5. This BEV encapsulation system is considered as an innovative nanotool for the next generation therapy, based on monoclonal antibody, of cardiovascular disease, i.e. atherosclerosis.

Chapter 3

Introduction

Tissue engineering represent a new alternative for the treatment of patients which is an interdisciplinary field involving engineering and life science [98]. This new branch of engineering has attracted many scientist and surgeon because it can avoid some many difficulties for the transplantation or the replacement of organs[99]. One of the purposes of this area is to mimic the fundamental structure of the tissue wanted to be replace,[100] moreover another important characteristic is the studies of the mechanical properties which should be as close as possible to the proper tissue[101].

Cardiovascular disease is an important issue for the Western wold because represent one of the first cause of death, a special attention should be given to the atherosclerosis (ATH), plague of the modern world accomplice the sedentary life, unbalanced diet, smoke and chronic disease as diabetes [8]. ATH is an inflammatory disease characterize by an endothelial disfunction with an attraction for the macrophage and an accumulation of low-density lipoproteins which induce the formation of the plaque[102].

The actual strategies for the treatment of the plaque in an advanced clinical stage is vascular surgery which has made huge progress in the last decades for obstructive diseases, but still suffers of some limitations to be faced, such as the replacement of vessels with a dimeter smaller than 6 mm. These prostheses can cause thrombogenic events which may occur considering the contact of the blood with the wall of the vessels due to the lower pressure in the peripherical system. Contrarily, for larger vessels many strategies are available. like grafts in polyethylene terephthalate (PET, commercially known as Dacron®) or in expanded poly tetrafluoroethylene (ePTFE, known as Teflon) which can substitute the vessels, but there are no good candidates as

substitutes for the replacement of small-caliber vessel [103]. Furthermore, their compliance mismatch at the anastomosis level, due to the fact that they are inelastic polymers, results in anastomic intimal hyperplasia and implies graft occlusion [103]. Electrospinning is a promising method for the fabrication of tissue engineering scaffold and this process can generate materials with a morphologic structure similar to the human tissue. It is possible to generate fibers with micrometres diameters using several different types of polymers[104], i.e., poly (ε-caprolactone) (PCL) and poly glycerol sebacate (PGS)[105].

In this chapter it will be describe in depth the production and the results regarding the properties obtained from the scaffold.

Electrospinning

Electrospinning has found significant use in the field of tissue engineering over the last ten years. The use of electrospinning to produce polymer fibrous scaffolds has been intensively investigated. Several types of polymers have been investigated including synthetic polymer, natural polymer, and polymer blends. The use of synthetic polymers increases the mechanicals properties shown better behaviour than natural polymers. Blending two synthetic polymers or two natural polymers could result in enhanced mechanical properties [106]. Electrospinning shows potential for the fabrication of scaffolds mimicking the blood vessels. This technique can generate fibrous, monitoring the fiber diameter, either nanoscale or microscale (micro- nano-fibers: 5µm – 50 nm) which can emulate the characteristics of ECM which compose the *avventitia* layer of native blood vessel. To sum up this system includes a process in which the interested solution is forced in a needle under a high electrostatic force and solidifies forming fibres on a cylindrical collector.

When the high voltage charges the polymeric solution the Taylor cone is formed at the end of the needle.

A thin flow emerges from the Taylor cone and a rapid solvent evaporation happen generating the fiber deposition on the tubular collector. This is a fibrous random-orientated deposition.

Our electrospinning apparatus is composed of:

• a syringe, containing the polymeric solution;

• a pump, to control the fluid that exits from the syringe;

• a high voltage DC generator (usually 30kV), connected to the syringe needle;

• a metallic collector, on the ground, that has the function to collect the fibers.

Electrospinning is indeed a method for the atomization of fluids, with application in mass spectrometry and in the industrial field of surface coating.

If the fluid employed for electrospinning has a low molecular weight, the stream becomes unstable before it reaches the collector and transforms just into a spray of electrostatically charged small drops. By using fluid polymers instead, the viscoelastic forces stabilize the stream, allowing the formation of thin charged filaments that deposit into a twist of fibers. The diameters are far smaller than those of extruded or mechanically stretched fibers (wet, dry a melt spinning where diameters are about 10m and over).

Fibrous mats from different natural or/or synthetic polymers have been generated using this technique. Electrospinning is a robust method that allows effective control over the morphology of the generated constructs and is easy-to-scale up. All these characteristics have made electrospinning an attractive process for fabrication of biomimetic scaffolds with tunable physical properties. Electrospun scaffolds have been used for many tissue engineering applications including bone, skin, cartilage and tendon tissue engineering.

Electrospinning has been paid much attention to because it can prepare three-dimensional nano-scale fibrous membranous or tubular scaffolds with an extremely large surface-to-volume and high porosity. Moreover, the composition and structure can be controlled to achieve desired properties

and functionality. Electrospinning has been applied widely in biomedical areas, such as nerve guidance conduit, wound dressing, bone regeneration, and vascular graft.

Presently, many reports and studies have been issued emphasizing on the electrospun natural and synthetic polymers used for biomaterials. Many studies demonstrate that cell attachment, spreading, and proliferation were enhanced greatly on these nanofibrous structures. The composition of the original material has a great influence on the morphological, mechanical, biodegradable, and biological properties of the electrospun scaffold.

Process parameters

The fiber morphology can be influenced by several parameters which can be divided in three different categories: proprieties of the polymeric solution, electrospinning setup, and environmental conditions.

Solution proprieties depend on its viscosity, electrical conductivity, and surface tension. Which are associated to the characteristics of the polymer and the solvent.

• Viscosity: it is one of the parameters with an important influence over the diameter and morphology of the fibers. The polymer structure and the molecular weight are correlate with the proper viscoelastic forces of the solution.

• Electrical conductivity: the increase of a solution's conductivity cause a greater repulsion of the flow's jet, and therefore a greater elongation of the fibers, which decrease in diameter [107].

Possible approaches to increase conductivity are the addition of salts [108] and the use of a more conductive solvent , such as N,N dimethylformamide (DMF)[109][110].

• Surface tension: To produce nanofibers, the electric charge must exceed the tension of the solution's surface. During the electrospinning process surface tension opposes the jet stretch, causing the formation of drops or fibers with drops. To avoid this phenomenon, is better to use a solution with a low surface tension.

Parameters like the voltage, the flow rate, the distance from the collector and the distance from the needle must be setup because strictly related to the nanofiber produced.

• Voltage: increasing the voltage can causes a high electrostatic repulsion of the flow, obtaining fiber with good stretch and a thin diameter. Instead with large potential differences, fiber diameters become larger [111].

• Distance between the needle and the collector: this distance influences the travel time and the power of the electric field. Reducing the distance, the flow has a minimal time available to dry before reaching the collector, but the intensity of the electric field also increases, incrementing the flow's acceleration. For this reason the fiber size increases [107].

• Opening diameter: when is use a needle with a small internal diameter there is a reduction of number of drops and also the fiber diameter. A drop at the end of the needle will have smaller size and higher surface tension. More time is needed to stretch the flow and wear it thin before it reaches the collector[112].

• Humidity: an increase in humidity increases the size, number and distribution of pores on the fiber surface and it could alter the diameter fiber depending on the polymer solution used [113].

• Temperature: the increase in solution temperature has two opposed effects on the electrospinning process. Indeed, it increases solvent evaporation, therefore increasing fiber size, but is also decreases viscosity, with the opposed effect.

Temperature cannot be increased over a certain limit if enzymes or proteins are used in the process. [114] [115][116][117].

• Pumping flow rate: wide flow rates cause an increase in fiber size. Indeed, these do not have sufficient time to allow the solvent to evaporate [107]. This parameter is however less influential than others.

Polycaprolactone (PCL)

Polycaprolactone was synthesized by the Carothers group in the early 1930s [118]. Polycaprolactone (PCL) is a synthetic polymer largely used for biomedical application due to the biocompatibility and slow degradation characteristics[119]. Moreover, PCL present good mechanical properties giving to the electrospun material promising medical application. The degradation is induced by a hydrolytic mechanism, a slower degradation capmaring with other hydrophilic biomaterials, making it suitable for long-term implantable prostheses.

Poly (glycerol sebacate) (PGS)

Poly (glycerol sebacate) (PGS) is a polymer which present a good biocompatibility, high hydrophilicity and good biodegradability. It is synthetized from the condensation of glycerol and sebacic acid. Controlling curing time, curing temperature and the reagents concentration, is possible to modulate the degradation kinetic and mechanical properties of the resulting polymer. Usually is used in tissue engineering to formulate soft tissue as vessels, retina, cartilage and cardiac muscle[120].

Gelatin

Gelatin derives from the hydrolysis of collagen and it is largely used in pharmaceutical and medical fields. Is a chep and biodegradable natural polymer easy to use. It is easy to solubilize in water to form gels.

Quercetin

Quercetin, a plant flavonoid widely distributed in fruits and vegetables such as apples, berries, and onions. It can be used as an ingredient in supplements, beverages, or foods[121] [122] [123]. Like many other bioflavonoids, quercetin present antioxidant, anti-atherogenic, and anti-carcinogenic

properties. The U. S. Food and Drug Administration has not approved any health claims for quercetin. It's chemical structure is:

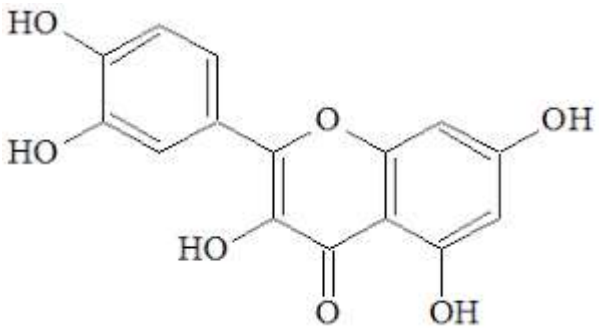

Figure 25. Representative quercetin structure. Adapted from Sanda Teda et al. [124]

The daily intake of various flavonoids has been estimated to be around 23–34 mg and quercetin constitutes a major fraction. It has been estimated that sometimes quercetin may represent as much as 60% of the total flavonoids consumed[125][126]. Quercetin, related flavonoids, and plant extracts from tea and ginkgo have been reported to have various clinically relevant properties such as antioxidant [127][128][129][130], anti-inflammatory, and tumoricidal activity[131]. Furthermore, beneficial associations between the consumption of quercetin and lower incidences of coronary heart diseases and stroke have been reported [132][133]. Particularly it is interesting the pharmacological activities of flavonoids as anti-inflammatory agents playing an important role in the regulation of cell adhesion processes. The adhesion of leukocytes to the vascular endothelial cells is a critical step in the inflammatory response and involves recruitment and infiltration of leukocytes to the site of tissue injury, infection, or lesion formation.

Bioreactors

A bioreactor is defined as a system which can simulate the physiological environment and can controlled single variable like the cellular migration, proliferation and differentiation. But bioreactor can also use to test the behaviour of the produced scaffold. In this study is fundamental the use of

a bioreactor in order to simulate or at least get closer to the future *in vivo* implant situation and predict the bio-prosthesis performance. Our bioreactor is made up a chamber where the bio prosthesis is insert, a manometer which register the pressure impress, a peristaltic pump, and a reservoir. This bioreactor is filled with PBS which is flux continually trough the pump. The bioreactor is placed in an incubator at 37 °C to simulate the physiological temperature.

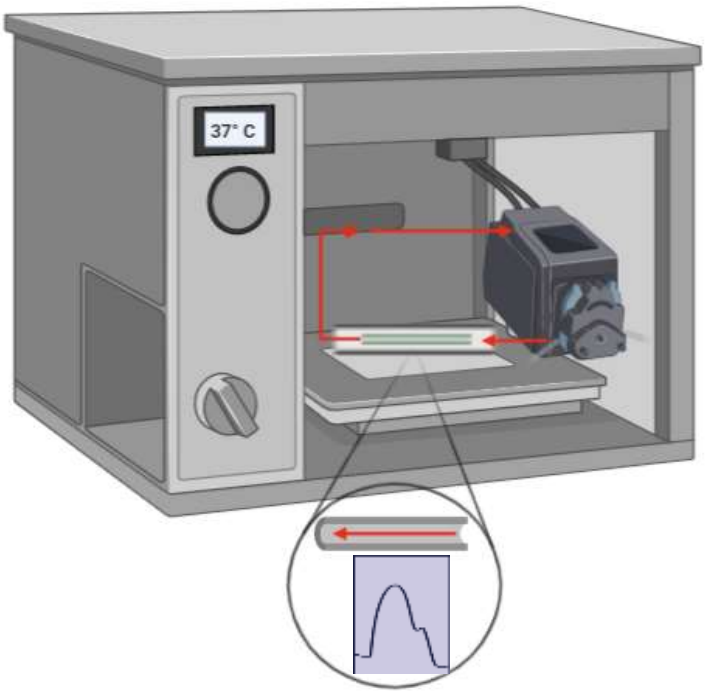

Figure 26. Schematic representation of bioreactor. Created with Biorender.com

Materials and methods

Preparation of polymeric solution

Poly(ε-caprolactone) (molecular weight= 8 x 104 Dalton) (Sigma-Aldrich, St. Louis, MO, USA) (PCL) and poly (glycerol sebacate) (PGS) were used as polymers for the electrospinning process. PGS was prepared as shown in Wang et al.[116]: briefly, glycerol and sebacate acid were mixed together in 2:3 molar ratio; later the bland was dissolved at 120°C in presence of an argon flux for 24 hours. At the end, the mix was kept in vacuum at the same temperature for 48 hours to obtain a very viscous pre-polymer.

Two different kind of solution were prepared for the electrospinning process: PCL: PGS 1:1 (v/v) and quercetin added PCL:PGS 1:1 (v/v). To prepare the solutions of PCL 20% (w/v) and PGS 20% (w/v), chloroform and ethanol 9:1 (v/v) were used as solvent. In the second case, quercetin (Sigma-Aldrich, St. Louis, MO, USA) at 0.05% (w/v) was added. Successively, each obtained solution was kept in agitation for 12 hours at room temperature 25 ± 2°C. Then PCL 20% and PGS 20% were mixed in 1:1 ratio (v/v) and the final copolymeric solution was kept in agitation for at least two hours before electrospinning.

Synthesis of prostheses by electrospinning technique

The electrospinning apparatus used (SPINBOW, Bologna, Italy) consisted of three components: a high voltage power supply (PCM series, Spellman, NY, USA), a syringe pump (KSD-100, KD Scientific , Holliston, MA, USA) , and a grounded collector. The collector was a cylinder 13 cm long and it was possible to choose the external diameter: 2 mm or 5 mm.

The polymer solution was loaded into a glass syringe 5 mL (FORTUNA® OPTIMA®, Poulten & Graf GmbH, Wertheim, Germany) and was extruded from a flat needle tip at a vertically distance of 18 cm from the collector. The total volume processed was 2.00 mL.

Table 3 electrospinning operating parameters.

Needle diameter (G)	16
Flux ratio (mL/h)	1.10
Voltage (kV)	17
Rotational speed (rpm)	500
Translation speed (mm/min)	600
Right limit(mm)	115
Left limit(mm)	15

Two different kind of scaffold were realized through the electrospinning technique: PCL:PGS 1:1 (v/v) and PCL:PGS 1:1 (v/v) functionalized with quercetin. The scaffold containing quercetin where electrospun in dark conditions because this antioxidant is photosensitive.

Figure 27. representative scaffold made of PCL:PGS (1:1) (left) and one functionalized with Q (right).

Coating with gelatin

To reduce water permeability, scaffolds were coated with gelatin (Sigma-Aldrich, St. Louis, MO, USA). The gelatin solution was obtained mixing on a hotplate gelatin and milli-Q water to achieve a final concentration of 67 mg/ml. A gelatin film was obtained putting the sample in a collector (Kirk 510 Bicasa, Italy) connected to a mechanical mixer and immersed into the gelatin solution kept at 37 ± 2°C by a hotplate (Heidolph MR 3001 K, Germany) for one hour under agitation at a costant

velocity of 135 rpm. After all, it was placed under UV-lamp for one hour in order to allow the cross-linking of gelatin with fibers. At the end, the gelatin-coated scaffold was put into a desiccator overnight. The gelatin coating was performed for both quercetin-functionalized and non-functionalized scaffolds.

Scanning electron microscopy analysis of PCL: PGS-based electrospun scaffold

The morphological properties of the fabricated constructs can give significant, especially to understand their behaviour with cells once in vivo implanted. Scanning electron microscopy (SEM) analyses were performed to study the morphology of native bio prostheses and after degradation. Samples were cut in small pieces and immobilized on a metallic support with adhesive tape in order to undergo a process of metallization with gold to make them conductive. Images were acquired with a Hitachi S-2500 (Tokyo, Japan) and to measure the fibers of the polymeric constructs, diameters were measured in at least two different images for each type of scaffold by image processing software (Image J, USA). For each sample, at least fifty fibers were considered in order to obtain a meaningful statistical value.

Kinetic of blood coagulation on electrospun vascular prostheses

The blood coagulation on PCL:PGS-based vascular graft was studied considering the release of free haemoglobin for the red blood cells caused from their rupture. In fact, this protein is the most common marker analyzed in the dedicated literature for the studies of how materials influence the kinetic of blood coagulation. Blood was collected by healthy volunteer in agreement with the local ethic committee. 16 µL of a solution of CaCl2 (0.2 M) were added to 64 µL of EDTA blood was dropped above the internal surface (32 mm^2 in area) and mixed. After time-points (15, 30, 60, and

120 minutes), each sample was put in 16 mL of deionized water and they were incubated at 37°C for 5 minutes. The concentration of free haemoglobin in water was registered by collecting the absorbance values at 540 nm using the spectrophotometer Jeneway (Genova). Glass was used as reference material for prothrombotic activity.

Fluid uptake

The fluid uptake on biomaterials which need to be sutured with organs have been performed because it can influence alteration in different characteristics of the graft, as the possibility to increase the volume, process known as swelling, by absorbing the liquid, the possibility to change its mechanical properties, the biological response, and eventually the drug release behaviour[134]. Fluid uptake was studied under three different conditions, neutral, acid and basic conditions to cover all the possibility that the scaffold could undergo once implanted.

Degradation

Scaffolds biodegradability is one of the most important characteristics for biomaterials. These tests were performed in static, dynamic condition and under different pression using a bioreactor to simulate some physiological pressure. To evaluate it, degradation tests were implemented using phosphate buffered saline solution (PBS) as a function of time.

Static condition

To evaluate the biodegradability in static condition versus time scaffolds was cut into cylindric pieces (5 x 5 mm); after, each fragment has been weighted using an analytic balance and then they have been immersed into 1,5 ml of PBS at 37°C ± 2°C. Considering gelatin-coated scaffolds (with or without quercetin), the analysis was led for 49 days. On the other hand, PCL:PGS 1:1 containing or

not quercetin were studied for 77 days. Samples has been taken weekly, as following: they were washed three times with deionized water and one time with milli-Q water to remove all the salts remained. Therefore, they have been frozen overnight and they have been lyophilized (freeze drier Christ model Alpha1-2LD$_{plus}$, Osterode am Hartz, Germany). At the end of the freeze drying, all the pieces have been weighted again on the same analytic balance described above.

Dynamic condition

To study the degradation in dynamic condition the scaffold where divided in pieces of 5mm and weighted using the same balance reported above. The pieces have been immersed into 4 ml of PBS at 37°C ± 2°C in an incubator and 200 rpm. Weekly the pieces were taken, washed with milli-Q water and left in a dissector for one night and weighted again.

Bioreactor

In this case scaffold were placed in the bioreactor chamber and a PBS solution was pass through the bio prostheses. Three representative pressure where chosen 60mmHg, 80mmHg and 100mmHg.The analysis was performed for 1 week, daily a 10% of total volume of PBS was collect and replace with fresh solution. At the end of the analysis the scaffold previously weighted were washed with milli-Q water, left in a dissector for one night and weighted again in the same balance.

The mass loss percentage, for all the three cases was calculated dividing the loss of weight with the initial weight, as shown in the following equation (6):

$$\text{Degradation } (\%) = \frac{\text{mf} - \text{mi}}{\text{mi}} \times 100$$

Where:

• mi is the initial weight of the sample (g);

• mf is the final weight of the sample (g)

Mechanical characterization

To perform mechanical loading tests in the axial direction on electrospun graft, uniaxial Z0.5 test machine (Zwich Roell, Ulm, Germany) was used.

Each tubular scaffold was cut to obtain rectangular specimen (length=30 mm, width=2 mm), as reported in figure 2.6 (a), with the short edge of each sample originally oriented circumferentially on the original tube. The thickness of each sample was measured using a digital caliber (Series 209, Mitutoyo, USA). Every segment was clamped at its cut ends and the crosshead speed was set at 20 mm/min with a preload of 0.1 N. Young's modulus was calculated considering stress and strain values between 0.5-2 % strain through a MATLAB algorithm. For each kind of scaffold, the measurement was repeated almost four times.

Quercetin release versus time

It is fundamental to understand the total amount of quercetin released by the scaffold, once it was implanted, in order to evaluate if this quantity is enough for its aim, so if it is able to show an anti-inflammatory effects in cells.

Static condition

To tested the release, a quercetin functionalized scaffold was cut in little pieces and all of them were immersed in 5 mL of PBS into a 50 mL test tube. For two months, sample were taken daily, with the same procedure used in gelatin release evaluation: 500 µL of solution was taken and then replaced with 500 µL of fresh PBS.

Dynamic condition

Functionalized scaffolds were cut into 0.5 cm pieces and put into a 50 mL test tube with 5 mL of PBS and, after, it was incubated at 37 ± 2°C, in order to mimic physiological conditions of human

body in the same incubator used for degradation assay, the test tube were subjected to a movement causing a scaffold sift. For one week, 10% of the solution were taken daily, and after the collected volume was replaced by 500 µL of fresh PBS. This procedure was repeated at each established sampling time.

Bioreactor

Entire scaffolds were placed in *ad-hoc* bioreactor at 37 ± 2°C. The bio-prostheses were tested at three different pressure to simulate the physiological pressure in peripheral vessels: 60, 80, 100 mmHg using PBS. For one week 10% of total solution was daily collected and replace with fresh PBS.

For all the three condition results were expressed in terms of percentage of the total amount of quercetin present in a scaffold after its production. It was not use as total amount of quercetin the quantity of this polyphenol added to the original spinning solution because, probably, during electrospinning process a quercetin loss happened.

The total amount of quercetin was evaluated through a liquid to solid extraction using ethanol as a solvent: an entire scaffold was cut in the smallest possible pieces, then they were put in ethanol and they were kept in agitation for 2 days at room temperature. The extraction was made in triplicate. After this, 150 µL of the solvent were collected and their absorbance analysed at 380 nm.

Gelatin release versus time

It was very important to analyse the gelatin release versus time, in order to have a complete knowing of what scaffold will emit during the time once it was implanted.

Static condition

An entire gelatin-coated scaffold cut into little pieces was put into a 50 mL test tube with 5 mL of PBS and, after, it was incubated at 37 ± 2°C, in order to mimic physiological conditions of human body in the same incubator used for degradation assay. For two months, 10% of the solution (500 µL) were taken daily, and after the collected volume was replaced by 500 µL of fresh PBS. This procedure was repeated at each established sampling time.

Bioreactor

An entire gelatin-coated scaffold was collocated in an *ad-hoc* bioreactor at 37 ± 2°C, in order to mimic physiological conditions of human body in the same incubator used for degradation assay. The bio-prostheses were tested at three different pressure to simulate the physiological pressure in peripheral vessels: 60, 80, 100 mmHg using PBS. For one week 10% of total solution was daily collected and replace with fresh PBS.

Gelatin released amount in each condition was determined via bicinchoninic acid assay (BCA) that permits to calculate the protein concentration with UV-Visible spectroscopy at 562 nm.

The BCA assay is a convenient tool, as it allows to measure very small volumes: in fact only 5 µL of the sample were mixed with 125 µL of the BCA reagent in an Eppendorf, and placed into an incubator at 37 ± 2°C for 30 minutes. After that, it was possible to measure the absorbance value of the sample (Microplate reader Tecan, Männendorf, Swiss), which was related to the concentration of the protein using an opportune calibration curve.

Morphology characterization

To analyse scaffold's morphology the scanning electron microscopy (SEM) (Hitachi model S-2500) technique was used. Before scanning, the samples have been covered by a 30 nm gold layer using a Polaron SEM system, operating at 0.1 Torr and 20 mA. This procedure makes the samples conductive, that is a necessary requirement for the process. SEM is an instrument that permits, through the emission of an electron beam, to analyze signals produced by the interaction of electrons in the beam with the sample. By processing these signals it is possible to obtain information about the sample. The extreme versatility of this instrument is proved by the variety of samples that can be analyzed (in terms of their nature, shape and dimensions) and the simplicity of sample preparation. Fiber mean diameter in at least two images of the scaffolds were measured using image processing software (Image J, USA). For each sample at least 100 fibers were measured to obtain a meaningful statistical value.

Results

Degradation

Biomaterial degradation is a key factor that can influence cell adhesion, proliferation and the tissue architecture reorganization and integration. Degradability of biomaterials is a possible drawback in tissue engineering which is associated to the polymer creep and weakening and must be kept into consideration[105]. When a biomaterial is used as prosthesis, slow degradation and integrity of the sample enables host body to gradually replace the implanted scaffold with native tissue over an extended period of time [135]. Nowadays the classical concept of tissue engineering, according to which the scaffold is described as a simple extracellular matrix-inspired framework, is overcome. The new concept is to fabricate constructs able to actively interact with cells during the regeneration process, releasing growth factors and chemoattractant proteins. Despite the majority of tissue engineering research is focused on the fabrication of the perfect vascular scaffold mimicking biochemical, physiological, biomechanical and architectural characteristics of the native tissues, the counteracting of the surgical-related inflammation represents today a new challenge. In fact, the post-surgical inflammation is able to affect negatively the cellular attachment and cellular growth on the bio-prostheses , inducing many damages to the microstructure of the biomaterials, compromising its physico-chemical and mechanical properties, leading, in the worst case, to the rejection of the graft. For this reason, PCL: PGS (1:1, v/v), the best performing scaffold, was functionalized with the direct addition of an antioxidant in the spinning solution. Among antioxidants, there is a class of compounds, known as polyphenols, that show anti-inflammatory activity both *in vitro* and *in vivo.*

Static condition

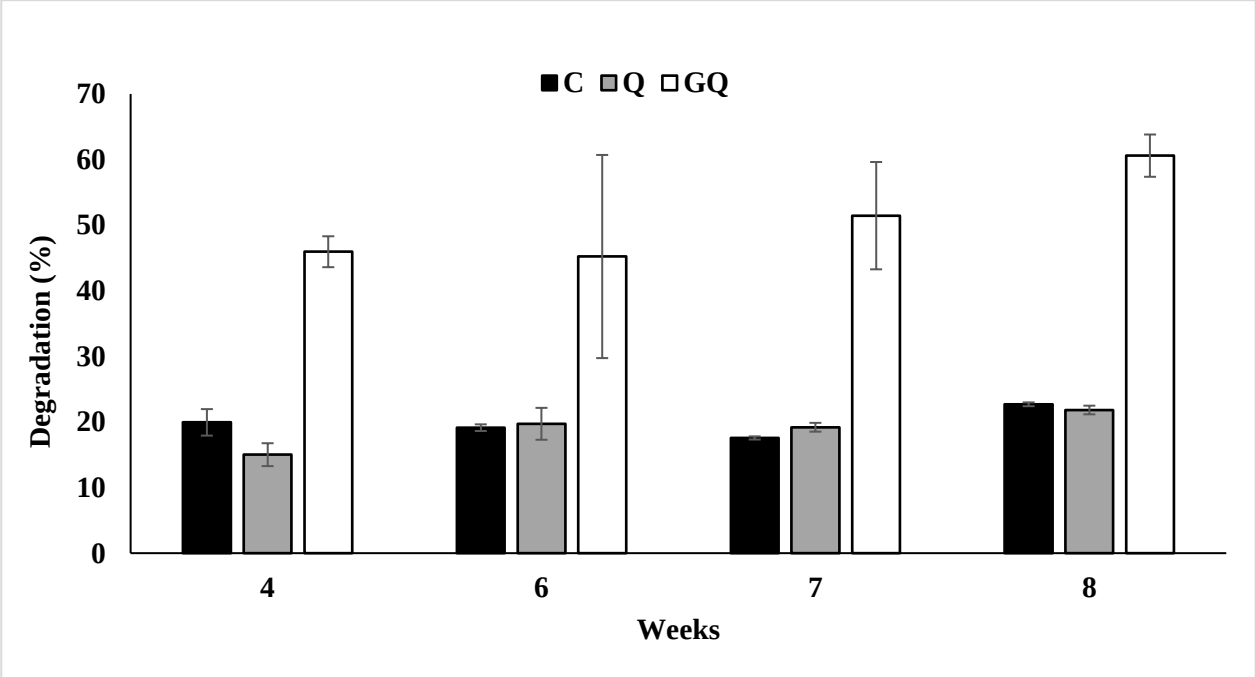

Figure 28. Degradation percentage in static condition of coated and uncoated scaffolds.

As shown in figure 28, degradation test was performed until 8 weeks. The percentage of degradation, in the case of PCL:PGS 1:1, after 4 weeks is about 20%, in completely agreement with data observed by other scientific works that used PGS like Sant et al. [136], Kharaziha et al. [137]and Salehi et al. (2014) [135]. In one of his works, Kharaziha [137] et al. attributed PCL:PGS scaffolds degradation (at 37°C and in DPBS) to ester bonds hydrolysis of monomer that compose it: sebacate acid and glycerol. Comparing the literature with the results obtained with quercetin functionalized samples, it's noticeable that quercetin did not influence significantly scaffold degradation for 4 weeks. In conclusion, the addiction of quercetin to the electrospinning mix solution do not change the degradation behavior of the scaffolds: PCL:PGS 1:1 scaffold (C) and quercetin functionalized ones (Q) have the same degradation profile in terms of trend and value. It's possible to notice that samples with gelatin coating (GQ) showed a major mass loss percentage than the uncoated ones, indeed after 4 weeks its degradation is about 45% against the 20% of uncoated grafts. This behaviour seems to be an accelerated kinetic of degradation but is just a superimposed effect due

to gelatin release. Samples seem to lose more mass about their original weight, that includes also gelatin-coating, since they're releasing gelatin that is incorporated in the mass loss percentage calculations. However, gelatin coated polymer was degradating itself in the same way of uncoated one. In conclusion, gelatin did not change degradation pathway of the polymer. Indeed, the trend of degradation of both coated and uncoated scaffolds was the same (10-15% a month), but in the case of coated grafts all the data were increased in absolute values.

Dynamic condition

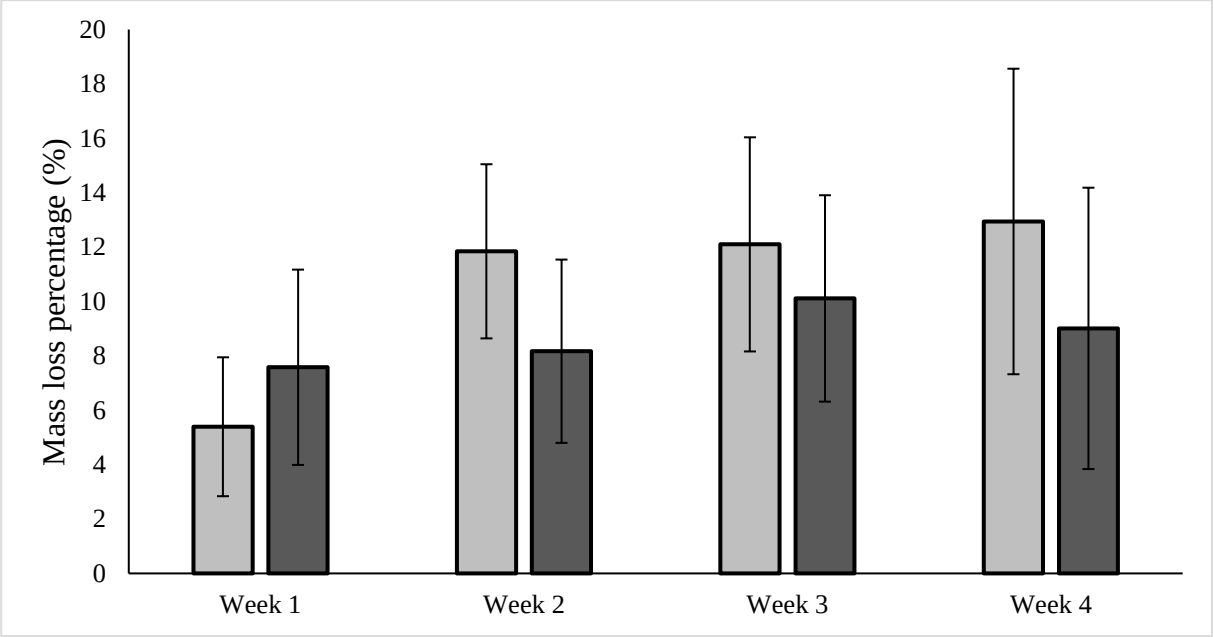

Figure 29. Degradation percentage in dynamic condition of functionalize with quercetin bio prostheses and control.

In general, biomaterial degradation plays a pivotal role in the formation of the new tissue since it can influence positively or negatively cell adhesion and proliferation. Biodegradability could be considered a possible disadvantage in tissue engineering, especially when it is associated with polymer creep and weakening during time. As shown in figure 29 degradation tests were performed until 4 weeks. The mass loss percentage in the case of control bio-prostheses after 4 weeks was about 10 %, according to data observed by other authors [135]. Comparing these data with those collected working with QS, it was noticeable that the addition of quercetin in the scaffold did not interfere with the degradation kinetic. In fact, both polymeric constructs showed the same degradation trend over 4 weeks**.**

Bioreactor

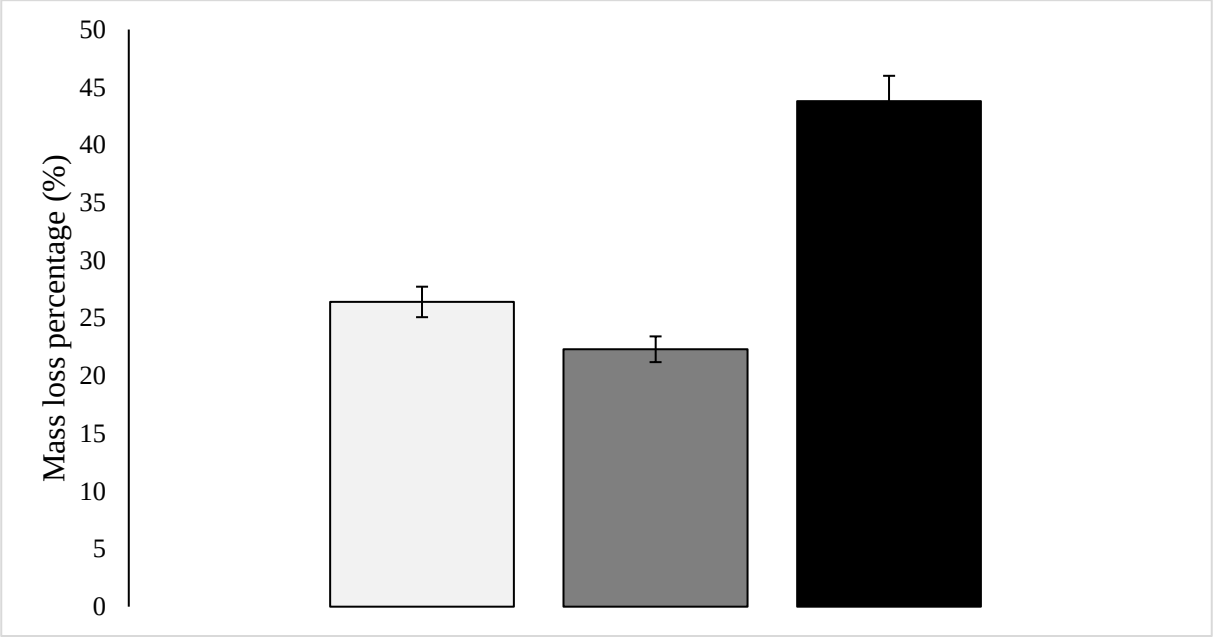

Figure 30. Degradation percentage of coated and functionalize bio-prostheses under ☐ 60 mmHg , ▒ 80mmHg, and ■ 100mmHg pressure after 1 week.

The results obtained in figure 30 shown a correlation between the degradation and the pressure condition. The polymeric graft covered with gelatin as coated agent were tested in a bioreactor using three different pressure which are representative the peripherical district of human body. The bio-prostheses reach a 45% of degradation in terms of mass loss percentage after 1 week if tested at 100mmHg.

These degradation results reported the importance of the pressure of the fluid forced on the scaffold wall.

Degradation in different pH condition

One of the most important parameters to be focused on in vascular tissue engineering is represented by the possibility to work with biodegradable and bioabsorbable polymers. In this case, two different biodegradable and bioabsorbable polymers were used, poly (caprolactone) and poly

(glycerol sebacate). The study of a short-period mass loss in conditions close to the physiological ones, could be predictive for the behaviour of the material once implanted. The period taken into consideration was 28 days working under neutral conditions (PBS) whereas working under basic or acid condition the period considered was just of 7 days. This study was performed since the basic and the acid conditions are considerable a good environment to study an accelerated *in vitro* degradation. Considering the neutral environment, no statistically significant differences were noticed among the different 4 weeks of study. The general mass loss was around 20 % of the initial weight and increasing the incubation time, the mass loss remained constant. Significant results were obtained when the degradation of the material was studied in the presence of a pH = 12 and a pH = 3. (Table 5)

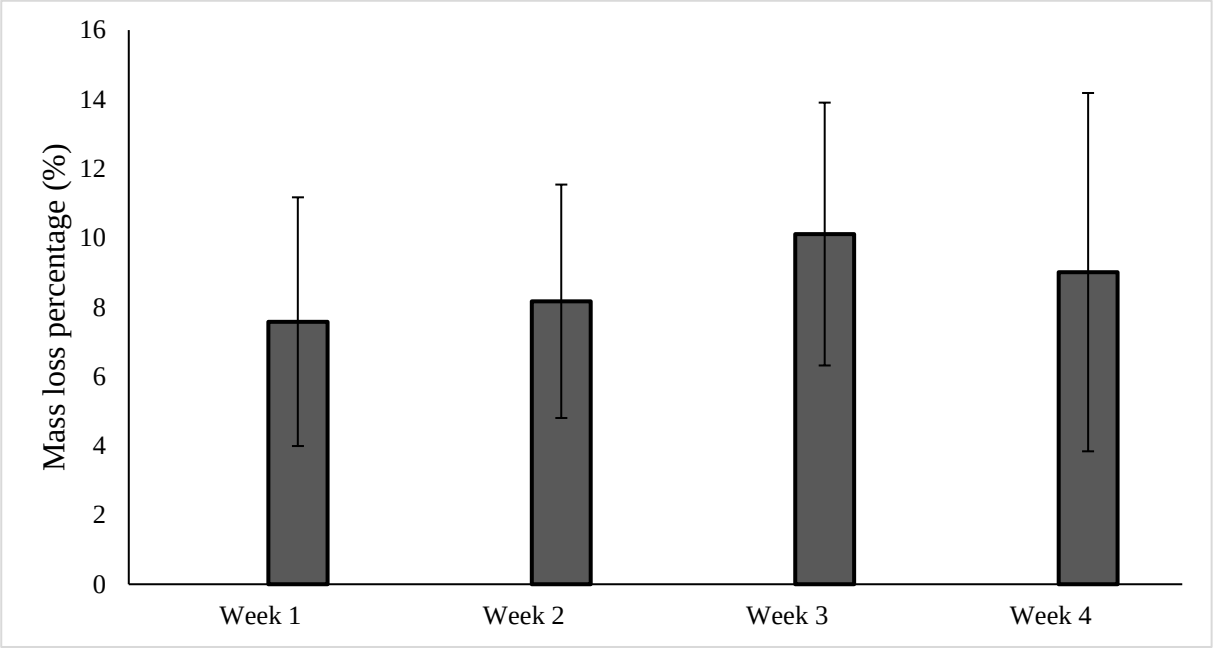

Figure 31. mass loss of PCL:PGS-based electrospun scaffold in neutral conditions.

Table 4. pH values of degradation media before and after mass loss experiments after 7 days.

Mass loss condition	Starting pH value	Final pH value
acidic	3.00	3.02 ± 0.03
basic	12.00	9.03 ± 0.69
neutral	7.40	6.82 ± 0.16

Table 5: mass loss percentage of bioprostheses in different pH solution values after 7 days.

Mass loss condition	Mass loss (%)	D.V.
acidic	9.15	± 0.60
basic	29.56	± 10.69
neutral	9.68	± 0.25

Quercetin release

Static condition

As shown in figure 32, studying the release behaviour of uncoated functionalized scaffold, it's possible to notice that for the first 10 days the release was very low. Then, the kinetic of the release accelerated reaching 1% of the total quercetin in the scaffold after 15 days and a final value of 2,15% at the end of the observing time (53 days). This quantity of quercetin was very low and this fact is probably due to quercetin low solubility in aqueous solutions. All these experiments were performed in PBS.

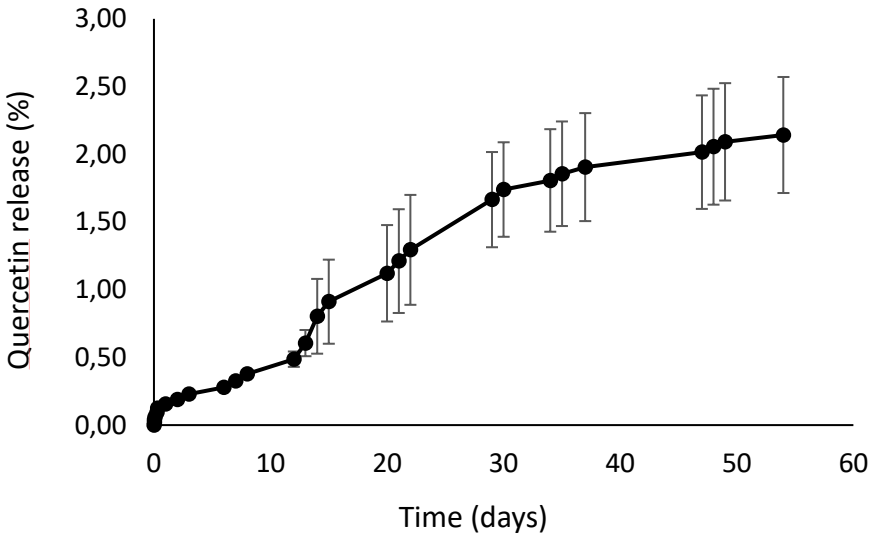

Figure 32. Quercetin release from uncoated bio-prostheses.

Comparing the results obtained with uncoated samples with those of coated ones (figure 32), it was found that curves had the same trend, meaning that gelatin coating does not interfere with the release kinetic.

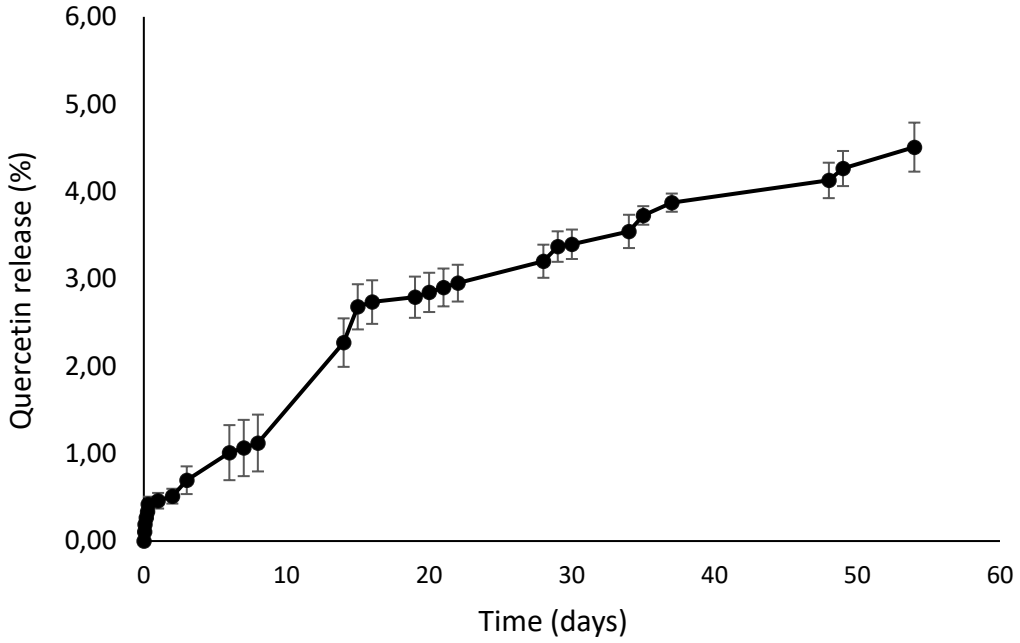

Figure 33. Quercetin release from coated bio-prosteses.

However, in the coated sample release curve, (figure 33) there were higher values of percentage at the same time: after 15 days, the percentage was about 2.15% and the final value reached after 53 days was 4.5%. This increasing effect in quercetin percentage can be explained in two different possible ways: first one is that gelatin, leaving the scaffold, induced a co-release of quercetin, which during the gelatin crosslinking phase has bonded with the coating agent; another possibility is that the presence of gelatin preserve quercetin from oxidation and this is reflected in an enhancing of quercetin release percentage. In fact, in this case the percentage of quercetin released in both scaffolds could be the same, but during spectrophotometric analysis only active quercetin and not the oxidized form is detected. This aspect needs a more detailed study.

As functionalizing agent, quercetin must express an anti-inflammatory effect: in order to reach its aim is necessary to understand if the amount of quercetin release is enough for obtaining the expected results on cells. As explained by Kobuchi et al.,[135] quercetin shows an anti-inflammatory effect after 24 hours starting from a concentration of 1µM that is equivalent to 3.02×10^{-4} mg/mL

that is always overcome in the release from the beginning in both coated and uncoated samples. In the same work, it is demonstrated that a more significant anti-inflammatory activity is shown with a concentration of 50 µM (0.015 mg/mL). This value was reached after 5 days in case of uncoated quercetin functionalized samples and after just few hours for gelatin coated ones. In conclusion, it is possible to affirm that the functionalized electrospun scaffold incorporated an amount of quercetin suitable for anti-inflammatory activity.

Dynamic condition

As showed in figure 34 quercetin release in dynamic condition after one week reach 60% of bioactive compound release. The bio-prostheses tested were uncoated and the dynamic condition have a significant effect on the quercetin release. Is important to focus on the initial burst release in the initial hours. As reported above 50 µM of quercetin have an important anti-inflammatory activity, in this condition the concentration is reached after 24 hours. This show that the bio-grafts present an anti-inflammatory activity barely after 24 hours after the implant.

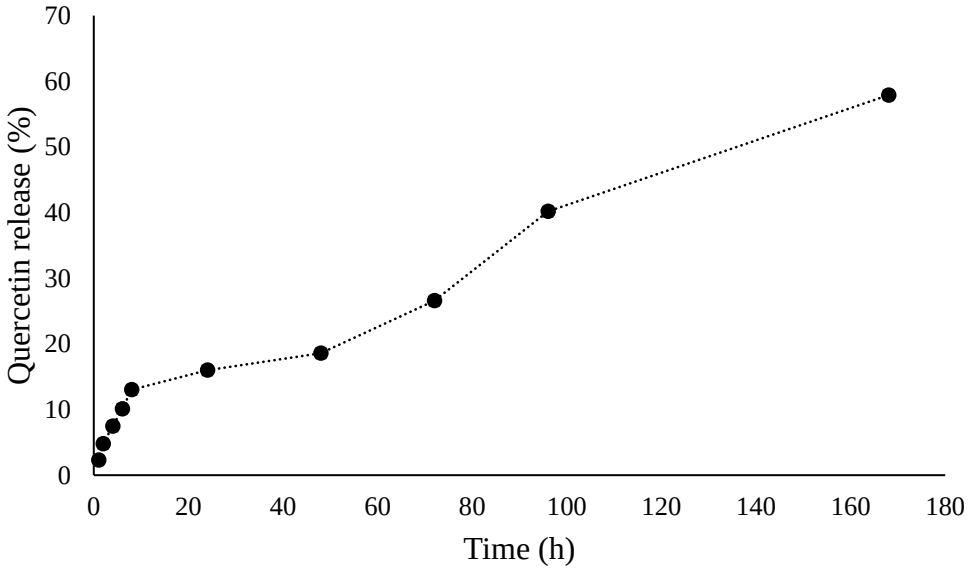

Figure 34. Quercetin release studied in dynamic condition after seven days.

Bioreactor

As showed in figure 35 quercetin release is proportionally connected with the pressure imposed in the scaffold internal wall. Indeed, the scaffold under 100mmHg release 40% of quercetin after one week while the one under 60mmHg reach just the 28%. Even if the release compared to the one in dynamic condition is lower the percentage is still ideal for an anti-inflammatory activity.

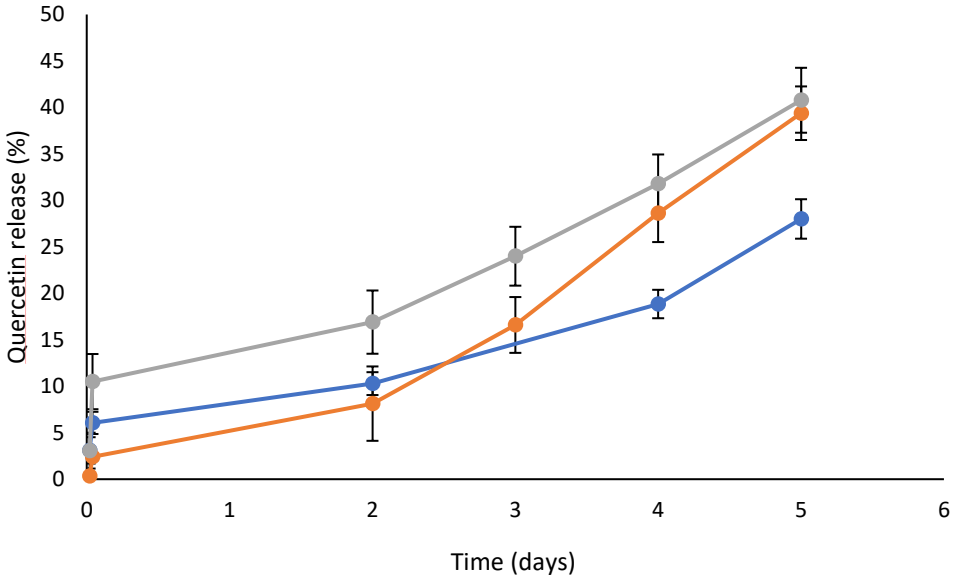

Figure 35. Degradation percentage of coated and functionalize bio-prostheses under 60 mmHg, 80mmHg, and 100mmHg pressure after 1 week.

Gelatin release

Static condition

As shown in figure 36, the cumulative curve of gelatin release showed a logarithmic trend. There was a brief initial phase where a large amount of gelatin is released, reaching value of 30% of the total coating in only 8 hours; after, a plateau is reached in about two weeks with a value of 60% of gelatin released from the total coating. This trend of gelatin release curve, with a peak in the first hours of immersion, can explain the different behavior in degradation and fluid uptake tests

between coated and uncoated samples. Although this significant percentage of gelatin released in first hours seems not to be in agreement with the aim of the coating, it has to be taken in consideration that not only gelatin will reduce graft permeability, once the prosthesis has been implanted, but it will be assisted by coagulation of blood in direct contact with scaffolds surface at the same time. It has to be verified by opportune simulations if the value of the curve plateau permits to reach a steady state in which it would be possible to have safe working conditions of the graft in vivo.

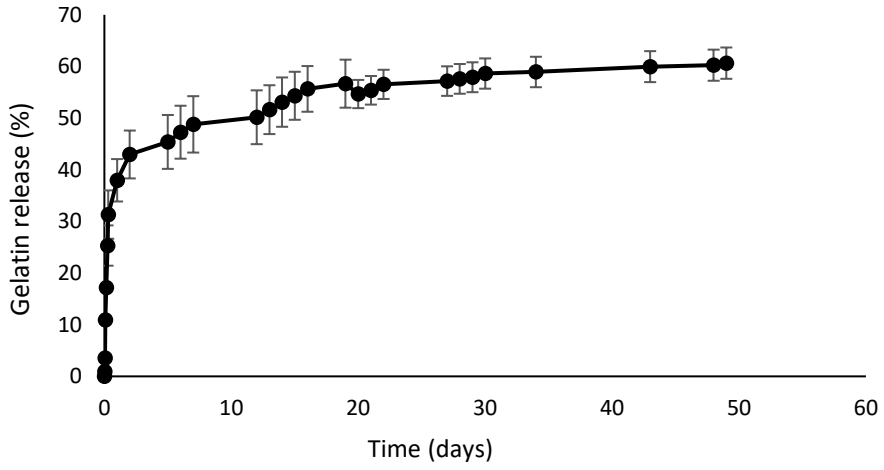

Figure 36. Gelatin release cumulation curve in time.

Bioreactor

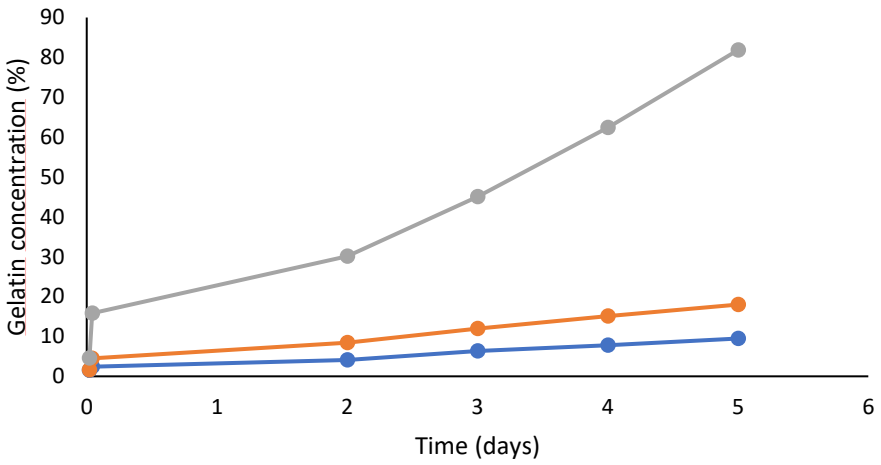

Figure 37. Gelatin release from bio-prostheses under 60 mmHg, 80mmHg, and 100mmHg pressure after 1 week.

This graph (figure 37) shows how prostheses subjected to higher pressure (in terms of mmHg) show a higher percentage release than those subjected to lower pressure. This release is adequate to prevent blood loss. The results are shown in percentage terms of the total amount used to form the layer around the prosthesis. The total amount of gelatin was obtained by subtracting the weight of the prosthesis after the gelatin coating process.

Mechanical characterization

To tested mechanical properties of scaffolds, Young's modulus, tensile strength and elongation were evaluated.

Surprisingly, all the tested samples showed a comparable tensile strength without any relevant differences. Comparing quercetin functionalized scaffolds (Q) behaviour with PCL:PGS 1:1 (C), it was possible to notice that there were not any substantial differences between them in all the mechanical parameters tested. These results shown that scaffolds mechanical behaviour did not change although the direct addiction of a new molecule in the electrospinning mixture, after having optimized the process parameters.

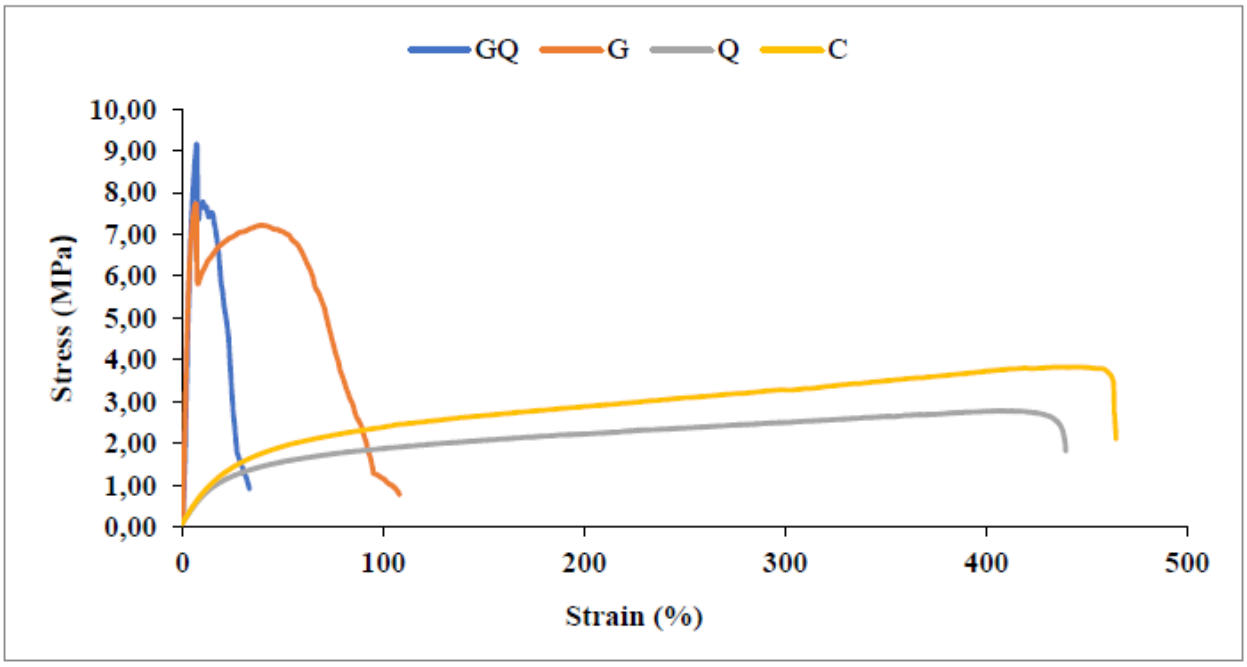

Figure 38. stress-strain curve for all type of scaffolds analyzed.

Observing stress-strain curves shown in figure 38, it was evident that uncoated samples PCL:PGS 1:1 (C) and quercetin functionalized PCL:PGS 1:1 (Q), after an initial elastic behaviour, had a typical ductile curve characterized by the possibility of having high notable elongations before rupture.

Conversely, dry gelatin-coated scaffolds with (GQ) or without (G) quercetin showed very different behaviour under a mechanical point of view in comparison with all the other samples.

Indeed, all dry gelatin-coated samples had shown a more brittle and harder behaviour than uncoated ones, presenting a higher Young's modulus (from 12 to 20 times bigger) and a lower breaking elongation (from 5 to 10 times lower). This hardening property was overcome immersing gelatin-covered scaffolds in a NaCl solution (0.9 %, w/v). The hardening of the polymeric samples caused by the surface modification with gelatin was responsible of low values in elongation. Following vascular surgery procedures, gelatine coated scaffolds were immersed in a NaCl solution and their mechanical responses were investigated again.

Surprisingly, the wet state restored the ductile behaviour of the gelatine-coated samples, removing the hardening property of dry gelatine, but showing a lower rupture elongation.

Wet samples were considered to correspond better than dry samples to the final application of the prostheses, and therefore, taken together, all these data suggested that the coating with gelatin did not modify the mechanical properties of native scaffolds. In particular, the condition of hydration facilitated the sliding of polymer chains under mechanical deformation, both in the case of gelatin coated and uncoated samples.

The mechanical properties of samples tested in the bioreactor under different pressure were evaluated in terms of young modulus, tensile strength and elongation. All the samples, compared with native human artery, present results in the same stage. As reported by the analysis on bio-prostheses treated in static condition these results proving that the electrospun scaffold under physiological pressure did not undergo change caused by the pressure.

Table 6. Young's modulus, tensile strength and elongation of comparation of bioprotheses.

Samples	Young's modulus (MPa)	Tensile strength (MPa)	Elongation (%)
60 mmHg	1.62 ± 0.64	1.34 ± 0.42	48.98 ± 12.07
80 mmHg	7.29 ± 0.07	4.47 ± 0.35	66.97 ± 3.28
100 mmHg	3.93 ± 0.25	3.30 ± 0.22	50.66 ± 7.87
Native material	7.61 ± 0.92	3.14 ± 1.47	218.48 ± 27.72
Native human artery	2.58 ± 0.34	1.13 ± 0.06	46.54 ± 11.31

Morphology

Images obtained with Scanning Electron Microscope (SEM) of internal and external scaffold surface are shown in figure 39.

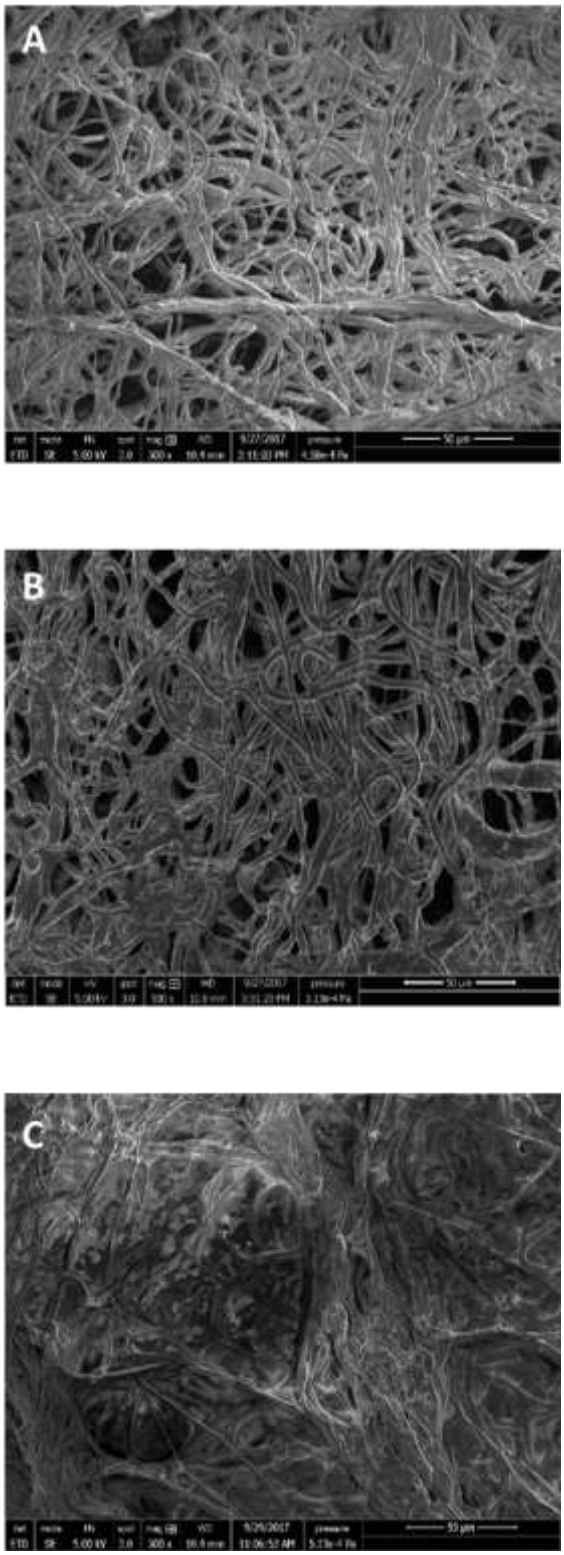

Figure 39. SEM images of surface of A (PCL: PGS ,1:1), B (PCL:PGS,1:1+Q) and C (PCL:PGS,1:1+Q coated with gelatin) scaffold.

Samples analyzed were: PCL:PGS 1:1 (C), gelatin coated PCL:PGS 1:1 (G), quercetin functionalized PCL:PGS 1:1 (Q) and quercetin functionalized gelatin coated PCL:PGS 1:1 (GQ). Their analysis revealed a completely random fibers orientation and disposure. Fiber dimensions in both internal (data not shown) and external surface of all kinds of scaffolds can be considered as microfibers with a range of diameters variation from 5.29 ± 1.31 (PCL:PGS 1:1) to 6.60 ± 2.05 (gelatin coated PCL:PGS 1:1). Among all the analyzed samples there were not any significant variation regarding fibers diameters.

Table 7. Fiber diameters of different kinds of scaffolds considered.

	PCL:PGS 1:1	**With quercetin**	**With gelatin and quercetin**
Fiber diameters (µm)	5.29 ± 1.31	5.38 ± 2.52	5.50 ± 2.08

Generally, biomaterials with micrometric fibers are better that nanometric fibers ones, because their pores of bigger dimension are preferable for cellular attachment and proliferation and also for nutritional substances diffusion in cellular culture [138][139]. The gelatin coating modified fibers disposition sticking them together and making them more undefined. Indeed, cross-linking of fibers it's the aim of the coating in order to reduce scaffolds permeability and porosity so that it can handle the hematic flux enough, until the blood clotting on the internal surface of the prosthesis happens.

Scanning electron microscopy

The morphology of biomaterials is a crucial aspect to be taken into consideration. It provides information regarding the morphology and the 3D architecture of the scaffold. These characteristics influence other parameters directly related to mass loss over time, fluid uptake, cell compatibility, and interactions with blood. Nanofibers, as an example, show a degradation rate that could be higher if compared to microfiber. For all these reasons, morphology analyses of PCL:PGS-based

electrospun scaffold were performed by scanning electron microscopy (SEM). SEM images revealed a marked difference between the internal and the external surface of this scaffold (data not shown). The external surface was constituted by bead-free microfibers, randomly oriented (Figure 37A) whereas the internal one is characterized by fused fibers. This fact finds an explanation in the use of mineral oil distributed on the collector before the deposition of fibers prior to the electrospinning process. Morphology analyses were performed even taking into consideration samples after 28 days of soaking in PBS.

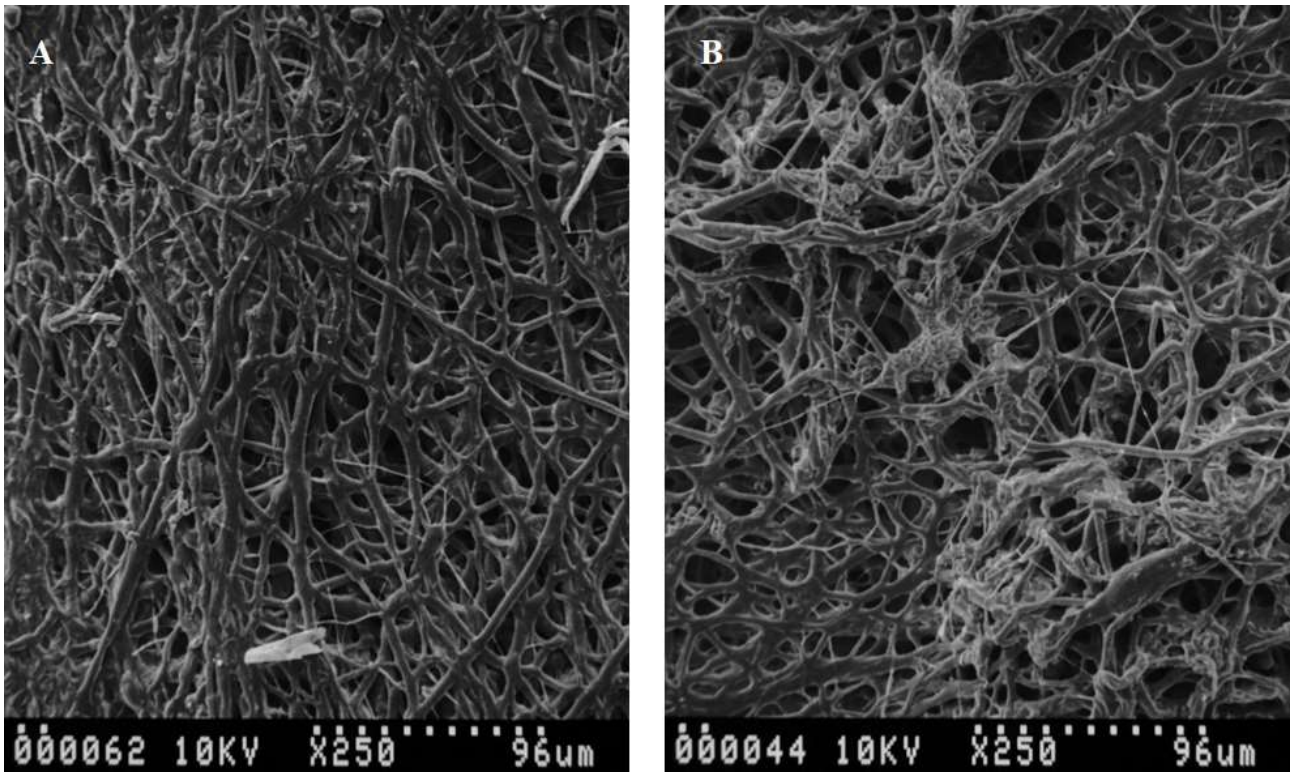

Figure 40. Representative micrographs of PCL:PGS-based surface (a) before and (b) after 28 days of degradation.

Figure 40 shows the fibers of electrospun PCL:PGS-based material after 4 weeks of soaking in PBS. They maintain their overall 3D architecture with randomly oriented microfibers. It was noticed the presence of fiber agglomeration that indicate an initial weakening and collapse of fibers. The images are representative even for the porosity of the studied material. After 4 days, the number and the

dimension of the pores increased due to effect of fiber degradation. This mass loss is to be considered positive because of it will be parallel to the deposition of extracellular matrix that will replace the electrospun fibers.

Kinetic of blood coagulation on electrospun vascular prostheses

Hemocompatibility is a biological characteristic that all the biomaterial must possess to be used in vivo. Different properties are comprised in the concept of hemocompatibility, i.e., hemolysis, complement activation, and kinetic clotting time. The blood coagulation is one of the process that is the basis of different cardiovascular diseases and it is directly related to the formation of thrombotic event. The most prominent limitations of artificial prostheses are the high frequency of thrombosis working with small-diameter graft. For this reason, it is crucial that the material that is the basis of the construct must be non-thrombogenic. The PCL:PGS-based material was put in contact with blood for 15, 30, 60, and 120 minutes and it was registered the quantity of released haemoglobin. Glass was used as a reference procoagulant material.

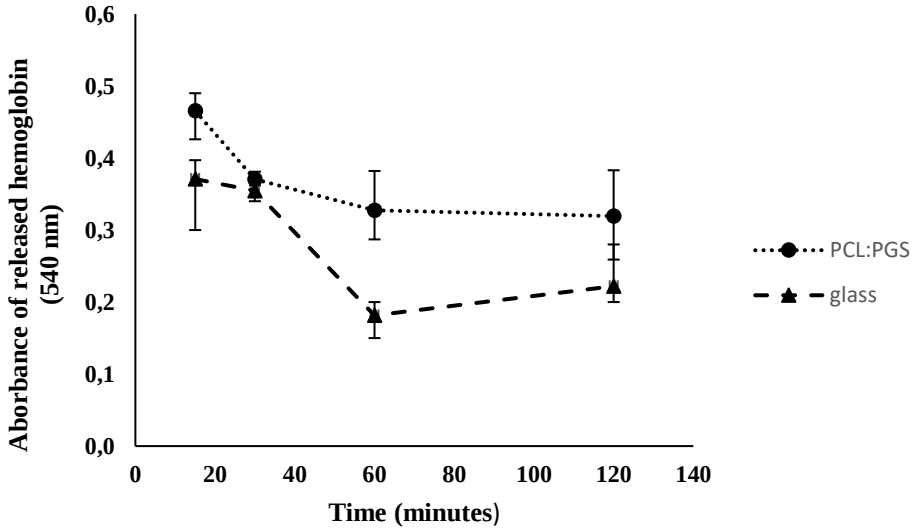

Figure 41. Coagulation kinetic of PCL:PGS-based scaffold. Glass was used as reference material.

Figure 41 shows the kinetic of blood clotting on the tested material and on glass. The quantity of released haemoglobin was markedly higher for the studied sample in comparison with the glass. This means that a higher number of erythrocytes are maintained free, because they are not entrapped in the formed clot, and are lysed by adding deionized water. The haemoglobin released from the sample is related to the number of free erythrocytes and thus with the dimension of the blood clot that is present on the studied material. Lower is the absorbance of haemoglobin, lower are the procoagulant properties of the scaffold.

Fluid uptake

One of the principles of tissue engineering is represented by having biodegradable materials that during their degradation allow the regeneration of the replaced organ. In order to mimic better the scaffold behaviour *in vivo* conditions, mass loss and fluid uptake experiments were performed under dynamic conditions using a tube rotator at 22 rpm in an incubator at 37°C (Bicasa, Bernareggio, Italy). These studies were carried out in the presence of three different pH, acidic (in a solution of hydrochloric acid, pH = 3), basic (in a solution of sodium hydroxide, pH = 12), and neutral (in PBS, pH = 7.4). To register the mass loss of the tubular constructs under pH-based conditions, they were cut in small pieces (5 × 5 mm^2), weighted on an analytical balance, immersed in the opportune solution, and incubated at 37°C for a total period of 7 days. After one week of experimentation, samples were collected, washed with deionized water, and put in desiccator overnight prior to be weighted again. Furthermore, to study the mass loss for samples soaked in PBS, in addition to one week even samples after 14, 21, and 28 days were taken into consideration.

The percentage of mass loss was calculated as follows (equation 6):

$$\text{mass loss } (\%) = \frac{m_i - m_f}{m_i} \times 100$$

where m_i and m_f are the mass of the sample before and after soaking, respectively. All experiments were performed in triplicate.

Similarly, for fluid uptake experiments, small pieces of the construct were obtained as reported above and weighted. Then, they were soaked in PBS and after 15, 30, 60, 120, 180, 240 minutes, and 24 hours, once removed the excess of water on their surface, they were weighted again. The fluid uptake percentage was as reported above by the equation.

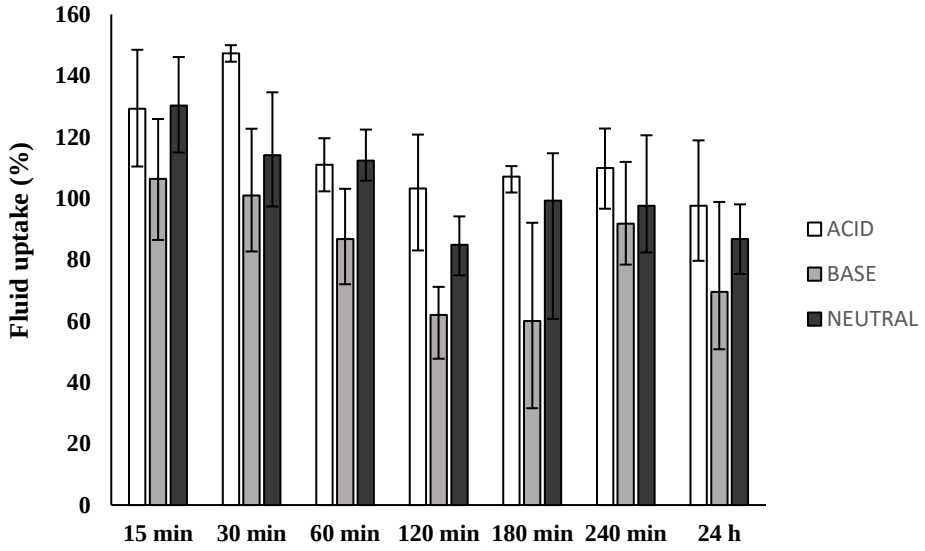

Figure 42. Fluid uptake of PCL:PGS-based electrospun scaffold in acid, basic, and neutral conditions.

For all samples, an increase in mass was registered even after 15 minutes of soaking, regardless of the pH of the solution used. The influence of different pH values started to have effects after 30 minutes of soaking. In fact, after 30, 60, 120, and 180 minutes, the samples immersed in the solution of NaOH (pH = 12) decreased their mass in comparison with the other samples. This behaviour finds explanation in the capability by basic compounds of better degrading the electrospun fibers. Considering the acidic and the neutral solutions, the mass of the samples was maintained constant for most of the time used for the experimentation. No evidences of significant differences were noticed between the samples soaked in acidic solution (pH = 3) and those immersed in PBS. After 240 minutes, the fluid uptake was similar for all the pH conditions.

Overall conclusion

The present work is focused on innovative tools for the atherosclerosis. For the treatment of early-stage of atherosclerosis nanoparticles were developed for a target drug delivery while for the development of the plaque an innovative bioresorbable and biocompatible polymeric graft was studied.

Focusing on the results obtained from the nanocarriers studied, liposomes and PLGA based nanoparticles showed comparable mean size, PDIs, and morphological properties. A notable difference regarded the entrapment efficiency which resulted be significantly higher for the polymeric nanoparticles reaching a maximum of 98.01±0.05%. An advantage of liposomes was given from the release profile which resulted to be more sustainable due to the presence of the lipidic bilayer, avoiding a burst release of the entrapped protein.

The hemolytic activity resulted to be streactly related to the concentration of the entrapped drug, probably due to the presence of absorbed protein on the external surface of the carrier. Although the PLGA-based nanoparticles present in all the studied cases an hemolytic activity lower than 5%, even the high amount of encapsulated protein, considering biocompatibility, using the MTS assay on EA. hy926 human endothelial cells, both the carries present no cytotoxic effect neither for loaded nor empty carriers.

Taking into account these results, more extensive studied was performed on polymeric nanoparticles. These analyses were done at the Instituto de Investigação e Inovação em Saúde da Universidade do Porto (Porto, Portugal) during the research period abroad. In order to have a more sustained release, a PEG coating was made on PLGA particles, this procedure commonly used to facilitate a possible graft on nanoparticle surface of molecules able to drive the nanocarriers. Indeed, the aim of this experimentation is the production of functionalized nanoparticles for

targeted delivery to atherosclerotic plaque using the IUG-1. Results showed that nanoparticles are a good candidate as innovative tools for target delivery, with good PDIs, mean size, zeta-potential, and morphological properties. Furthermore, the stability of entrapped drug was evaluated using the CD analysis until one week. The effectively functionalization of IUG-1 was established both from the ATR-FTIR analysis profiles and the significant differences in terms of zeta-potential and dimension in respect to bare nanoparticles. Also, a good biocompatibility and hemocompatibility, in terms of hemolysis, were revealed even using 100 μg/mL of loaded drug.

Another topic was focused on the production of bio prostheses using the electrospinning technique. In the case of we are in the present of a partial or severe occlusion, the advantage of the developed nanocarrier are limited. In this case, it is more opportune the use of a vascular biodegradable and bioabsorbable vascular prostheses with small diameter (less than 6.00 mm).

After the setting of working parameters, studies of degradation and release were performed. In order to decrease the permeability of the blend of polymeric solution, we have decided to fabricate prostheses coated with gelatin after the electrospinning process. Furthermore, the produced scaffolds, were functionalized with quercetin as anti-inflammatory agent. The coated and functionalized scaffolds were studied in three different conditions: static, dynamic and in a bioreactor to test its performance in several circumstance. Results showed and trying to move towards a different profile of degradation and release in the different condition indicating a correlation with the mechanical forces induced by the physiological environmental flow present in the bioreactor. All the obtained result allowed us to plan an *in vivo* experimentation in the next future.

Reference

[1] N. J. Pagidipati and T. A. Gaziano, “Estimating deaths from cardiovascular disease: A review of global methodologies of mortality measurement,” *Circulation*, vol. 127, no. 6, pp. 749–756, 2013.

[2] A. Timmis *et al.*, “European society of Cardiology: Cardiovascular disease statistics 2019 (executive summary),” *Eur. Hear. J. - Qual. Care Clin. Outcomes*, vol. 6, no. 1, pp. 7–9, 2020.

[3] J. Bejarano *et al.*, “Nanoparticles for diagnosis and therapy of atherosclerosis and myocardial infarction: Evolution toward prospective theranostic approaches,” *Theranostics*, vol. 8, no. 17, pp. 4710–4732, 2018.

[4] A. Nakhlband *et al.*, “Combating atherosclerosis with targeted nanomedicines: Recent advances and future prospective,” *BioImpacts*, vol. 8, no. 1, pp. 59–75, 2018.

[5] C. C. Chang, Y. C. Chang, W. L. Hu, and Y. C. Hung, “Oxidative Stress and Salvia miltiorrhiza in Aging-Associated Cardiovascular Diseases,” *Oxid. Med. Cell. Longev.*, vol. 2016, 2016.

[6] C. J. Marrocco and H. R. L. Bush, “Peripheral arterial disease,” *High Risk Diabet. Foot Treat. Prev.*, vol. 358, pp. 1–8, 2010.

[7] J. W. Olin and B. A. Sealove, “Peripheral artery disease: Current insight into the disease and its diagnosis and management,” *Mayo Clin. Proc.*, vol. 85, no. 7, pp. 678–692, 2010.

[8] D. Beconcini, F. Felice, A. Fabiano, B. Sarmento, Y. Zambito, and R. Di Stefano, “Antioxidant and anti-inflammatory properties of cherry extract: Nanosystems-based strategies to improve endothelial function and intestinal absorption,” *Foods*, vol. 9, no. 2, 2020.

[9] C. Fava and M. Montagnana, “Atherosclerosis is an inflammatory disease which lacks a common anti-inflammatory therapy: How human genetics can help to this issue. A narrative review,” *Front. Pharmacol.*, vol. 9, no. FEB, pp. 1–9, 2018.

[10] M. Rafieian-kopaei, M. Setorki, M. Doudi, A. Baradaran, and H. Nasri, “Atherosclerosis : Process,Indicators, Risk Factors and Background,” *Int. J. Prev. Med.*, vol. 5, no. 8, pp. 927–946, 2018.

[11] E. Falk, “Pathogenesis of Atherosclerosis,” *J. Am. Coll. Cardiol.*, vol. 47, no. 8 SUPPL., pp. 0–5, 2006.

[12] M. H. Criqui, “Peripheral arterial disease - Epidemiological aspects,” *Vasc. Med.*, vol. 6, no. 3 SUPPL., pp. 3–7, 2001.

[13] C. Camaré, M. Pucelle, A. Nègre-Salvayre, and R. Salvayre, “Angiogenesis in the atherosclerotic plaque,” *Redox Biol.*, vol. 12, no. November 2016, pp. 18–34, 2017.

[14] R. Ross, “The pathogenesis of atherosclerosis: A perspective for the 1990s,” *Nature*, vol. 362, no. 6423, pp. 801–809, 1993.

[15] P. Libby and J. Plutzky, “Atherosclerosis: An inflammatory disease,” *Int. Congr. Symp. Ser. - R. Soc. Med.*, no. 243, pp. 27–31, 2000.

[16] B. D. Lamon and D. P. Hajjar, “Inflammation at the molecular interface of atherogenesis: An Anthropological Journey,” *Am. J. Pathol.*, vol. 173, no. 5, pp. 1253–1264, 2008.

[17] C. F. Krieglstein and D. N. Granger, “Adhesion molecules and their role in vascular disease,” *Am. J. Hypertens.*, vol. 14, no. 6 II, pp. 44–54, 2001.

[18] P. Libby, P. M. Ridker, and A. Maseri, “Inflammation and atherosclerosis,” *Circulation*, vol. 105, no. 9, pp. 1135–1143, 2002.

[19] A. Tedgui and Z. Mallat, “Cytokines in atherosclerosis: Pathogenic and regulatory pathways,” *Physiol. Rev.*, vol. 86, no. 2, pp. 515–581, 2006.

[20] N. Wilck and A. Ludwig, “Targeting the ubiquitin-proteasome system in atherosclerosis: Status Quo, challenges, and perspectives,” *Antioxidants Redox Signal.*, vol. 21, no. 17, pp. 2344–2363, 2014.

[21] H. Stary *et al.*, “AHA Medical / Scientific Statement Special Report A Definition of Initial , Fatty Streak , and Intermediate Lesions of Atherosclerosis,” *Circulation*, vol. 89, pp. 2462–2478, 1994.

[22] H. C. Stary *et al.*, “A definition of advanced types of atherosclerotic lesions and a histological classification of atherosclerosis: A report from the Committee on Vascular Lesions of the council on arteriosclerosis, American heart association,” *Circulation*, vol. 92, no. 5, pp. 1355–1374, 1995.

[23] G. Riccioni and V. Sblendorio, “Atherosclerosis: From biology to pharmacological treatment,” *J. Geriatr. Cardiol.*, vol. 9, no. 3, pp. 305–317, 2012.

[24] A. Endo, Y. Tsujita, M. Kuroda, and K. Tanzawa, “by ML-236A and ML-236B , Competitive Inhibitors of 3-Hydroxy-3-methylglutaryl-Coenzyme A Reductase,” *Eur. J. Biochem.*, vol. 77, pp. 31–36, 1977.

[25] F. G. Cunningham *et al.*, *Universal Free E-Book Store Universal Free E-Book Store*. 2014.

[26] S. Bellosta and A. Corsini, “RASSEGNA STATINE : INTERAZIONI TRA FARMACI ED EVENTI AVVERSI CORRELATI Statins : drug interactions and related adverse reactions,” vol. 10, no. 2, pp. 5–13, 2018.

[27] D. R. Greaves and S. Gordon, “Immunity, atherosclerosis and cardiovascular disease,” *Trends Immunol.*, vol. 22, no. 4, pp. 180–181, 2001.

[28] K. L. West, T. L. Zern, D. N. Butteiger, B. T. Keller, and M. L. Fernandez, “SC-435, an ileal apical sodium co-dependent bile acid transporter (ASBT) inhibitor lowers plasma cholesterol and reduces atherosclerosis in guinea pigs,” *Atherosclerosis*, vol. 171, no. 2, pp. 201–210, 2003.

[29] J. M. Donkers, R. L. P. Roscam Abbing, and S. F. J. van de Graaf, *Developments in bile salt based therapies: A critical overview*, vol. 161. Elsevier Inc., 2019.

[30] B. A. P. Phan, T. D. Dayspring, and P. P. Toth, “Ezetimibe therapy: Mechanism of action and clinical update,” *Vasc. Health Risk Manag.*, vol. 8, no. 1, pp. 415–427, 2012.

[31] L. Ge *et al.*, “The Cholesterol Absorption Inhibitor Ezetimibe Acts by Blocking the Sterol-Induced Internalization of NPC1L1,” *Cell Metab.*, vol. 7, no. 6, pp. 508–519, 2008.

[32] K. Tsujita *et al.*, “Impact of dual lipid-lowering strategy with ezetimibe and atorvastatin on coronary plaque regression in patients with percutaneous coronary intervention: The multicenter randomized controlled PRECISE-IVUS trial,” *J. Am. Coll. Cardiol.*, vol. 66, no. 5,

pp. 495–507, 2015.

[33] J. A. van Diepen, J. F. P. Berbée, L. M. Havekes, and P. C. N. Rensen, “Interactions between inflammation and lipid metabolism: Relevance for efficacy of anti-inflammatory drugs in the treatment of atherosclerosis,” *Atherosclerosis*, vol. 228, no. 2, pp. 306–315, 2013.

[34] T. Cyrus, S. Sung, L. Zhao, C. D. Funk, S. Tang, and D. Praticò, “Effect of low-dose aspirin on vascular inflammation, plaque stability, and atherogenesis in low-density lipoprotein receptor-deficient mice,” *Circulation*, vol. 106, no. 10, pp. 1282–1287, 2002.

[35] M. J. Yin, Y. Yamamoto, and R. B. Gaynor, “The anti-inflammatory agents aspirin and salicylate inhibit the activity of I(kappa)B kinase-beta [see comments],” *Nature*, vol. 396, no. 6706, pp. 77–80, 1998.

[36] K. Brand *et al.*, “Activated transcription factor nuclear factor-kappa B is present in the atherosclerotic lesion,” *J. Clin. Invest.*, vol. 97, no. 7, pp. 1715–1722, 1996.

[37] P. M. Ridker *et al.*, “Antiinflammatory Therapy with Canakinumab for Atherosclerotic Disease,” *N. Engl. J. Med.*, vol. 377, no. 12, pp. 1119–1131, 2017.

[38] P. M. Ridker, T. Thuren, A. Zalewski, and P. Libby, “Interleukin-1β inhibition and the prevention of recurrent cardiovascular events: Rationale and Design of the Canakinumab Anti-inflammatory Thrombosis Outcomes Study (CANTOS),” *Am. Heart J.*, vol. 162, no. 4, pp. 597–605, 2011.

[39] I. Ultrasonography *et al.*, “Article Annals of Internal Medicine -Blockers and Progression of Coronary Atherosclerosis : Pooled,” *Changes*, 2017.

[40] C. Stigliano *et al.*, “Methotraxate-Loaded Hybrid Nanoconstructs Target Vascular Lesions and Inhibit Atherosclerosis Progression in ApoE−/− Mice,” *Adv. Healthc. Mater.*, vol. 6, no. 13, pp. 1–9, 2017.

[41] S. K. Sahoo and V. Labhasetwar, “Nanotech approaches to drug delivery and imaging,” *Drug Discov. Today*, vol. 8, no. 24, pp. 1112–1120, 2003.

[42] O. C. Farokhzad and R. Langer, “Impact of nanotechnology on drug delivery,” *ACS Nano*, vol. 3, no. 1, pp. 16–20, 2009.

[43] R. BAZAK, M. HOURI, S. EL ACHY, W. HUSSEIN, and T. REFAAT, “Passive targeting of nanoparticles to cancer: A comprehensive review of the literature,” *Mol. Clin. Oncol.*, vol. 2, no. 6, pp. 904–908, 2014.

[44] J. V. Jokerst, T. Lobovkina, R. N. Zare, and S. S. Gambhir, “Nanoparticle PEGylation for imaging and therapy,” *Nanomedicine*, vol. 6, no. 4, pp. 715–728, 2011.

[45] M. E. Lobatto, V. Fuster, Z. A. Fayad, and W. J. M. Mulder, “Perspectives and opportunities for nanomedicine in the management of atherosclerosis,” *Nat. Rev. Drug Discov.*, vol. 10, no. 11, pp. 835–852, 2011.

[46] I. E. Santo, R. Campardelli, E. C. Albuquerque, S. V. de Melo, G. Della Porta, and E. Reverchon, “Liposomes preparation using a supercritical fluid assisted continuous process,” *Chem. Eng. J.*, vol. 249, pp. 153–159, 2014.

[47] J. Swaminathan and C. Ehrhardt, “Liposomes for Pulmonary Drug Delivery,” in *Controlled Pulmonary Drug Delivery*, H. D. C. Smyth and A. J. Hickey, Eds. New York, NY: Springer New

York, 2011, pp. 313–334.

[48] B. Maherani, E. Arab-Tehrany, M. R. Mozafari, C. Gaiani, and M. Linder, “Liposomes: A Review of Manufacturing Techniques and Targeting Strategies,” *Curr. Nanosci.*, vol. 7, no. 3, pp. 436–452, 2011.

[49] M. Chandarana, A. Curtis, and C. Hoskins, “The use of nanotechnology in cardiovascular disease,” *Appl. Nanosci.*, vol. 8, no. 7, pp. 1607–1619, 2018.

[50] A. Saito *et al.*, “Immunoliposomal drug-delivery system targeting lectin-like oxidized low-density lipoprotein receptor-1 for carotid plaque lesions in rats: Laboratory investigation,” *J. Neurosurg.*, vol. 115, no. 4, pp. 720–727, 2011.

[51] B. H. Simon Cho, J. R. Park, M. T. Nakamura, B. M. Odintsov, M. A. Wallig, and B. H. Chung, “Synthetic dimyristoylphosphatidylcholine liposomes assimilating into high-density lipoprotein promote regression of atherosclerotic lesions in cholesterol-fed rabbits,” *Exp. Biol. Med.*, vol. 235, no. 10, pp. 1194–1203, 2010.

[52] K. K. Gupta, S. Ali, and R. S. Sanghera, “Pharmacological Options in Atherosclerosis: A Review of the Existing Evidence,” *Cardiol. Ther.*, vol. 8, no. 1, pp. 5–20, 2019.

[53] M. Giannouli, V. Karagkiozaki, F. Pappa, I. Moutsios, C. Gravalidis, and S. Logothetidis, “Fabrication of quercetin-loaded PLGA nanoparticles via electrohydrodynamic atomization for cardiovascular disease,” *Mater. Today Proc.*, vol. 5, no. 8, pp. 15998–16005, 2018.

[54] M. R. Hirpara *et al.*, “Long circulating PEGylated-chitosan nanoparticles of rosuvastatin calcium: Development and in vitro and in vivo evaluations,” *Int. J. Biol. Macromol.*, vol. 107, pp. 2190–2200, 2018.

[55] B. L. Sanchez-Gaytan *et al.*, “HDL-Mimetic PLGA Nanoparticle To Target Atherosclerosis Plaque Macrophages,” *Bioconjug. Chem.*, vol. 26, no. 3, pp. 443–451, 2015.

[56] Z. Yang *et al.*, “Sustained release of heparin from polymeric particles for inhibition of human vascular smooth muscle cell proliferation,” *J. Control. Release*, vol. 60, no. 2–3, pp. 269–277, 1999.

[57] H. Kim, J. Han, and J. H. Park, “Cyclodextrin polymer improves atherosclerosis therapy and reduces ototoxicity,” *J. Control. Release*, vol. 319, no. August 2019, pp. 77–86, 2020.

[58] M. Yu *et al.*, “Nanoparticles targeting extra domain b of fibronectin− specific to the atherosclerotic lesion types III, IV, and v−enhance plaque detection and cargo delivery,” *Theranostics*, vol. 8, no. 21, pp. 6008–6024, 2018.

[59] X. Li *et al.*, “Synergistic effects of liposomes encapsulating atorvastatin calcium and curcumin and targeting dysfunctional endothelial cells in reducing atherosclerosis,” *Int. J. Nanomedicine*, vol. 14, pp. 649–665, 2019.

[60] D. Vllasaliu, R. Fowler, and S. Stolnik, “PEGylated nanomedicines: Recent progress and remaining concerns,” *Expert Opin. Drug Deliv.*, vol. 11, no. 1, pp. 139–154, 2014.

[61] C. Martins, F. Sousa, F. Araújo, and B. Sarmento, “Functionalizing PLGA and PLGA Derivatives for Drug Delivery and Tissue Regeneration Applications,” *Adv. Healthc. Mater.*, vol. 7, no. 1, pp. 1–24, 2018.

[62] R. Campardelli *et al.*, “The Journal of Supercritical Fluids Efficient encapsulation of proteins

in submicro liposomes using a supercritical fluid assisted continuous process," *J. Supercrit. Fluids*, vol. 107, pp. 163–169, 2016.

[63] C. Fornaguera, G. Calderó, M. P. Vinardell, C. Solans, and C. Vauthier, "Interactions of PLGA nanoparticles with blood components: protein adsorption, coagulation, activation of the complement system and hemolysis studies," pp. 6045–6058, 2015.

[64] G. P. A. Michanetzis, E. Markoutsa, S. Mourtas, and Y. F. Missirlis, "Hemocompatibility of amyloid and / or brain targeted liposomes," vol. 11, pp. 693–705, 2019.

[65] T. Freytag, A. Dashevsky, L. Tillman, G. E. Hardee, and R. Bodmeier, "Improvement of the encapsulation efficiency of oligonucleotide-containing biodegradable microspheres," vol. 69, pp. 197–207, 2000.

[66] R. Alex and R. Bodmeiers, "Encapsulation of water-soluble drugs by a modified solvent evaporation method . I . Effect of process and formulation variables on drug entrapment," vol. 7, no. 3, pp. 347–355, 1990.

[67] "Hermann et al.pdf." .

[68] L. Q. Chen, L. Fang, J. Ling, C. Z. Ding, B. Kang, and C. Z. Huang, "Nanotoxicity of Silver Nanoparticles to Red Blood Cells : Size Dependent Adsorption , Uptake , and Hemolytic Activity," 2015.

[69] P. Perrotta, B. Emini Veseli, B. Van der Veken, L. Roth, W. Martinet, and G. R. Y. De Meyer, "Pharmacological strategies to inhibit intra-plaque angiogenesis in atherosclerosis," *Vascul. Pharmacol.*, vol. 112, no. March 2018, pp. 72–78, 2019.

[70] C. Stefanadis, K. Toutouzas, E. Stefanadi, A. Lazaris, E. Patsouris, and N. Kipshidze, "Inhibition of plaque neovascularization and intimal hyperplasia by specific targeting vascular endothelial growth factor with bevacizumab-eluting stent: An experimental study," *Atherosclerosis*, vol. 195, no. 2, pp. 269–276, 2007.

[71] H. K. Makadia and S. J. Siegel, "Poly Lactic-co-Glycolic Acid (PLGA) as biodegradable controlled drug delivery carrier," *Polymers (Basel).*, vol. 3, no. 3, pp. 1377–1397, 2011.

[72] P. F. Ferrari, B. Aliakbarian, E. Zattera, L. Pastorino, D. Palombo, and P. Perego, "Engineered CaCO3 nanoparticles with targeting activity: A simple approach for a vascular intended drug delivery system," *Can. J. Chem. Eng.*, vol. 95, no. 9, pp. 1683–1689, 2017.

[73] Z. Amoozgar, J. Park, Q. Lin, J. H. Weidle, and Y. Yeo, "Development of quinic acid-conjugated nanoparticles as a drug carrier to solid tumors," *Biomacromolecules*, vol. 14, no. 7, pp. 2389–2395, 2013.

[74] C. Dempsey, I. Lee, K. R. Cowan, and J. Suh, "Coating barium titanate nanoparticles with polyethylenimine improves cellular uptake and allows for coupled imaging and gene delivery," *Colloids Surfaces B Biointerfaces*, vol. 112, pp. 108–112, 2013.

[75] J. S. Suk, Q. Xu, N. Kim, J. Hanes, and L. M. Ensign, "PEGylation as a strategy for improving nanoparticle-based drug and gene delivery," *Adv. Drug Deliv. Rev.*, vol. 99, pp. 28–51, 2016.

[76] A. C. Marques, P. J. Costa, S. Velho, and M. H. Amaral, "Functionalizing nanoparticles with cancer-targeting antibodies: A comparison of strategies," *J. Control. Release*, vol. 320, no. December 2019, pp. 180–200, 2020.

[77] S. Thalhauser and M. Breunig, “Considerations for efficient surface functionalization of nanoparticles with a high molecular weight protein as targeting ligand,” *Eur. J. Pharm. Sci.*, vol. 155, no. April, p. 105520, 2020.

[78] J. Zhao, F. Santino, D. Giacomini, and L. Gentilucci, “Integrin-targeting peptides for the design of functional cell-responsive biomaterials,” *Biomedicines*, vol. 8, no. 9, 2020.

[79] E. Ventura *et al.*, “Use of uteroglobin for the engineering of polyvalent, polyspecific fusion proteins,” *J. Biol. Chem.*, vol. 284, no. 39, pp. 26646–26654, 2009.

[80] F. Moroni, E. Ammirati, G. D. Norata, M. Magnoni, and P. G. Camici, “The role of monocytes and macrophages in human atherosclerosis, plaque neoangiogenesis, and atherothrombosis,” *Mediators Inflamm.*, vol. 2019, 2019.

[81] “Liang et al. 2013.” .

[82] F. Sousa, A. Cruz, P. Fonte, I. M. Pinto, M. T. Neves-Petersen, and B. Sarmento, “A new paradigm for antiangiogenic therapy through controlled release of bevacizumab from PLGA nanoparticles,” *Sci. Rep.*, vol. 7, no. 1, pp. 1–13, 2017.

[83] M. Varani *et al.*, “Theranostic Designed Near-Infrared Fluorescent Poly (Lactic-co-Glycolic Acid) Nanoparticles and Preliminary Studies with Functionalized VEGF-Nanoparticles,” *J. Clin. Med.*, vol. 9, no. 6, p. 1750, 2020.

[84] “Alam et al 2000-1.pdf.” .

[85] S. A. Townsend, G. D. Evrony, F. X. Gu, M. P. Schulz, R. H. Brown, and R. Langer, “Tetanus toxin C fragment-conjugated nanoparticles for targeted drug delivery to neurons,” *Biomaterials*, vol. 28, no. 34, pp. 5176–5184, 2007.

[86] A. Verma and F. Stellacci, “Effect of surface properties on nanoparticle-cell interactions,” *Small*, vol. 6, no. 1, pp. 12–21, 2010.

[87] D. E. Owens and N. A. Peppas, “Opsonization, biodistribution, and pharmacokinetics of polymeric nanoparticles,” *Int. J. Pharm.*, vol. 307, no. 1, pp. 93–102, 2006.

[88] A. Abuchowski, T. Van Es, N. C. Palczuk, and F. F. Davis, “Alteration of immunological properties of bovine serum albumin by covalent attachment of polyethylene glycol,” *J. Biol. Chem.*, vol. 252, no. 11, pp. 3578–3581, 1977.

[89] Z. Hussain, S. Khan, M. Imran, M. Sohail, S. W. A. Shah, and M. de Matas, “PEGylation: a promising strategy to overcome challenges to cancer-targeted nanomedicines: a review of challenges to clinical transition and promising resolution,” *Drug Deliv. Transl. Res.*, pp. 721–734, 2019.

[90] R. Roberts *et al.*, “Development of PLGA nanoparticles for sustained release of a connexin43 mimetic peptide to target glioblastoma cells,” *Mater. Sci. Eng. C*, vol. 108, no. August 2018, p. 110191, 2020.

[91] M. Pachauri, E. D. Gupta, and P. C. Ghosh, “Piperine loaded PEG-PLGA nanoparticles: Preparation, characterization and targeted delivery for adjuvant breast cancer chemotherapy,” *J. Drug Deliv. Sci. Technol.*, vol. 29, pp. 269–282, 2015.

[92] Y. Zhang, N. Kohler, and M. Zhang, “Surface modification of superparamagnetic magnetite nanoparticles and their intracellular uptake,” *Biomaterials*, vol. 23, no. 7, pp. 1553–1561,

2002.

[93] I. A. Mudunkotuwa, A. Al Minshid, and V. H. Grassian, “ATR-FTIR spectroscopy as a tool to probe surface adsorption on nanoparticles at the liquid-solid interface in environmentally and biologically relevant media,” *Analyst*, vol. 139, no. 5, pp. 870–881, 2014.

[94] R. Varshochian *et al.*, “The protective effect of albumin on bevacizumab activity and stability in PLGA nanoparticles intended for retinal and choroidal neovascularization treatments,” *Eur. J. Pharm. Sci.*, vol. 50, no. 3–4, pp. 341–352, 2013.

[95] M. Malakouti-Nejad *et al.*, “Formulation of nanoliposome-encapsulated bevacizumab (Avastin): Statistical optimization for enhanced drug encapsulation and properties evaluation,” *Int. J. Pharm.*, vol. 590, no. September, p. 119895, 2020.

[96] A. R. Padalhin, N. T. Ba Linh, Y. Ki Min, and B. T. Lee, “Evaluation of the cytocompatibility hemocompatibility in vivo bone tissue regenerating capability of different PCL blends,” *J. Biomater. Sci. Polym. Ed.*, vol. 25, no. 5, pp. 487–503, 2014.

[97] N. Interactions *et al.*, “The Hemocompatibility of Nanoparticles : A Review,” *Cells*, vol. 8, no. 1209, pp. 1–25, 2019.

[98] J. P. Vacanti and R. Langer, “Tissue engineering: The design and fabrication of living replacement devices for surgical reconstruction and transplantation,” *Lancet*, vol. 354, no. SUPPL.1, pp. 32–34, 1999.

[99] H. Shin, S. Jo, and A. G. Mikos, “Biomimetic materials for tissue engineering,” *Biomaterials*, vol. 24, no. 24, pp. 4353–4364, 2003.

[100] J. Wang and Q. Mao, “Methodology Based on the PVT Behavior of Polymer for Injection Molding,” *Adv. Polym. Technol.*, vol. 32, no. 2013, pp. 474–485, 2012.

[101] “Gomes et al., 1995.” p. 1995, 1995.

[102] P. Libby, “Inflammation in atherosclerosis,” *Arterioscler. Thromb. Vasc. Biol.*, vol. 32, no. 9, pp. 2045–2051, 2012.

[103] S. Drilling, J. Gaumer, and J. Lannutti, “Fabrication of burst pressure competent vascular grafts via electrospinning: Effects of microstructure,” *J. Biomed. Mater. Res. - Part A*, vol. 88, no. 4, pp. 923–934, 2009.

[104] M. Agarwal, Q. Xing, B. S. Shim, N. Kotov, K. Varahramyan, and Y. Lvov, “Conductive paper from lignocellulose wood microfibers coated with a nanocomposite of carbon nanotubes and conductive polymers,” *Nanotechnology*, vol. 20, no. 21, 2009.

[105] P. F. Ferrari, B. Aliakbarian, D. Palombo, and P. Perego, “Small diameter vascular grafts coated with gelatin,” *Chem. Eng. Trans.*, vol. 57, pp. 1441–1446, 2017.

[106] N. K. Awad, H. Niu, U. Ali, Y. S. Morsi, and T. Lin, “Electrospun fibrous scaffolds for small-diameter blood vessels: A review,” *Membranes (Basel).*, vol. 8, no. 1, pp. 1–26, 2018.

[107] L. Bosworth and S. Downes, “Biocompatible three-dimensional scaffolds for tendon tissue engineering using electrospinning,” *Cell. Response to Biomater.*, pp. 3–27, 2008.

[108] J. M. Deitzel, J. Kleinmeyer, D. Harris, and N. C. Beck Tan, “The effect of processing variables on the morphology of electrospun,” *Polymer (Guildf).*, vol. 42, pp. 261–272, 2001.

[109] C. Del Gaudio, A. Bianco, M. Folin, S. Baiguera, and M. Grigioni, “Structural characterization and cell response evaluation of electrospun PCL membranes: Micrometric versus submicrometric fibers,” *J. Biomed. Mater. Res. - Part A*, vol. 89, no. 4, pp. 1028–1039, 2009.

[110] V. Beachley and X. Wen, “Effect of electrospinning parameters on the nanofiber diameter and length,” *Mater. Sci. Eng. C*, vol. 29, no. 3, pp. 663–668, 2009.

[111] J. Venugopal, S. Low, A. T. Choon, and S. Ramakrishna, “Interaction of cells and nanofiber scaffolds in tissue engineering,” *J. Biomed. Mater. Res. - Part B Appl. Biomater.*, vol. 84, no. 1, pp. 34–48, 2008.

[112] L. Buruaga, A. Gonzalez, and J. J. Iruin, “Electrospinning of poly (2-ethyl-2-oxazoline),” *J. Mater. Sci.*, vol. 44, no. 12, pp. 3186–3191, 2009.

[113] X. M. Mo, C. Y. Xu, M. Kotaki, and S. Ramakrishna, “Electrospun P(LLA-CL) nanofiber: A biomimetic extracellular matrix for smooth muscle cell and endothelial cell proliferation,” *Biomaterials*, vol. 25, no. 10, pp. 1883–1890, 2004.

[114] S. Lingaiah, K. N. Shivakumar, R. Sadler, and M. Sharpe, “Electrospinning of nanofabrics,” *Int. SAMPE Symp. Exhib.*, vol. 52, no. January 2014, 2007.

[115] W. Cui, Y. Zhou, and J. Chang, “Electrospun nanofibrous materials for tissue engineering and drug delivery,” *Sci. Technol. Adv. Mater.*, vol. 11, no. 1, p. 014108, 2010.

[116] X. Wang, B. Ding, and B. Li, “Biomimetic electrospun nanofibrous structures for tissue engineering,” *Mater. Today*, vol. 16, no. 6, pp. 229–241, 2013.

[117] Z. Yang, H. Peng, W. Wang, and T. Liu, “Crystallization behavior of poly(ε-caprolactone)/layered double hydroxide nanocomposites,” *J. Appl. Polym. Sci.*, vol. 116, no. 5, pp. 2658–2667, 2010.

[118] M. Janmohammadi and M. S. Nourbakhsh, “Electrospun polycaprolactone scaffolds for tissue engineering: a review,” *Int. J. Polym. Mater. Polym. Biomater.*, vol. 68, no. 9, pp. 527–539, 2019.

[119] M. J. Mochane, T. S. Motsoeneng, E. R. Sadiku, T. C. Mokhena, and J. S. Sefadi, “Morphology and properties of electrospun PCL and its composites for medical applications: A mini review,” *Appl. Sci.*, vol. 9, no. 11, pp. 1–17, 2019.

[120] R. Rai, M. Tallawi, A. Grigore, and A. R. Boccaccini, “Synthesis, properties and biomedical applications of poly(glycerol sebacate) (PGS): A review,” *Prog. Polym. Sci.*, vol. 37, no. 8, pp. 1051–1078, 2012.

[121] H. Kobuchi, S. Roy, C. K. Sen, H. G. Nguyen, and L. Packer, “Quercetin inhibits inducible ICAM-1 expression in human endothelial cells through the JNK pathway,” *Am. J. Physiol. - Cell Physiol.*, vol. 277, no. 3 46-3, pp. 403–411, 1999.

[122] I. Crespo, M. V. García-Mediavilla, B. Gutiérrez, S. Sánchez-Campos, M. J. Tuñón, and J. González-Gallego, “A comparison of the effects of kaempferol and quercetin on cytokine-induced pro-inflammatory status of cultured human endothelial cells,” *Br. J. Nutr.*, vol. 100, no. 5, pp. 968–976, 2008.

[123] A. W. Boots, G. R. M. M. Haenen, and A. Bast, “Health effects of quercetin: From antioxidant to nutraceutical,” *Eur. J. Pharmacol.*, vol. 585, no. 2–3, pp. 325–337, 2008.

[124] V. Sanda *et al.*, “Lipoxygenase-Quercetin Interaction: A Kinetic Study Through Biochemical and Spectroscopy Approaches,” *Biochem. Test.*, 2012.

[125] J. H. M. De Vries, P. L. T. M. K. Janssen, P. C. H. Hollman, W. A. Van Staveren, and M. B. Katan, “Consumption of quercetin and kaempferol in free-living subjects eating a variety of diets,” *Cancer Lett.*, vol. 114, no. 1–2, pp. 141–144, 1997.

[126] M. E. Gerritsen *et al.*, “Flavonoids inhibit cytokine-induced endothelial cell adhesion protein gene expression,” *Am. J. Pathol.*, vol. 147, no. 2, pp. 278–292, 1995.

[127] I. Morel *et al.*, “Antioxidant and iron-chelating activities of the flavonoids catechin, quercetin and diosmetin on iron-loaded rat hepatocyte cultures,” *Biochem. Pharmacol.*, vol. 45, no. 1, pp. 13–19, 1993.

[128] A. Nègre-Salvayre and R. Salvayre, “Quercetin prevents the cytotoxicity of oxidized LDL on lymphoid cell lines,” *Free Radic. Biol. Med.*, vol. 12, no. 2, pp. 101–106, 1992.

[129] and C. R.-E. Nida salah, Nicholas J. Miller, George Paganga, Lilian Tijburg, G.Paul Bolwell, “1-s2.0-S0003986185714737-main.pdf,” *Archives of Biochemistry and Biophysics*, vol. 322, no. 2. pp. 339–346, 1995.

[130] C. A. Rice-Evans, N. J. Miller, and G. Paganga, “Structure-antioxidant activity relationships of flavonoids and phenolic acids,” *Free Radic. Biol. Med.*, vol. 20, no. 7, pp. 933–956, 1996.

[131] M. A. Avila, J. A. Velasco, J. Cansado, and V. Notano, “Quercetin Mediates the Down-Regulation of Mutant p53 in the Human Breast Cancer Cell Line MDA-MB468,” *Cancer Res.*, vol. 54, no. 9, pp. 2424–2428, 1994.

[132] S. O. Keli, M. G. L. Hertog, E. J. M. Feskens, and D. Kromhout, “Dietary flavonoids, antioxidant vitamins, and incidence of stroke: The Zutphen study,” *Arch. Intern. Med.*, vol. 156, no. 6, pp. 637–642, 1996.

[133] M. G. L. Hertog, P. C. H. Hollman, M. B. Katan, D. Daan, and K. Kromhout, “Intake of potentially anticarcinogenic flavonoids and their determinants in adults in the netherlands,” *Nutr. Cancer*, vol. 20, no. 1, pp. 21–29, 1993.

[134] J. K. Loreto M. Valenzuela, Bozena Michniak, “Variability of Water Uptake Studies of Biomedical Polymers,” *J. Appl. Polym. Sci.*, vol. 121, no. 3, pp. 1311–1320, 2011.

[135] S. Salehi *et al.*, “Generation of PGS/PCL blend nanofibrous scaffolds mimicking corneal stroma structure,” *Macromol. Mater. Eng.*, vol. 299, no. 4, pp. 455–469, 2014.

[136] S. Sant, D. Iyer, A. K. Gaharwar, A. Patel, and A. Khademhosseini, “Effect of biodegradation and de novo matrix synthesis on the mechanical properties of valvular interstitial cell-seeded polyglycerol sebacate-polycaprolactone scaffolds,” *Acta Biomater.*, vol. 9, no. 4, pp. 5963–5973, 2013.

[137] M. Kharaziha *et al.*, “PGS:Gelatin nanofibrous scaffolds with tunable mechanical and structural properties for engineering cardiac tissues,” *Biomaterials*, vol. 34, no. 27, pp. 6355–6366, 2013.

[138] Q. P. Pham, U. Sharma, and A. G. Mikos, “Pham2006,” *Tissue Eng.*, vol. 12, no. 5, pp. 1197–1211, 2006.

[139] A. Balguid, A. Mol, M. H. Van Marion, R. A. Bank, C. V. C. Bouten, and F. P. T. Baaijens,

“Tailoring fiber diameter in electrospun poly(ε-Caprolactone) scaffolds for optimal cellular infiltration in cardiovascular tissue engineering,” *Tissue Eng. - Part A*, vol. 15, no. 2, pp. 437–444, 2009.

Appendix

Papers published on international journal

- De Negri Atanasio, G.; Ferrari, P.F.; Campardelli, R.; Perego, P.; Palombo, D. Poly (Lactic-co-Glycolic Acid) Nanoparticles and Nanoliposomes for Protein Delivery in Targeted Therapy: A Comparative In Vitro Study. Polymers 2020, 12, 2566.
- Ferrari, P.F., Pettinato, M., Casazza, A.A., De Negri Atanasio, G., Palombo, D., Perego, P. Polyphenols from Nerone Gold 26/6, a new pigmented rice, via non-conventional extractions: antioxidant properties and biological validation. Journal of Chemical Technology and Biotechnology, 2021.

Oral presentation

- Perego P., Ferrari P.F., De Negri Atanasio G., Pane B. and Palombo D. 'From chemical engineering to tissue engineering: functionalization of small-diameter vascular prostheses with bioactive compounds' presentato al 8th International Conference 'Biomaterials, Tissue Engineering & Medical Devices' BIOMMEDD 2018, Cluj-Napoca Romanian.
- Ferrari P.F., De Negri Atanasio G., Pralits O.J., Perego P. and Palombo D. 'Study of engineered vascular bioprostheses in bioreactor' al 68th congress internazional organized from European Society of Cardiovascular Surgery (ESCVS) 2018.
- Ferrari P.F., De Negri Atanasio G., Pralits O.J., Perego P. and Palombo D. 'Biodegradable engineered small-diameter vascular scaffold: a study in bioreactor' ESVB 2019 Strasbourg, France. (oral presentation)
- De Negri Atanasio G., Ferrari P.F., Campardelli R., Palombo D. and Perego P. 'Production and characterization of polymeric nanoparticles for the controlled release of model proteins' National congress 'Il contributo dell'Ingegneria Chimica Italiana alla sostenibiltà globale' Palermo, Mondello 3-6 July 2019.

Poster presentation

- De Negri Atanasio G., Ferrari P.F., Pane B., Pralits O.J. Palombo D. and Perego P. 'Study of vascular prosthesis in bioreactor' National congress 'Il contributo dell'Ingegneria Chimica Italiana alla sostenibiltà globale' Palermo, Mondello 3-6 July 2019.

Summer school

- Comprehensive summer school on tissue engineering Trento, Italy, 2018
- GRICU summer school Palermo, Italy, 2019.

Research Period abroad

i3S - Instituto de Investigação e Inovação em Saúde da Universidade do Porto, Portugal

Supervisor: Prof. Bruno Sarmento

Topic: Production, functionalization, and characterization of polymeric nanoparticles for the targeted therapy for atherosclerosis disease.

Period: from January to July 2020.